THE ESSENTIAL ROLE OF BONE MORPHOGENETIC PROTEIN (BMP) SIGNALING
IN ORGANOGENESIS

Rongqin Ren

A dissertation submitted to the faculty of the University of North Carolina at Chapel Hill in partial fulfillment of the requirements for the degree of Doctor of Philosophy in the Department of Cell and Developmental Biology.

Chapel Hill
2007

Approved by:

Cam Patterson

Frank Conlon

Nobuyo Maeda

Mike Schaller

Dazhi Wang

ABSTRACT

Rongqin Ren: The Essential Role of Bone Morphogenetic Protein (BMP)

Signaling in Organogenesis

(Under the direction of Cam Patterson)

Signaling through the bone morphogenetic protein (BMP) pathway is essential to

organ developments. In this dissertation, two aspects of the BMP pathway were studied:

downstream targets and extracellular regulators of BMP signaling. To identify downstream

BMP mediators in angiogenesis, we performed microarray analysis on endothelial cells

(ECs) treated with BMP6 and identified cyclooxygenase 2 (Cox2) as a potential target of

BMP6. Upregulation of Cox2 as detected in the microarray was confirmed at the

transcriptional level by reverse transcriptase-polymerase chain reaction (RT-PCR) analysis

and by reporter assays. BMP6-induced endothelial cell proliferation, migration and tube

formation activities were all blocked by selective pharmacologic inhibition of Cox2. Both

genetic deletion and pharmacologic inhibition of Cox2 markedly attenuated BMP6-

dependent angiogenesis in an aortic ring assay. Targeted deletion of *BMP-binding*

endothelial precursor-derived regulator (*Bmper*), encoding an extracellular regulator of

BMP signaling, demonstrates its essential role as a BMP signal controller in early

development. Among other phenotypes, loss of Bmper activity caused abnormal branching

ii

morphogenesis in the lung and induced hypertrophy in cardiomyocytes. Transcriptional analysis using quatititive real-time PCR revealed the upregulation of hypertrophy markers and BMP signals in *Bmper* knockout cardiomyocytes and is consistent with a protective role for Bmper in cardiac hypertrophy via the downregulation of BMP pathway components. In summary, this research implicates that both BMP downstream mediators and their extracellular regulators as potential therapeutic targets in physiopathological events associated with abnormal BMP activities.

ACKNOWLEDGEMENTS

I would first like to thank my dissertation advisor, Cam Patterson, for the countless scientific, careers, and life lessons learned under his tutelage. Thanks to all the members of the Patterson Lab, past and present, for scientific discussions and support at all hours. Thanks to my committee members: Dr. Nobuyo Maeda, Dr. Frank Colon, Dr. Dazhi Wang, and Dr. Mike Schaller for their support and direction. Most of all, thanks to my parents for their support through the good times and the bad.

TABLE OF CONTENTS

LIST OF TABLES

Table

LIST OF FIGURES

CHAPTER I

Introduction

A. Organogenesis and Disease

During early development, organogenesis is an essential process describing the formation of the internal organs by the ectoderm, endoderm, and mesoderm. Our research is focused on three aspects of development: vasculature development, lung morphogenesis, and heart formation.

Vessel Development

Establishment of the vasculature during embryogenesis involves two distinctive processes: vasculogenesis and angiogenesis. Vasculogenesis occurs when new blood vessels are generated *de novo* from blood islands in a highly regulated manner, while angiogenesis involves the formation of new blood vessels from preexisting vasculature [1]. The generation of the primary capillary plexus by vasculogenesis follows four important steps: 1) the generation of angioblasts; 2) angioblast aggregation and assembly into tube-like forms; 3) the construction of vessel lumens; and 4) the establishment of vascular networks [2,3]. The primary vasculature undergoes continuous remodeling into mature circulatory vessels by angiogenesis [4,5].

Angiogenesis is not only a required event during embryogenesis for the establishment of blood vessel networks and the circulatory system, but is also found in many pathological events in adults, such as rheumatoid arthritis, psoriasis, tumorigenesis, and diabetic retinopathy [6]. Angiogenesis can be roughly divided into two phases: the activation phase and

the maturation phase. In the activation phase, endothelial cells (ECs) migrate into the

extracellular space by penetrating the peri-vascular basement membrane. They continue to

proliferate and form capillary sprouts and tubular structures. In the maturation phase, ECs

stop migration and proliferation to reconstitute a basement membrane and vessel wall by the

recruitment of smooth muscle cells. During this highly regulated process, a balance between

pro- and anti-angiogenic factors regulates the sequential steps of angiogenesis. Several

growth factors are considered to be pro-angiogenic in this process, including basic fibroblast

growth factor (FGF), platelet-derived growth factor (PDGF), vascular endothelial growth

factor (VEGF), and transforming growth factor beta 1 (TGF-β1). Since ECs are essential

components of angiogenesis, the abilities of these growth factors to stimulate angiogenesis

are tightly associated with their effects on ECs. For example, VEGF-C is able to promote the

migration and proliferation of ECs *in vitro* and *in vivo* [7]. To illustrate the regulation of

individual growth factor pathways and the cooperation among these angiogenic factors in

angiogenesis is an area of study with much to be learned.

Lung Morphogenesis

Normal embryonic development of lung is essential to initiate and maintain the

oxygen exchange after birth. In mouse, lung formation initiates at embryonic day 9.5 (E9.5)

as a pair of primary buds that are formed with foregut originated endoderm evaginated from

the laryngotracheal groove into the surrounding splanchnic mesenchyme[8]. Early lung

development can be divided into four stages. First, the bronchial and respiratory bronchiole

tree is formed during the pseudoglandular stage (E9.5- E16.6) [9]. Second, at the canalicular

stage (E16.6- E17.4), the distal epithelium and mesenchyme undergo extensive branching

into terminal sacs adjacent to the mesoderm-derived capillaries. Third, terminal sacs and

vasculature are further developed along with the maturation of alveolar epithelial type I and II cells during the terminal sac stage [E17.5 to postnatal day 5 (P5)]. Lastly, the alveolar stage (P5 to P30) is characterized by differentiation of the terminal respiratory sacs into alveolar ducts and sacs.

The mature respiratory system is composed of different types of epithelial cells. The location along the proximal to distal airway determines the type of epithelial cells [9]. The larynx is lined with squamous epithelial cells. The upper airways are characterized by a mixture of ciliated columnar and mucus-secreting goblet cells with clusters of pulmonary neuroendocrine cells (PNECs) [10]. The primary bronchioles contain clara cells, which are important for detoxifying harmful substances [11]. The terminal alveolar sacs are composed of two types of epithelial cells. Type I epithelial cells enable gas exchange with the circulation by forming tight junctions with the pulmonary endothelial cells. Type II epithelial cells secrete surfactant proteins, which are essential to reduce surface tension of alveoli and facilitate their expansion [12,13].

Many growth factor pathways are involved in lung branching morphogenesis and epithelial cell differentiation. For example, genetic deletion of fibroblast growth factor 10 (*Fgf10*) in the lung mesenchyme or FGF10 receptor (*Fgfr2IIIb*) in the epithelium lead to severe pulmonary agenesis, which indicates the essential role of the FGF pathway in early lung morphogenesis [14,15]. Another important growth factor is sonic hedgehog (SHH). Several human congenital pulmonary defects have been related to abnormalities in the SHH signaling [16-19]. The *Shh* deficient lungs display a hypoplastic phenotype, missing distal lung tissues, and delaying type II epithelial cell differentiation [20-22].

Cardiac Development

Congenital heart diseases are among the most common human birth defects, and occur in approximately 1% of the newborn population [23]. Two major forms of these malformations are cardiac septation defects and valvular anomalies, which are related to problems in cardiac cushion formation and valve development. At E8.0, the mouse heart has a tubular structure formed by a myocardial outer layer and an endocardial inner layer [24-26]. The linear heart tube undergoes elongation and looping to generate these major components from anterior to posterior, including outflow tract (OFT), primitive ventricle, atrioventricular canal (AVC), atria and inflow tract [26,27]. Following the looping of heart, ECs in the AVC and OFT start an epithelial-to-mesenchymal transformation (EMT) to form the AVC cushions located between the future atria and ventricle around E9.5, and to contribute to the endocardial ridges at the OFT slightly later. The OFT is closed to separate the aorta from the pulmonary trunk by the fusion of the endocardial ridges. These cushion formations result in left to right separation of the heart [28].

Another important event for heart formation is valvulogenesis. Cardiac valves start to develop along with the endocardial cushion formation at the AVC and OFT region during the looping stage at E9.5 [29]. Within the endocardial cushions undifferentiated heart valve progenitor cells first undergo proliferation followed by the remodeling stage, including decreased proliferation and production of extracellular matrix layers abundant in collagen, elastin and proteoglycan. At the end, endocardial ridges contribute to the semilunar valves located in the aorta and pulmonary artery, while the leaflets of the mitral and tricuspid valves are derived from the AVC cushion and direct the blood flow from atria to ventricles [29-31].

Multiple growth factor pathways are involved in normal heart formation. The lack of FGF10 causes defects in the positioning of heart in the thoracic cavity, while the loss of *Fgfr2IIIb* leads to malformations in the OFT septation and ventricular morphogenetic abnormalities [32]. The ablation of either one of two members of the FGF family, *Fgf8* and *Fgf15*, results in abnormalities in OFT and the right ventricle during early heart development [33,34]. Heparin-binding EGF-like growth factor (HB-EGF) is essential for cardiac valve formation and normal function [35]. The cardiac defects of *Pdgfb* null mice induce dilated ventricular chambers, reduced ventricular wall thickness, myocardial hypertrabeculation and septal malformations [36-39].
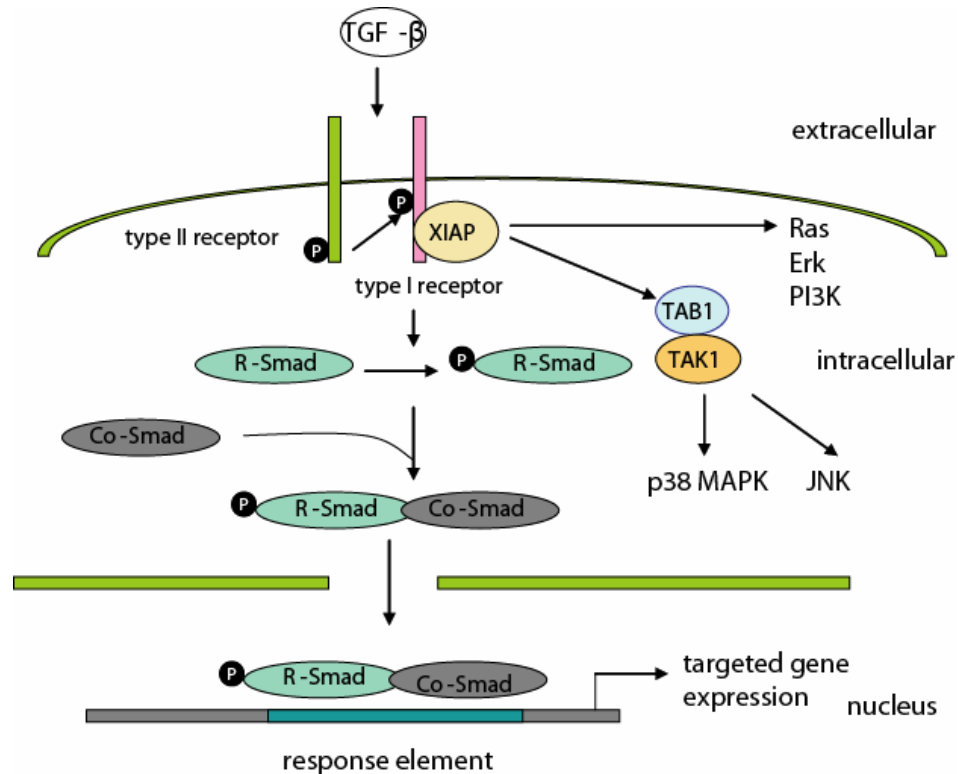
B. TGF-β superfamily

FIG. 1.1. TGF-β pathway components and its Smad-dependent and independent signaling.

The bone morphogenetic protein (BMP) family belongs to the TGF-β superfamily, which is composed of three other major sub-families: the Mullerian inhibitory substance

(MIS) family, the inhibin/activin family, and the TGF- β family [40,41]. An overall brief introduction of TGF-β signaling is described below as the BMP signal pathways share many similarities with the rest of the members.

TGF-β ligands

TGF-β superfamily ligands are synthesized as large precursor proteins which are proteolytically cleaved at the amino-terminal (N-terminal) and the mature carboxy-terminal (C-terminal) region are secreted into extracellular matrix [41-44]. The active C-terminal domain contains a "cysteine knot" folding motif formed by six intra-strand disulfide bonds [45-50]. Except for growth and differentiation factor 3 (GDF3) and GDF9 [51], TGF-β superfamily members possess the conserved seventh cysteine residue that can covalently bind to extracellular domains of their cell surface receptors [50,52,53].

TGF-β receptors

Receptors for TGF-β superfamily members are formed with an extracellular ligand-binding domain, a single trans-membrane, and an intracellular serine-threonine kinase domain [54-57]. Receptors are divided into two groups, types I and II receptors. Only type I receptors have a glycine-serine rich juxta-membrane domain (the GS box), which is essential for their activation [58]. Seven different type I receptors have been identified, including activin receptor-like kinase (Alk) 1 to 7 [59,60]. Five total type II receptors contain TGF-β receptor II (TGF-βRII), BMPRII, Activin type II A receptor (ActRIIA), ActRIIB, and MISRII [55,57,61,62].

BMP and activin membrane bound inhibitor (BAMBI) is a pseudoreceptor for the TGF-β pathway. [63] This protein has the extracellular ligand-binding and trans-membrane domains that resemble type I receptors, but it lacks the intercellular kinase activity. Due to its special structure, BAMBI is able to compete with type I receptors for ligand interaction

and block the downstream signaling of the TGF-β family [63,64]. BAMBI is coexpressed with BMP4 during development [63-65] and its expression is induced by TGF-β and BMP signaling, resulting in negative-feedback regulation [66,67].

Structure and function of Smads

Upon ligand binding, type I TGF-β receptors are trans-phosphorylated by the constitutively phosphorylated type II receptor [58]. The activated type I receptor phosphorylates receptor-regulated Smads (R-Smads), which in turn bind to the common partner Smad (Co-Smad) [68,69]. In vertebrates, Smad was named by combining *Drosophila mother against decapentaplegic proteins (Mad)* and the related *C. elegans Sma* [70]. These heteromeric complexes translocate to the nucleus and regulate the transcription of target genes by interacting with other transcription factors [68,71]. In mammalians, Smads can be divided into three functional groups: the R-Smads (Smad1, Smad2, Smad3, Smad5, and Smad8), Co-Smad (Smad 4), and Inhibitory Smads (I-Smads, Smad6 and Smad7) [72].
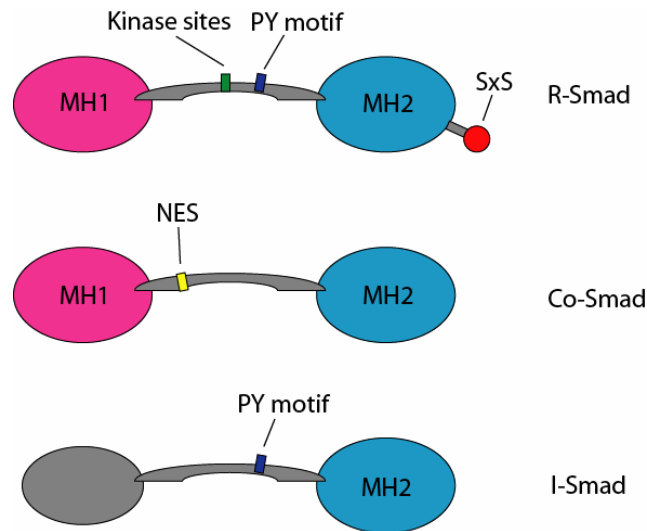
Fig. 1.2. Difference in protein structures of R-Smads, Co-Smads, and I-Smads. MH1: Mad Homology 1; PY motif: PXXY site, which binds to Smurfs; SxS: phosphorylation site for type I receptors; NES: nucleus export signal.

Smad proteins consist of two conserved globular domains: the N-terminal Mad Homology1 (MH1) domain and C-terminal MH2 domain, which are connected by a linker region [73,74]. The MH1 domain is only found in R-Smads and Smad4 but not I-Smads, and the MH2 domain is shared in all Smads [75]. The featured structures and functions of each domain are described as follows. First, the MH1 domain contains a β-hairpin structure, which is important for its DNA-binding activity [76]. Second, in the linker region, R-Smads have multiple phosphorylation sites for Mitogen Activated Protein Kinases (MAPKs) [70,77], Ca^{++}- and Calmodulin-dependent kinase II (Cam Kinase II) [78], Cyclin-dependent kinase (CDKs) [79], and G protein-coupled Receptor Kinase 2 (GRK-2) [80]. These phosphorylation events inhibit the functions of R-Smads in transducing TGF-β signaling [78,80-82]. Both R-Smads and I-Smads have a PY motif (PPXY sequence) recognized by the E3 ubiquitin ligases, Smad ubiquitin regulatory factor 1 (Smurf1) and Smurf2, leading to the degradation of R-Smads [83-85] or TGF-β receptors [86,87], respectively. A functional leucine-rich nuclear export signal (NES) is only found in the linker region of Smad4 and is important for exporting Smad4 from nucleus to cytoplasm under unstimulated conditions [88]. Finally, the conserved MH2 domain mediates multiple protein-protein interactions, including the dimerization of R- and Co-Smads [89,90], the interaction between I-Smads and type I receptors [91,92], and the binding of R- and Co-Smads with transcriptional coactivators such as p300 and the cAMP-response element-binding protein (CREB) binding protein (CBP) [93-96]. R-Smads have an additional Ser-X-Ser motif at the C-terminal that is phosphorylated by activated type I receptors and this modification is required for downstream signaling [69,97-99].

Transcriptional activity of Smads

R-Smads and Co-Smads complexes bind to the Smad-binding element (SBE) on the promoter region which transcriptionally regulates the expression level of the TGF-β downstream targets. Currently, the known SBEs include: 1) CAGA motif (CAGACA), which is found in the promoters of many TGF-β and BMP target genes [75,100-104]; 2) GTCT motif (GTCTAGAC) [104]; and 3) GCCG motif ($GCCG_nCGC$) [66,105,106]. The low affinity of Smad proteins for the SBE motifs does not secure the interaction of a Smad complex to one SBE site *in vivo* [103]. In *in vitro* assays, this problem can be overcomed by using concatemers with multiple SBEs to increase the binding affinity for transcriptional activation [104]. Since the promoters of Smad targets contain fewer repeats of SBEs *in vivo*, the high affinity of the Smad complex to DNA is achieved by cooperating with DNA-binding cofactors [107]. The different combination of Smad partners in various tissues and cell types can also help to determine the activation or repression of the transcription of specific genes. One example of Smad-binding co-transcription factors is the forkhead family protein, FoxH1. The interaction between FoxH1 with Smad2/Smad4 complex is essential for the binding of the complex to the *Mix2* promoter region, which leads to transcriptional activation of this promoter [108,109]

Smad-independent signaling

In addition to the Smad-dependent signaling pathway, the TGF-β-activated kinase 1 (TAK1) pathway is one of the Smad-independent signal pathways that transduce TGF-β downstream effects [110]. Upon the binding of TGF-β ligands to their receptors, TAK1 activity is stimulated through TAK1-binding protein (TAB1) and X-chromosome-linked inhibitor of apoptosis (XIAP), an E3 ubiquitin ligase [111]. TAK1 is reported to activate the p38 MAPK and c-Jun N-terminal kinase (JNK), which mediates the apoptotic effect induced by TGF-β

9

signaling [112-115]. TGF-β pathway can also interact with Ras , Erk and the phosphatidylinositol 3-kinase (PI3K) signaling and this crosstalk is important for TGF-β induced apoptosis, proliferation, and differentiation [116,117].

Different functions of TGF-β sub-families

Each subfamily of the TGF-β superfamily has its distinctive function in development. MIS functions as an important inducer for regression of the embryonic Mullerian duct in males [118]. The inhibins and activins are well known by their ability to regulate biosynthesis and secretion of follicle-stimulating hormone, a key hormone in the regulation of follicle release from the ovaries [119-121]. The TGF-β sub-family consists of 3 isoforms: TGF-β1, TGF-β2, and TGF-β3 [41], which regulate multiple events during embryonic development, including yolk sac vasculogenesis, haematopoiesis, cardiac development, and lung morphogenesis [122-124]. BMPs were originally found to induce ectopic bone formation when implanted into muscle [125]. Later studies connected BMPs to other processes in development, such as anterior-posterior axis formation, neurogenesis, and gonadogenesis [126-128]. The contribution of BMPs to vessel, lung, and heart developments is described below.

C. The BMP signal pathway

Similar to the rest of TGF-β members, BMPs are synthesized as large precursor proteins, which are proteolytically cleaved at an Arg-X-X-Arg site located at the N-terminus, and then the mature C-terminal region is secreted into the extracellular matrix [44]. Over thirty members of the BMP family have been identified from different species [126,129]. In mammals, the BMP family is composed of the BMP group (BMP2 to BMP17) and the GDF group (GDF1, 3, 5, 8, 9, 10) [130]. For BMP signaling, there are currently four major BMP type I receptors: Alk1, Alk2, Alk3 (BMP type IA receptor, BMPR-IA), and Alk6 (BMPR-IB); and

three type II receptors: BMP RII, Activin type II A receptor (ActR-IIA) and ActR-IIB

[60,131,132 133]. The R-Smads for BMP downstream signaling are Smad1, Smad5, and Smad8

[134]. A list of BMP direct target genes, which mediate BMP-dependent functions in different

cells and tissues have previously been identified, including *Xvent2, Xvent2B, msx1, msx2,*

Id1, Id2, Id3, GATA2, Dlx5, Tob, and *FGFR2* [106,135-142].

The BMP pathway can also activate both Smad-dependent and independent signals.

There are two forms of type I and type II receptor complexs on the cell surface: One is the

preformed receptor complex (PFC) and the other is BMP-induced signaling complex (BISC).

The stimulation of PFC by BMP ligands initiates the activation of the Smad signaling,

whereas ligand-induced complex, BISC, directs signals through the Smad-independent, p38

MAPK-dependent pathway, which results in the induction of alkaline phosphatase [143].

BMP pathway in angiogeneisis

BMPs have important but incompletely understood effects on angiogenesis by

affecting EC differentiation, migration and proliferation. BMP4 induces EC differentiation of

mouse embryonic stem cells, and this induction is blocked by the expression of a dominant

negative BMP receptor [144,145]. In developing *Xenopus* embryos, progenitor cells in dorsal

and ventral marginal zones fail to differentiate into ECs in the ventral blood island region

when BMP signaling is blocked by injection of RNA coding for a dominant negative,

truncated form of the BMP type I receptor [146]. Both BMP2 and BMP4 stimulate EC

migration and tube formation activity, which contribute to their ability to promote

neovascularization in tumors[147,148]. BMP6 is a potent agonist for EC migration and tube

formation *in vitro* [149]. On the other hand, the transcorneal injection of BMP4 in rats

promotes apoptosis of capillary ECs [150], suggesting that BMP4 contributes to EC apoptosis

during rat papillary membrane regression. Taken together, these studies demonstrate an important yet complex role for BMPs in angiogenesis.

BMP pathway in lung morphogenesis

Several BMPs and their receptors have been found to be expressed during lung development. During the pseudoglandular and canalicular stages, *Bmp4* is expressed in both the distal tips of the epithelium and in the mesenchyme adjacent to the more proximal developing airways. *Bmp4* expression is downregulated in the epithelium of the terminal sacs but remains in the capillary endothelium prior to birth [151]. On the other hand, *Bmp5* and *Bmp7* expression predominantly exist in the mesenchyme and endoderm, respectively[152,153]. Three type I receptors mediating BMP signaling are also expressed in the embryonic lung. Alk2 is found in mesenchyme specifically, while Alk3 and Alk6 are localized in both the epithelial and mesenchymal populations[154,155].

The functional importance of BMPs in lung morphogenesis has been supported by transgenic and knock-out studies of BMP ligands and their receptors. Most lines of evidence suggest that BMP signaling positively regulates the proliferation of the distal epithelium. BMP4 promotes branching morphogenesis of the whole embryonic lung culture [156], while inhibition of BMP signaling by overexpression of BMP4 antagonist Noggin or Gremlin results in reduction in lung size and an expansion of proximal bronchial epithelium to the periphery[157,158]. Conditional deletion of Alk3 in lung epithelium leads to a decline in proliferation, an increase in apoptosis, and defects in morphogenesis[159]. However, BMP4 transgenic lungs are smaller in size, have fewer and cystic epithelial terminal sacs, and have decreased cell proliferation[153]. This finding indicates that BMP4 activity at very high levels may activate different pathways, which elicit negative responses to proliferation. Taken

12

together, BMP signals play an essential role in lung branching morphogenesis and homeogenesis.

BMP signals in heart development

BMP signals are involved at different stages of cardiac development, including the initial stage of cardiac myogenesis and the later stage of endocardial cushion development and cardiac valve maturation[160-163]. BMP ligands are present in heart during early embryonic development. During E9.5 and E10.5, *Bmp2* is expressed in the AVC region, while *Bmp*4 expression is located at the OFT area and endocardial cushion[164]. The dynamic *Bmp6* expression starts in the endocardium at E9.5, then in the AVC cushions and in the myocardial layer of the left part of the OFT at E10.5, and is localized to the mesenchyme of the OFT at E12.5[163,165]. The distribution of *Bmp7* transcripts is ubiquitous throughout the myocardium from E8.5 to E15.5[166,167]. Receptors transducing BMP signals, including Alk2, Alk3 and BMPRII are also ubiquitously expressed in the developing heart [154,155,168,169]. Some of the BMP antagonists are also present at the heart forming region. Noggin mRNA is detected in the heart forming area as early as E7.5[170] and its expression remains in the ventricles and the myocardium of the AVC and OFT between E11.5 to E12.5[171].

Conditional knock-down of *Bmp2* in the heart leads to reduced mesenchymal components inside the AV cushions[172,173], while BMP4 deficiency results in malformations in proximal OFT septation and decreased proliferation of OFT mesenchyme[174]. Individual disruption of *Bmp5*, *Bmp6*, and *Bmp*7 expression does not show obvious cardiac abnormalities due to functional redundancy [175-177]. The *Bmp5* and *Bmp7* double knockout mouse has severe defects in cushion formation [167], while *Bmp6* and *Bmp7* double deletion also results in malformation in cardiac cushion[163]. Cardiac deletion of Alk3 results in a

hypoplastic AV cushion due to impaired epithelium-mesenchymal-transformation (EMT)
[178,179]. Homozygous *BmprII*[ΔE2/ΔE2] mice, which express a mutant BMPRII lacking the ligand-binding domain, show malformed septation of the conotruncus and absence of the semilunar valves [162]. Conditional *Noggin-/-* mice display thicken ventricular walls and enlarged AVC and OFT regions a result of elevated cell proliferation and EMT activity [171]. Based on these studies, the BMP pathway is essential to the formation of cardiac cushions and valves during heart development.

D. Modulation of BMP signaling

The modulation of BMP signals takes place in three locations: the intracellular area, the plasma membrane, and the extracellular matrix. Our research has been focused on studying extracellular antagonists, which bind to BMPs and interfere with their interaction with cell-surface receptors. At least seven antagonists have been found in vertebrates, including Noggin, Chordin, Chordin *like*, Follistatin, FSRP, the DAN/Cerberus protein family, and sclerostin[127]. These antagonists help to maintain proper levels of BMP signaling and play essential roles in organogenesis. For example, Noggin and Chordin are important in developmental events, including neurogenesis and pharyngeal development [180-182].

Bmper protein structure and expression

Previous studies in our lab found that *Bmper* mRNA is enriched in the fetal liver kinase (Flk1)-positive population in differentiated mouse ES cells[144]. Bmper has a 39-amino-acid signal peptide at the amino terminus, five cysteine-rich (CR) von Willebrand C-like domains, one von Willebrand D domain, and a carboxy-terminal Trypsin Inhibitor-like cysteine rich domain (Figure 1.3) [144]. Bmper protein shares 30% overall identity (44%

14

similarity) with its *Drosophila* homolog, crossveinless2 (cv2)[183]. The presence of CR

domains indicates Bmper as a BMP binding protein like chordin. The expression profile of

 Bmper in both adult and embryonic mice was examined. *Bmper* mRNA expression was

FIG. 1.3. Structures of CV2, and Chordin in comparison to that of Bmper. Total amino acid number of each protein is indicated at C-terminal end. CR: cysteine-rich; VWD: von Willebrand D domain; TI: Trypsin Inhibitor-like.

highest in heart, lung and skin in adults[144,183]. The expression pattern of *BMPER* in

developing embryos is highly dynamic. Bmper is first expressed in the proximal part of the

embryonic region during mid-gastrulation [183]. At E10.5, *in situ* hybridization reveals Bmper

expression in two important early angiogenesis regions, yolk sac where BMP2, BMP4 and

BMP6 activity has been found[184], and the aorto-gonadal-mesonephric (AGM) region, which

contains EC cell precursors and where a high level of BMP4 is found[185]. At E14.5, *Bmper*

transcripts are found in lung mesenchymal tissues and cartilage of the developing skeleton

[183]. Based on its structure and expression pattern, Bmper may play an important role in

organogenesis where BMP signals are involved.

Anti- and pro-BMP activity of Bmper

The effect of Bmper on the BMP pathway is closely related to its ability to bind to

BMP2, BMP4, and BMP6 [144]. Studies show evidence supporting both anti- and pro-BMP

activity for Bmper. For example, ectopic expression of Bmper dorsalizes *Xenopus*

embryos[144,186]. Bmper inhibits BMP-induced osteoblast and chondrocyte differentiation *in*

vitro [187]. Bmper inhibits BMP4-stimulated luciferase activity in the Smad-dependent reporter

assay and blocks BMP4-induced EC differentiation from ES cells [144]. On the contrary, other

studies indicate that Bmper has pro-BMP effects. Bmper activity is important for the

formation of cross-veins in fly wing [188,189,190,191]. Bmper enhances phosphorylation of Smad1

stimulated by BMP4 in COS7 cells [192]. Injection of both Bmper and BMP4 RNA in animal

caps synergistically induces the expression of the mesoderm marker, *Xbra* [186]. A hypothesis

proposed by Hammerschmidt's group suggests that Bmper activity on BMP signaling is

dependent on its proteolytic processing; uncleaved Bmper is an anti-BMP regulator, whereas

cleaved Bmper plays a pro-BMP role because only uncleaved Bmper can bind to the

extracellular matrix through heparin [193].
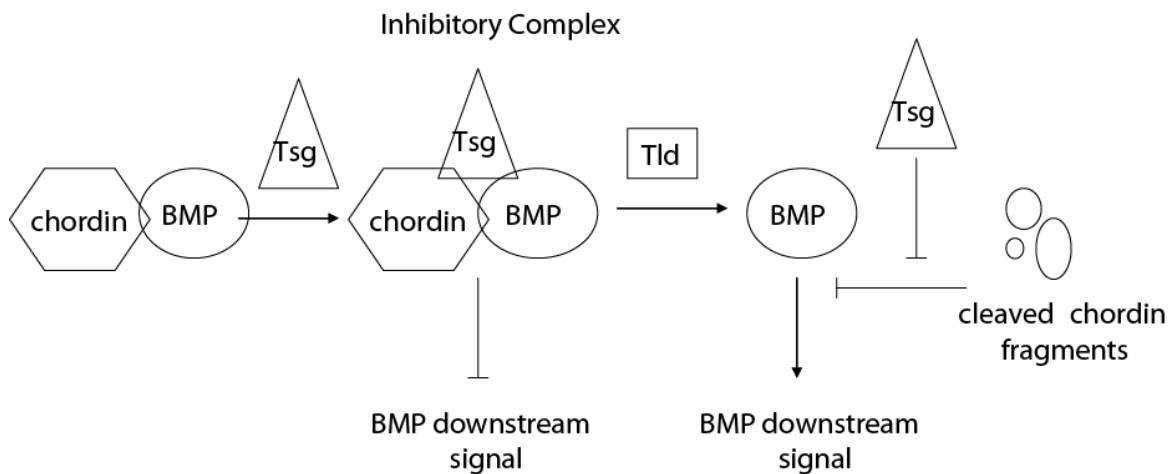
FIG. 1.4. The interaction of twisted gastrulation, chordin and BMP. Tsg stabilizes the chordin and BMP complex to inhibit BMP signals. In the presence of Tolloid, Tsg facilitates the cleavage of chordin and blocks the binding of cleaved fragments to BMP. This leads to an activated BMP pathway.

This proteolysis-dependent pro-BMP activity is also observed on two BMP

antagonists, Chordin and Twisted gastrulation (Tsg) (Figure 1.4). First, full length chordin

directly binds to BMP through its four CR domains [194]. This binding is stabilized by Tsg and

a trimolecular BMP–Tsg–Chordin complex is formed [195,196]. This complex sequesters BMP

from its cell surface receptors, which results in inhibition of BMP signaling[196-200].

Tolloid/Xolloid proteases cleave chordin and release BMP, which in turn activates

downstream signaling[201-204]. This proteolytic cleavage of Chordin by Tolloid/Xolloid is

facilitated by Tsg [198,199,204]. Cleaved Chordin fragments containing CR domains are still able

to bind and inhibit BMP and this remaining inhibitory activity is also blocked by Tsg

[194,195,199,205]. Thus, the presence of Tolloid/Xolloid can determine the anti- or pro-BMP

activity of Chordin and Tsg. Based on this model, the different action of Bmper on BMP

signaling may also be affected by the expression of an unidentified protease, which cleaves

Bmper proteins.

Despite structural similarity of Bmper and Chordin, there are two important

differences between these two BMP extracellular regulators. First, Bmper is expressed in

areas where high BMP activity has been found and its expression is BMP signaling

dependent [184,193]. On the other hand, *Chordin* transcripts, are found in regions with low BMP

activity and its expression is negatively regulated by BMP signaling [181,206]. Second, the

binding of Bmper to BMPs does not block their interaction to cell surface receptors [193], while

the Chordin and BMPs complex cannot bind to the receptors [194]. This suggests that Bmper

may have its own regulatory mechanism different from the previously described mode for

Chordin and Tsg.

CHAPTER II

Gene Expression Profiles Identify a Role for Cyclooxygenase 2–dependent Prostanoid Generation in BMP6-induced Angiogenic Responses

Rongqin Ren*, Peter C. Charles*¶, Chunlian Zhang*, Yaxu Wu*, Hong Wang*, and Cam Patterson*¶

Carolina Cardiovascular Biology Center* and Department of Medicine¶, University of North Carolina, Chapel Hill, NC

Running title: Cox2 in BMP-dependent angiogenesis

Authors' contributions:

Designed research: RR, HW, CP

Performed research: RR, CZ, YW, HW

Analyzed data: RR, PCC, CP

Wrote paper: RR, CP

Scientific heading: Hemostasis, thrombosis, and vascular biology

Address correspondence and inquiries to:

Cam Patterson, M.D.

Director, Division of Cardiology and Carolina Cardiovascular Biology Center

8200 Medical Biomolecular Research Building

Chapel Hill, NC 27599-7126

Telephone: 919-843-6477

Fax: 919-843-4585

e-mail: cpatters@med.unc.edu

Abstract

The bone morphogenetic protein (BMP) family of proteins participates in regulation of angiogenesis in physiological and pathological conditions. To investigate the molecular mechanisms that contribute to BMP-dependent angiogenic signaling, we performed gene expression profiling of BMP6-treated mouse endothelial cells. We detected 77 mRNAs that were differentially regulated after BMP6 stimulation. Of these, cyclooxygenase 2 (Cox2) was among the most highly upregulated by BMP stimulation, suggesting a role for Cox2 as a downstream regulator of BMP-induced angiogenesis. Upregulation of Cox2 by BMP6 was detected at both mRNA and protein levels in endothelial cells, and BMP6 increased production of prostaglandins in a Cox2-dependent fashion. BMP6 upregulated Cox2 at the transcriptional level through upstream SMAD-binding sites in the Cox2 promoter. Pharmacologic inhibition of Cox2, but not Cox1, blocked BMP6-induced endothelial cell proliferation, migration and network assembly. BMP6-dependent microvessel outgrowth was markedly attenuated in aortic rings from Cox2–/– mice or after pharmacologic inhibition of Cox2 in aortas from wild-type mice. These results support a necessary role for Cox2 in mediating proangiogenic activities of BMP6. These data indicate that Cox2 may serve as a unifying component downstream of disparate pathways to modulate angiogenic responses in diseases in which neovascularization plays an underlying pathophysiologic role.

Introduction

During the tightly regulated process of angiogenesis, a balance between pro- and anti-angiogenic factors results in the sequential steps required for new blood vessel formation. Several mitogens are considered pro-angiogenic, including members of the basic fibroblast growth factor, platelet derived growth factor, vascular endothelial growth factor, and transforming growth factor beta families. Since endothelial cells (ECs) are essential components of angiogenesis, the abilities of these growth factors to stimulate angiogenesis are tightly associated with their effects on ECs.

BMPs belong to the TGF-β superfamily, and over thirty members of the BMP family have been identified from different species [126,129]. BMPs are synthesized as precursor proteins, then are proteolytically cleaved at the N-terminus and secreted into the extracellular matrix. BMPs dimerize through disulfide bonds and initiate signaling by binding cooperatively to both type I and type II membrane-bound serine/threonine kinase receptors[207,208]. The constitutively active type II receptors trans-phosphorylate type I receptors, which then activate intracellular substrates by phosphorylation, and thus determine the specificity of intracellular signals. In vertebrates, small mothers against decapentaplegic proteins (Smads) are downstream signaling molecules for the receptors. Receptor-regulated Smads (R-Smads) bind to the common partner Smad (Smad4), and these heteromeric complexes translocate to the nucleus and regulate the transcription of target genes by interacting with other transcription factors at *cis*-acting elements defined by the sequence CAGAC[A] [209,210].

BMPs have important but incompletely understood effects on angiogenesis by affecting EC differentiation, migration and proliferation. BMP6 is a potent agonist for EC

migration and tube formation *in vitro* [149]. BMP2 enhances neovascularization in tumors and this activity may involve the stimulation of EC proliferation, migration, and tube formation by BMP2 [147]. BMP4 induces EC differentiation of mouse embryonic stem cells, and this induction is blocked by the expression of a dominant negative BMP receptor [144,145]. On the other hand, the transcorneal injection of BMP4 in rats promotes apoptosis of capillary ECs [150], suggesting that BMP4 contributes to EC apoptosis during rat papillary membrane regression. In developing *Xenopus* embryos, progenitor cells in dorsal and ventral marginal zones fail to differentiate into ECs in the ventral blood island region when BMP signaling is blocked by injection of RNA coding for a dominant negative, truncated form of the BMP type I receptor [146]. Taken together, these studies demonstrate an important yet complex role for BMPs in angiogenesis.

Though many lines of evidence indicate that BMPs are important in angiogenesis, there are still unresolved issues, in particular the delineation of downstream effectors that respond to BMP signaling during angiogenesis. This study has taken advantage of microarray technology to analyze the BMP6-mediated signaling network in ECs. Among the list of differentially expressed genes, we have selected Cox2 for further analysis based on the sustained change in transcription levels. Cox2, which catalyses the conversion of arachidonic acid to prostaglandins (PGs), is linked to several physiological and pathogenetic pathways that participate in angiogenesis, inflammation and invasiveness [211]. The increased risk of heart attack and stroke among patients taking Cox2 inhibitors [212-216] indicates a complicated role for Cox2 activity in maintaining vascular homeostasis. Our expression and EC functional studies indicate that Cox2 is an essential downstream component mediating

BMP6-dependent EC activation, which could be one of the mechanisms underlying its

cardioprotective effects.

Materials and methods

Plasmids and reagents

Recombinant human BMP6 protein was obtained from R&D systems. A selective Cox2 inhibitor, NS398, the Cox1 inhibitor, SC560, and immunoassay kits for PGE2 and 6-keto-PGF1α were obtained from Cayman (Ann Arbor, MI). Cox2 promoter regions from −8653 to +53 bp and −7444 to +53 bp were inserted into pGL3-Basic vector (Promega, Madison, WI). Two similar Cox2 reporter constructs (−1500 to +1 bp and −371 to +70 bp) were kindly provided by Dr. Curtis C. Harris from National Institutes of Health [217] and Dr. Carol C. Pilbeam from University of Connecticut [218].

Microarray analysis

Mouse intraembryonic endothelial cells (MECs) were cultured as previously described 9. Total RNA was extracted from MECs treated with BMP6 for 4, 12, or 24h, or from mock-treated controls. Universal mouse reference RNA was used as a reference [219], and was labeled with Cy3 florescence dye using the Fluorescent Linear Amplification Kit (Agilent Technologies, CA). Samples of MEC RNA were labeled with Cy5, and equimolar mixtures of the two florescence dye-labeled probes were hybridized to Agilent 22k Mouse Development Oligo Microarrays (G4120A, Agilent Technologies). Microarrays were scanned with a GenePix 4000B scanner and images were quantified with GenePix Pro 5.0 Software (Molecular Devices, Sunnyvale, CA). Each experimental group included independent triplicate biological replications. Raw expression data were normalized via a modified quantiles local algorithm (X. He and C. Patterson, manuscript in preparation). Differentially expressed genes were identified with a two-tailed type 2 Student t-test. Cluster analysis and visualization using Java-TreeView were accomplished as previously described

23

[220]. Selected genes were validated by RT-PCR. The complete, MIAME-compliant dataset is available at the Gene Expression Omnibus (http://www.ncbi.nlm.nih.gov/projects/geo/, reference # GSE4909).

Reporter gene analysis and gel mobility shift assays

Luciferase reporter assays were performed as previously described [144]. Electrophoretic gel mobility assays (EMSA) were performed essentially as described [134] with 3 μg of nuclear extract. DNA and protein complexes were resolved on a non-denaturing 4% polyacrylamide gel and visualized by autoradiography. The probes used were –8147—AGG CAG ACA GAC AGA CAA CCA GAT AGA TA— –8119 (*sense*) and –8119— TCC GTC TGT CTG TCT GTT GGT CTA TCT AT— –8147 (*antisense*).

Cell proliferation, migration and tube formation assays

Cell proliferation assays were performed as described previously [221]. The migration assays were prepared using a 48-well chamber apparatus (NeuroProbe, Cabin John, MD). The lower chambers of the apparatus were filled with DMEM with or without BMP6 and then covered with the gelatin-coated filter and the upper chambers. Cell suspensions in DMEM with or without Cox inhibitors were then added to the upper chambers. After incubating for 6 h at 37°C, cells present on the lower surface were identified with the 10 X objective on a Nikon Eclipse TS100 inverted microscope. EC tube formation was analyzed with the Matrigel-based tube formation assay [149]. Chilled 24-well plates were coated with Matrigel (Becton Dickinson) that was polymerized at 37°C for 30 minutes. MECs were serum-starved overnight, trypsinized, and plated at equal numbers into each Matrigel-coated well. After 16 h of incubation in the absence or presence of BMP6 and/or Cox inhibitors, the formation of tubes was photographed. Images were processed with Adobe Photoshop® CS.

Mouse aortic ring angiogenesis assays

Mouse aortic ring assays were performed with modifications from a previously reported method [222]. Thoracic aortas were removed from 2 month old mice, aortic rings were sectioned and then embedded in rat tail collagen gel (1.5 mg/ml) prepared by mixing 7.5 volumes of 2 mg/ml collagen, 1 volume of 10X MEM, 1.5 volume of NaHCO3 (15.6mg/ml) and 0.1 volume of 1M NaOH. Each well containing the aortic rings was incubated in 250 μl of MCDB131 supplemented with 25 mM NaHCO3 and 1% mouse serum. Images of aortic rings were taken with an Olympus microscope at Day 6.

Results

Characterization of the BMP-responsive transcriptome in ECs

We utilized MECs to characterize BMP6-responsive transcriptional events in ECs for two reasons. First, MECs express all the components of the BMP signaling pathway from cell surface receptors to Smads (*data not shown*). Second, Id1, a well-characterized target of BMP6 signaling in ECs [149], is faithfully upregulated in MECs (Figure 2.1). To characterize the BMP6-dependent transcriptome in ECs, RNA samples extracted from MECs with or without BMP6 treatment for 4, 12, or 24 h were analyzed with microarrays. Differentially expressed genes were identified by Student's ttest ($p < 0.05$) and then filtered for fold change. As expected, Id1 was upregulated at each time point in this analysis, confirming the validity of our dataset and the sensitivity of this approach for identifying BMP-responsive genes (Table 2.2).

Out of 20,000 genes surveyed, a total of 37 genes were upregulated and 40 genes were downregulated by treatment with BMP-6 at any time point using relatively stringent criteria to reduce false-positive results (representative genes shown in Tables 2.1 and 2.2). Two groups of differentially expressed genes were identified by hierarchical clustering analysis (Figure 2.2). The first group comprised genes downregulated by BMP6, including two members of the metalloproteinase family (Adamts1 and Adamts5) that are known inhibitors of neovascularization [223]. The second group contains genes upregulated by BMP6. Wnt2, Cox2, Id1, two other members of the Id family (Id2 and 3), CD44, Tnfrsf12a (tumor necrosis factor receptor superfamily), Snail1 (a Wnt-regulated transcriptional factor) and Timp1 (an inhibitor of metalloproteinases) are present in this cluster. To establish the validity of the microarray dataset, we performed RT-PCR analysis for several selected genes,

confirming that Cox2, Wnt2, Timp1 and Adamts1 were indeed differentially regulated by BMP6 at the mRNA level (Figure 2.3*A*). In addition, the upregulation of Cox2 after BMP6 treatment was also demonstrated at the protein level by Western blotting (Figure 2.3*B*).

Enhanced production of prostanoids through the upregulation of Cox2 by BMP6

Because cyclooxygenases catalyze the formation of prostaglandins from arachidonic acid, we next investigated whether stimulation of ECs by BMP6 also leads to increased PG production by MECs. These experiments were performed in the presence of arachidonic acid concentrations that favored prostaglandin generation by Cox2 over Cox1 and measured the two functional important PGs in ECs, PGE2 and the dominant form PGI2 [224]. BMP6 potently increased generation of PGE2 and 6-keto-PGF1α (a stable metabolism of PGI2) in MEC, as determined by accumulation of these prostanoids in the culture media after BMP stimulation (Figure 2.4*A* and *B*). Generation of PGE2 and 6-keto-PGF1α was abolished by pretreatment with the Cox2 inhibitor NS398 but not the Cox1 inhibitor SC560, indicating their derivation via a Cox2-dependent mechanism.

Transcriptional activation of the Cox2 promoter by BMP6

Because Cox2 is primarily regulated at the transcriptional level by factors such as interleukin-1β [224,225] and tumor necrosis factor-α [226], we reasoned that the rapid upregulation of Cox2 mRNA by BMP6 might also occur at the transcriptional level. To investigate the mechanism of transactivation of the Cox2 promoter by BMP6, we tested four Cox2 promoter-luciferase reporter constructs containing various lengths of Cox2 promoter regions upstream of its transcription start site (Figure 2.5*A*). These constructs were transiently transfected into MECs, which were then treated with or without BMP6. Only the −8653 to +53 bp promoter construct, but not those containing smaller fragments of the Cox2 promoter,

could be stimulated by BMP6 (Figure 2.5*B*). In addition, we observed a 5 fold activation of this 8.7 kb reporter when Smad1 was co-transfected into MECs, which is consistent with previous observations that overexpressed Smad proteins can transactivate BMP target genes in a ligand-independent manner [227,228]. These data indicate that necessary BMP-responsive elements in the Cox2 promoter are located between base pairs –8653 and –7444.

Interestingly, this interval in the Cox2 promoter contains a tight cluster of putative Smad-binding elements (identified using the Vector NTI algorithm) between base pairs –8147 and –8119 (Figure 2.5*A*). To further characterize the BMP6-responsive element in the Cox2 promoter, we used this 29-bp sequence as a probe in gel shift assays after performing pilot experiments to exclude the possibility that other potential Smad-binding sites within the promoter had nuclear protein-binding activity. Using this 29-bp fragment as a probe, we found that extracts from MECs contained a DNA binding activity that migrates with slower mobility than the probe alone (Figure 2.5*C*). This binding was competed away by addition of unlabeled specific probe at 50-fold excess but not by 100-fold excess of unlabeled nonspecific competitor, indicating its specificity. To analyze whether this binding is related to Smad-binding activity, we tested a consensus Smad-binding element sequence in competition assays [229]. This sequence efficiently inhibited binding of the labeled probe to nuclear proteins, which strongly suggested that Smads are required nuclear proteins in the extract for binding to the 29-bp Cox2 element. Stimulation of MECs with BMP6 for 4 h retarded the mobility and enhanced the intensity of the DNA-protein interaction (Figure 2.5*D*), suggested that BMP6 remodels or post-translationally modifies the protein complex that binds to this element. In addition, the coexpression of Flag-tagged Smad1 and Smad4 caused an additional DNA-protein complex of slightly slower mobility. Known difficulties in

28

supershifting Smad proteins preclude definitive testing that the endogenous complexes contains proteins within this family, but our data are most consistent with a necessary role for Smad binding within the Cox2 promoter in mediating BMP6-dependent *trans*-activation.

Inhibition of Cox2 blocks BMP6-induced EC proliferation, migration and tube formation

To determine whether the upregulation of Cox2 plays a necessary intermediary role in BMP6-dependent endothelial functions, we examined whether changes in BMP6-mediated MEC proliferation and migration occur after inhibition of Cox2. At the concentrations used here, NS398 exerted specific inhibition of Cox2 over Cox1, as determined by measurement of PGE2 production (*data not shown*). In cell counting assays as an index of proliferation, BMP6 stimulated cell growth at both 48 and 72 h after treatment (Figure 2.6*A*). Inhibition of Cox2 blocked BMP6-dependent MEC proliferation almost totally, whereas a specific Cox1 inhibitor, SC560, had no effect. We next measured cell migration activity using two assays: wound healing and Boyden chambers. BMP6 potently enhanced migration through wells, as has been previously described [149], and the addition of NS398 prevented BMP6-stimulated migration whereas SC560 had no effect (Figure 2.6*B*). Similar results were observed in wound healing assays (*data not shown*). We also tested the role of BMP6-dependent Cox2 activation on EC tube formation using Matrigel tube formation assays. The addition of BMP6 alone increased the number of enclosing tubes by over 2-fold, and this increase could only be blocked by cotreatment with NS398, but not SC560 (Figures 2.6*C* and *D*). The results from these functional assays strongly support a model in which Cox2 is a necessary mediator of the effects of BMP6 on EC function.

Requirement of Cox2 activity in BMP6-induced microvessel outgrowth

To better understand the effect of Cox2 activity in BMP6-induced angiogenesis, mouse aortic ring assays were selected to mimic an *in vivo* environment [222]. Mouse thoracic aortas were sectioned, embedded in collagen gel, and incubated with or without BMP6 and/or Cox inhibitors. To minimize the background of microvessel outgrowth under control conditions, only 1% mouse serum was added to media. After a 6-day incubation, BMP6 treatment increased the total number of outgrowing microvessels from aortic rings (Figures 2.7*A* and *B*). Cotreatment with NS398 reduced BMP6-activated neovascular outgrowth to control levels, whereas SC560 had no effect. We also used genetic deletion of Cox2 to provide more definitive evidence of a role for endogenous Cox2 in mediating BMP6-dependent responses. Aortas from Cox2 –/– mice and Cox2 +/+ littermates were used in these experiments. The activation of microvessel outgrowth by BMP6 was abolished in aortas from Cox2 –/– mice (Figures 2.7*C* and *D*). Although Cox2 activity may not be necessary for all VEGF-mediated events [230], VEGF induces Cox2 expression in ECs [231] and this induction is required for VEGF-mediated angiogenesis [232]. Therefore we also tested the effects of Cox2 deletion on VEGF-induced neovascularization. The addition of recombinant VEGF (25 ng/ml) significantly increased microvessel outgrowth in WT aortas, but not in Cox2 –/– aortas (Figures 2.7*C* and *D*). These data indicate that BMP6 and VEGF signal pathways unexpectedly share common requisite downstream mediators in the regulation of angiogenesis.

Discussion

The BMP signaling pathway has an important but incompletely characterized role in mediating vascular development and angiogenesis. Mechanistically, little is known about downstream transcriptional targets of BMPs other than Id1 in EC [149]. In the present study, we have been able to generate a comprehensive list of BMP6 target genes in ECs using microarray technology. The accuracy of our dataset has been confirmed by both RT-PCR and western blotting (Figures 2.3*A* and *B* and *data not shown*). Three major clusters of BMP-responsive genes were identified based on their patterns of expression (Figure 2), suggesting that independent pathways for gene activation by BMPs exist in ECs. In this screen, we found angiogenesis-associated genes that participate in intracellular and extracellular signaling and matrix reorganization, indicating a coordinated program to allow vessel assembly and maturation, including Cox2, Wnt2, Timp1, Adamts1 and Adamts5. An independent microarray study in our laboratory also found that Wnt2 is enriched in flk1+ differentiated embryonic stem cells and that this Wnt signaling pathway plays a critical role in the regulation of angiogenesis [233]. The present studies indicate that BMP6 is likely to be upstream of Wnt2 expression in the cascade of blood vessel growth, an observation that will be helpful to establish network relationships of different signaling pathways in angiogenesis.

Our analyses indicate that Cox2 is indeed a bona fide transcriptional target of the BMP-responsive signaling pathway. Cox2 mediates the biosynthesis of PGs from arachidonic acid, and the expression of Cox2 is upregulated by cytokines, including VEGF and IL-1β [234]. Increased Cox2-dependent PG generation plays diverse roles in increasing cell proliferation [235], inhibiting apoptosis [236], and stimulating angiogenesis [237,238]. The present

results suggest that the role of Cox2 in angiogenesis in vivo may be due in part to its induction by BMPs acting on the vascular endothelium to alter prostanoid generation.

We have identified in these studies a heretofore-uncharacterized BMP-responsive enhancer located at –8147 bp upstream from the Cox2 transcription start site (Figure 2.5). A number of transcription factors and signaling events have been previously linked to Cox2 transcriptional activation; for example, VEGF induces Cox2 upregulation through p38 MAPK and JNK signaling pathways [232], and Wnt signaling increases Cox2 transcription via a β-catenin-dependent pathway that activates the Cox2 promoter through a Tcf-4-binding element [217]. In osteoblasts, BMP2 activates Cox2 transcription via a specific binding site on the Cox2 promoter for core-binding factor activity 1 (cbfa1) [218]; however, our data indicate that the induction of Cox2 by BMP6 follows different rules, at least in ECs, and these experiments provide the first link between Smad activation and Cox2 transcriptional regulation. Based on our analyses, we also predict the involvement of the EC-specific transcriptional factor GATA2 in BMP6-mediated Cox2 induction, since a GATA rich sequence is adjacent to the Smad-binding site (*data not shown*). Additional reporter studies are being performed to clarify the relationship among these angiogenic transcription factors in the regulation of Cox2 in ECs.

Results from *in vitro* EC function assays including proliferation, migration, and tube formation clearly show that Cox2 activity is required for BMP6-induced EC activation (Figure 2.6). In addition, pharmacological and genetic disruptions of Cox2 activity indicate that BMP6-activated microvessel outgrowth also requires Cox2 activity (Figure 2.7). At the same time, the inhibition of Cox1 does not attenuate angiogenesis stimulated by BMP6. Given the remarkable structural and kinetic similarity between these two enzymes, our

findings are consistent with other observations that Cox2, but not Cox1, plays an important role in mediating angiogenesis under both physiological and pathological situations [211,230]. Coupled with our own conclusions, this suggests that angiogenesis-promoting prostanoid generation in ECs must occur in a precise spatiotemporal fashion to activate the program of blood vessel growth. Remarkably, inhibition of Cox2 by NS398 reduces BMP6 mRNA and protein expression in bone cells [239]. This suggests that positive feedback loops may exist in the BMP6 and Cox2 pathway, and such an interaction could play an important role in amplifying the activation of ECs by BMP6. Taken together, these studies provide further support for the consideration of pharmacological Cox2-targeting strategies to modulate new vessel formation in diseases in which angiogenesis is a major component including cancer and cardiovascular disease.

Acknowledgements

Figure legends

FIG. 2.1. BMP6 induces the upregulation of Id1 in a time-dependent fashion. RT-PCR analysis of Id1 in MEC treated with or without BMP6. Total RNA was extracted from MECs collected at 4, 12, and 24 h after BMP6 treatment. GAPDH was used as a loading control.

FIG. 2.2. Hierarchical clustering of BMP6 target genes. Differentially expressed genes were selected with a p value ≤ 0.05 and ratio fold change $\geq \pm 1.5$, and were subjected to hierarchical cluster analysis. Median-centered clusters were viewed with JavaTreeView. Fold change relative to common reference is indicated by red (+1.5, full scale) and green (-1.5, full scale) intensity. (A) Global view of the clustered genes. (B) Detail of the clustered genes with selected genes labeled. Cluster 1 corresponds to genes in Table 1, and cluster 2 corresponds to genes in Table 2. The complete data set is accessible online through the UNC Microarray Database (http://genome.unc.edu).

FIG. 2.3. RT-PCR and Western blotting analysis of gene expression in BMP6-induced EC activation. (A) RT-PCR analysis of Wnt2, Cox2, Timp1 and Adamts1 expression using total RNA from MECs collected at 0, 4, 12, and 24 h after BMP6 treatment. GAPDH was used as a loading control. (B) Western blot analysis of Cox2 protein expression after BMP6 stimulation for the indicated times. β-actin was used as a loading control.

FIG. 2.4. Elevated levels of secreting prostaglandins derived from Cox2 after BMP6 stimulation. MECs were pretreated with NS398 (10 μM), SC560 (100 nM) or vehicle before BMP6 (100 ng/ml) treatment. Cox2-dependent prostanoid generation was determined by measurement of the major forms of PGs generated by ECs, PGE2 (A) and 6-keto-PGF1α (B) after 4 h of stimulation in the presence of exogenous arachidonic acid (2.5 μM). Data are expressed as mean ± SEM of 6 replicates.

FIG. 2.5. Activation of the Cox2 promoter by BMP signaling. (A) Depiction of 4 luciferase reporters of the Cox2 promoter, -8653 to +53 bp, -7444 to +53bp, -1500 to +1 bp, and −371 to +70 bp. Putative Smad-binding sites are denoted. (B) MECs were transfected with luciferase reporter plasmids carrying different lengths of the Cox2 promoter in the presence or absence of BMP6 treatment or the cotransfection of an active Smad1 expression vector. After 48 h, cells were lysed to measure luciferase activity. Luciferase activity was normalized using Renilla luciferase activity. Data shown are the mean ± S.D. of triplicates. (C) An end-labeled fragment containing the 29-bp Smad-responsive region was incubated with nuclear extracts from MECs and with different non-labeled competitors. Complexes were resolved on a nondenaturing 4% polyacrylamide gel followed by autoradiography of the dried gel. The addition of nuclear extract produced a specific shifting band denoted as I. The asterisk represents a nonspecific band. S: specific; NS: non-specific; SBE: Smad-binding element. (D) Nuclear extracts were extracted from MECs treated with BSA or BMP6 or cotransfected with Flag-Smad1 and Flag-Smad4. Overexpression of Smads induced a slower migrating complex labeled as II.

FIG. 2.6. Inhibiting Cox2 activity attenuates BMP6-induced MEC proliferation, migration and tube formation. (A) Time-dependent response of MEC proliferation to

BMP6 (100 ng/ml) treatment. MEC were pretreated with NS398 (10 μM), SC560 (100 nM), or vehicle before treatment with BMP6. Cells were counted at each time point. (B) MEC cell migration on gelatincoated filters to BMP6 was assayed after pre-treatment with NS398, SC560, or vehicle. After 6 hours, transmigrated cells were counted. (C) MECs were plated on Matrigel-coated 24-well plates, followed by treatment with BMP6, NS398, SC560 and/or vehicle. Images were taken 6 h after incubation. Original magnification, 10X. (D) The mean and SD of 3 replicate wells of a representative experiment is shown. The p-value was determined by Student's t test.

FIG. 2.7. The proangiogenic activity of BMP6 is blocked by Cox2 inhibition in a mouse aorta ring assay. (A) Mouse aorta rings (n = 4) were embedded in collagen gel in the presence of vehicle, BMP6, NS398, or SC560. Neovessel sprouts were blindly counted at Day 6. Original magnification, 4X. (B) Quantitative analysis of aortic ring assays. Columns indicate mean of triplicates. Bars indicate SD. Similar results were obtained in a second independent experiment. (C) Aortas from Cox2 +/+ and -/- mice were tested in this neoangiogenic assay. Images of microvessel outgrowth from aorta with or without BMP6 treatment are presented. (D) Statistical data of aortic ring assay using Cox2 -/- mice.

Table 2.1. Genes downregulated by BMP6 in MECs.

Gene Name	Accession No.	Fold Change			Gene Name	Accession No.	Fold Change		
		4 h	12 h	24 h			4 h	12 h	24 h
Mbl2	NM_010776.1	0.81	0.61	0.68	Fts	NM_010241.1	0.63	0.79	0.90
Matn2	NM_016762.1	0.86	0.66	0.80	Acadm	NM_007382.1	0.66	0.81	0.91
Ephx1	BC029636.1	0.83	0.63	0.77	Slc39a10	NM_172653.1	0.61	0.85	0.90
Smarca1	NM_053123.1	0.77	0.64	0.93	Lphn2	XM_131258.1	0.67	0.85	0.90
Cyp39a1	NM_018887.1	0.65	0.54	0.93	Sema3a	XM_131903.1	0.55	0.75	0.85
Sdh1	NM_146126.1	0.67	0.67	0.82	Adamts5	NM_007038.1	0.41	0.60	0.71
Tgtp	NM_011579.1	0.65	0.44	0.63	Sdpr	NM_138741.1	0.42	0.66	0.76
Chd3	NM_146019.1	0.67	0.65	0.84	Armcx3	NM_027870.1	0.60	0.76	0.98
Tef	NM_153484.1	0.60	0.72	0.92	Frmd4b	BC031369.1	0.61	0.67	0.91
Scel	AE014176.1	0.55	0.84	1.24	Adamts1	D67076.1	0.57	0.65	0.75
Arhgap18	NM_176837	0.64	0.74	0.85	Add3	BC037116.1	0.65	0.77	0.96
Slc39a10	NM_172653.1	0.63	0.82	0.84	Sap30	NM_021788.1	0.66	0.91	1.01
Prkcm	NM_002742.1	0.67	0.77	0.93	Sap30	NM_021788.1	0.63	0.82	1.01
Pmp22	NM_008885.1	0.62	0.77	0.87					

Table 2.2 Genes upregulated by BMP6 in MECs.

| Gene Name	Accession No.	Fold Change			Gene Name	Accession No.	Fold Change		
		4 h	12 h	24 h			4 h	12 h	24 h
Inhba	NM_008380.1	1.56	1.28	1.16	Cd44	XM_130536.1	1.85	1.21	1.05
Vcl	NM_009502.2	1.68	1.02	1.08	Gnb4	NM_013531.1	1.55	1.24	1.04
Itga5	NM_010577.1	1.60	1.08	1.03	Txnrd1	NM_015762.1	1.58	1.31	0.95
Cyp1b1	NM_009994.1	1.66	1.24	1.27	N4wbp4	BC022122.1	1.54	1.21	1.03
Vcl	NM_009502.2	1.70	0.98	0.98	Fosl1	NM_010235.1	1.54	1.30	1.11
Ctgf	NM_010217.1	2.64	1.03	0.88	Hmga2	NM_003483.3	1.94	1.53	1.08
Tmepai	BC036995.1	1.85	1.36	1.05	Timp1	NM_011593.1	1.65	1.66	1.12
Errfi1	NM_133753.1	1.62	0.97	0.87	Timp1	M59906.1	1.45	1.56	1.17
Etv5	NM_023794.2	1.62	1.00	0.88	Snai1	NM_011427.1	1.72	1.53	1.32
Hmox1	NM_010442.1	1.56	0.99	0.94	Wnt2	BC026373.1	2.71	1.97	1.45
Slc20a1	NM_015747.1	1.52	1.16	0.95	Id1	U43884.1	1.94	1.91	2.06
Cox2	X98792.1	2.48	1.52	1.19	Pcolce2	NM_029620.1	1.21	1.64	1.42
Dtr	NM_010415.1	1.98	1.38	1.16	Id2	XM_176747.1	1.76	2.34	2.23
Tnfrsf12a	NM_013749.1	2.19	1.56	1.11	Id3	NM_008321.1	1.54	1.72	1.88
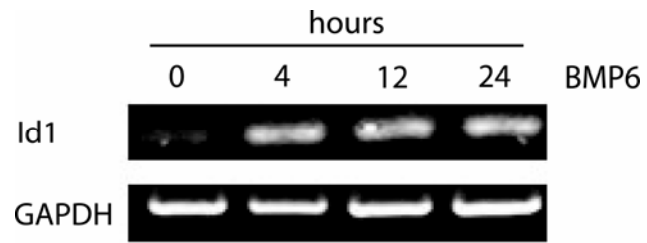
FIG. 2.1. BMP6 induces the upregulation of Id1 in a time-dependent fashion.
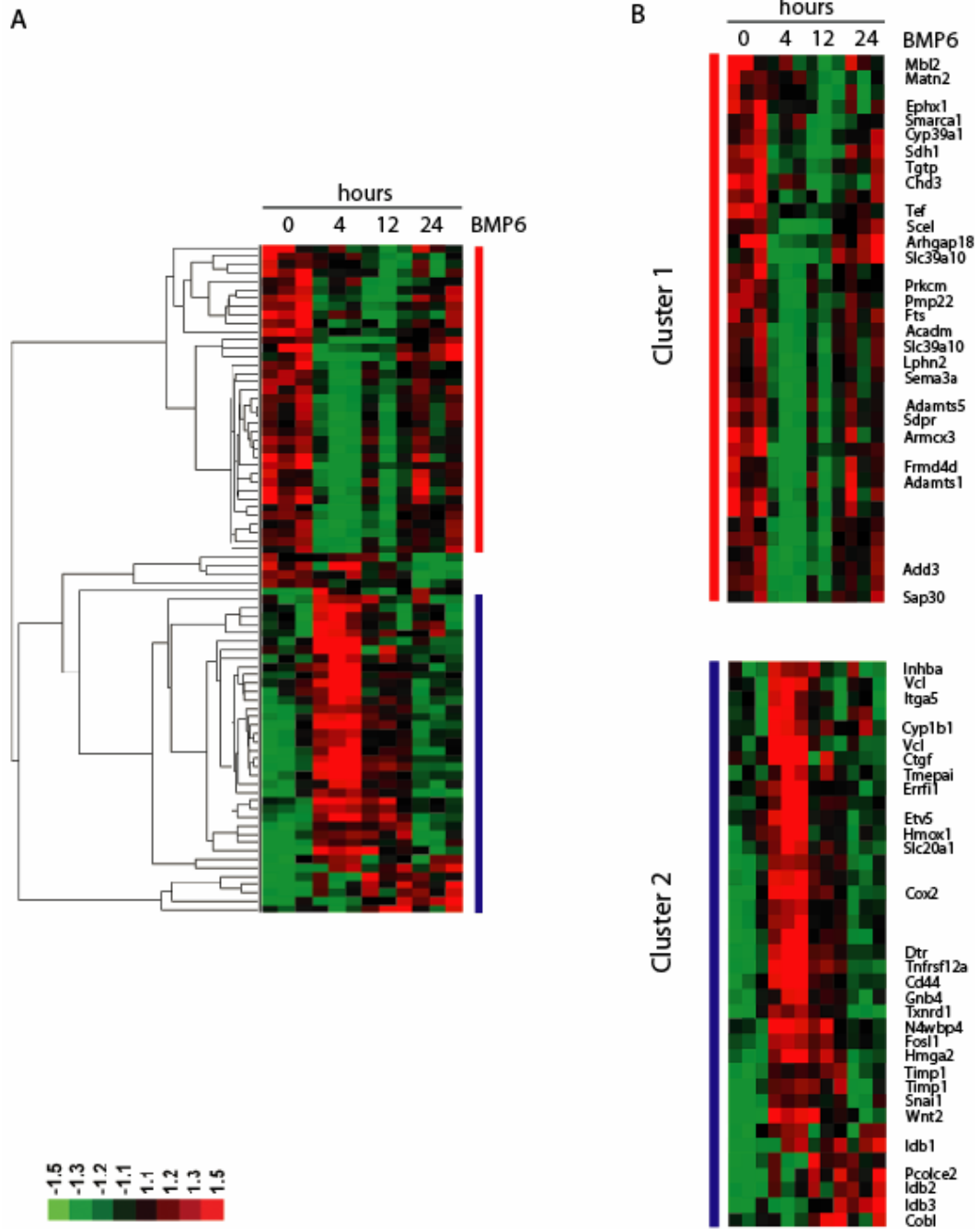
FIG. 2.2. Hierarchical clustering of BMP6 target genes.
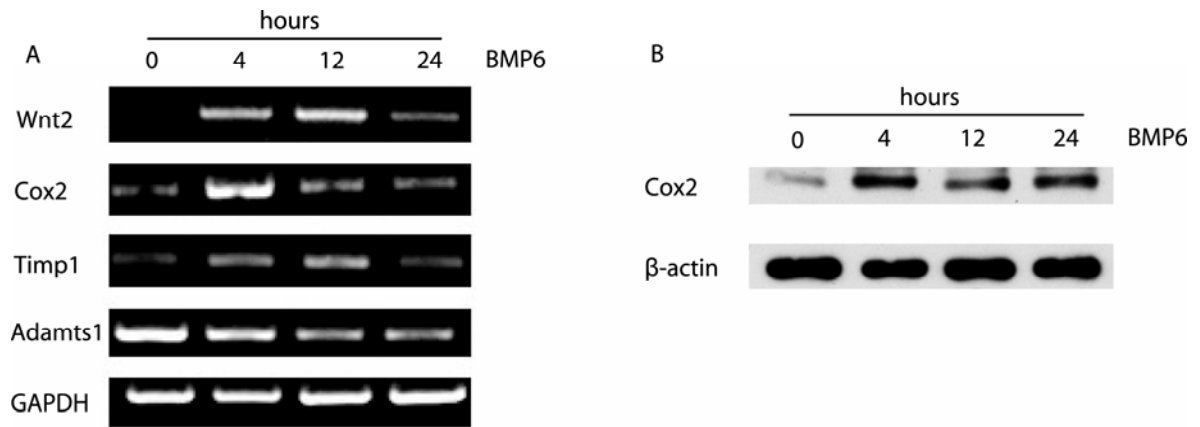
FIG. 2.3. RT-PCR and Western blotting analysis of gene expression in BMP6-induced EC activation.

FIG. 2.4. Elevated levels of secreting prostaglandins derived from Cox2 after BMP6 stimulation.

FIG. 2.5. Activation of the Cox2 promoter by BMP signaling.

FIG. 2.6. Inhibiting Cox2 activity attenuates BMP6-induced MEC proliferation, migration and tube formation.

FIG. 2.7. The proangiogenic activity of BMP6 is blocked by Cox2 inhibition in a mouse aorta ring assay.

CHAPTER III
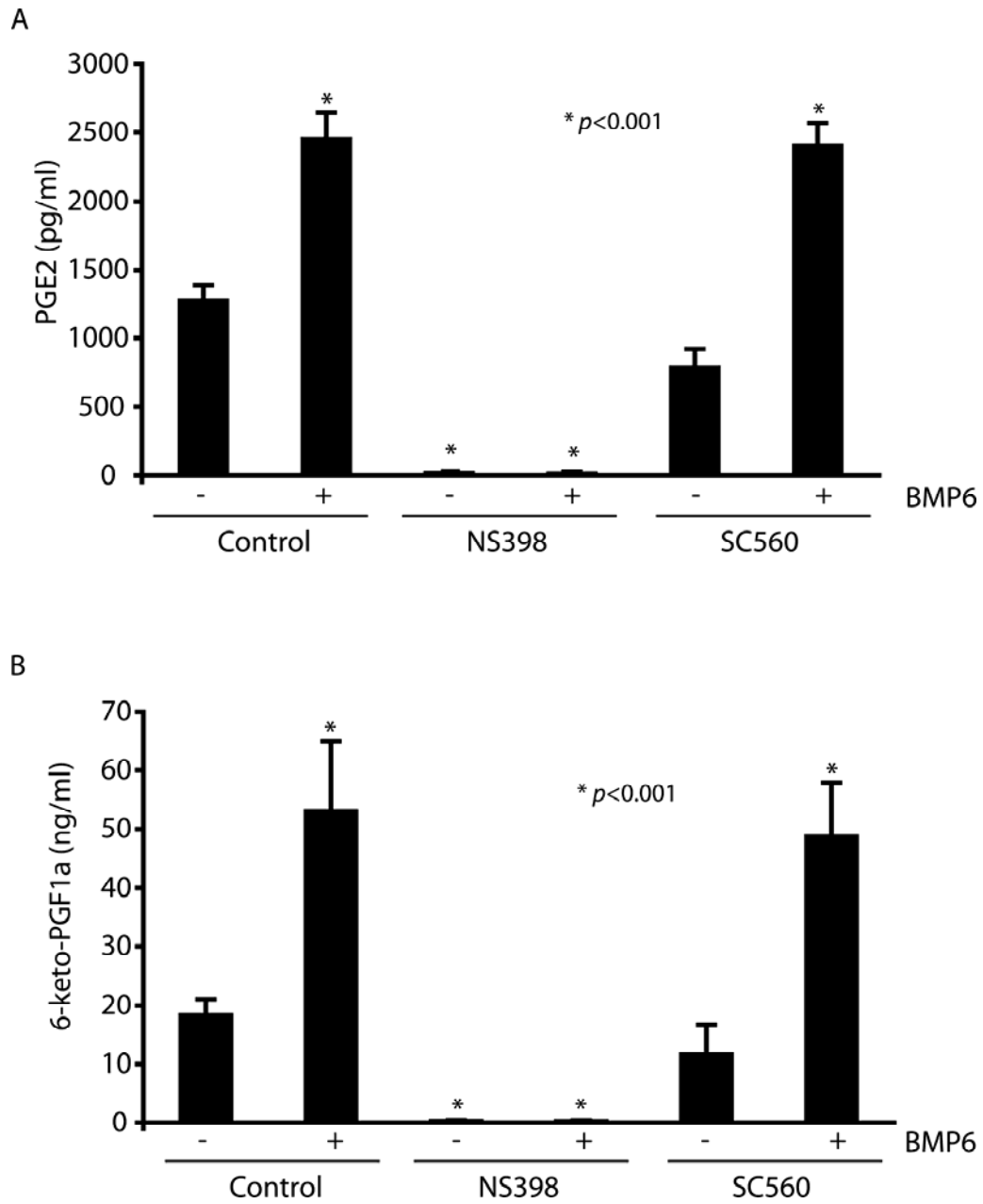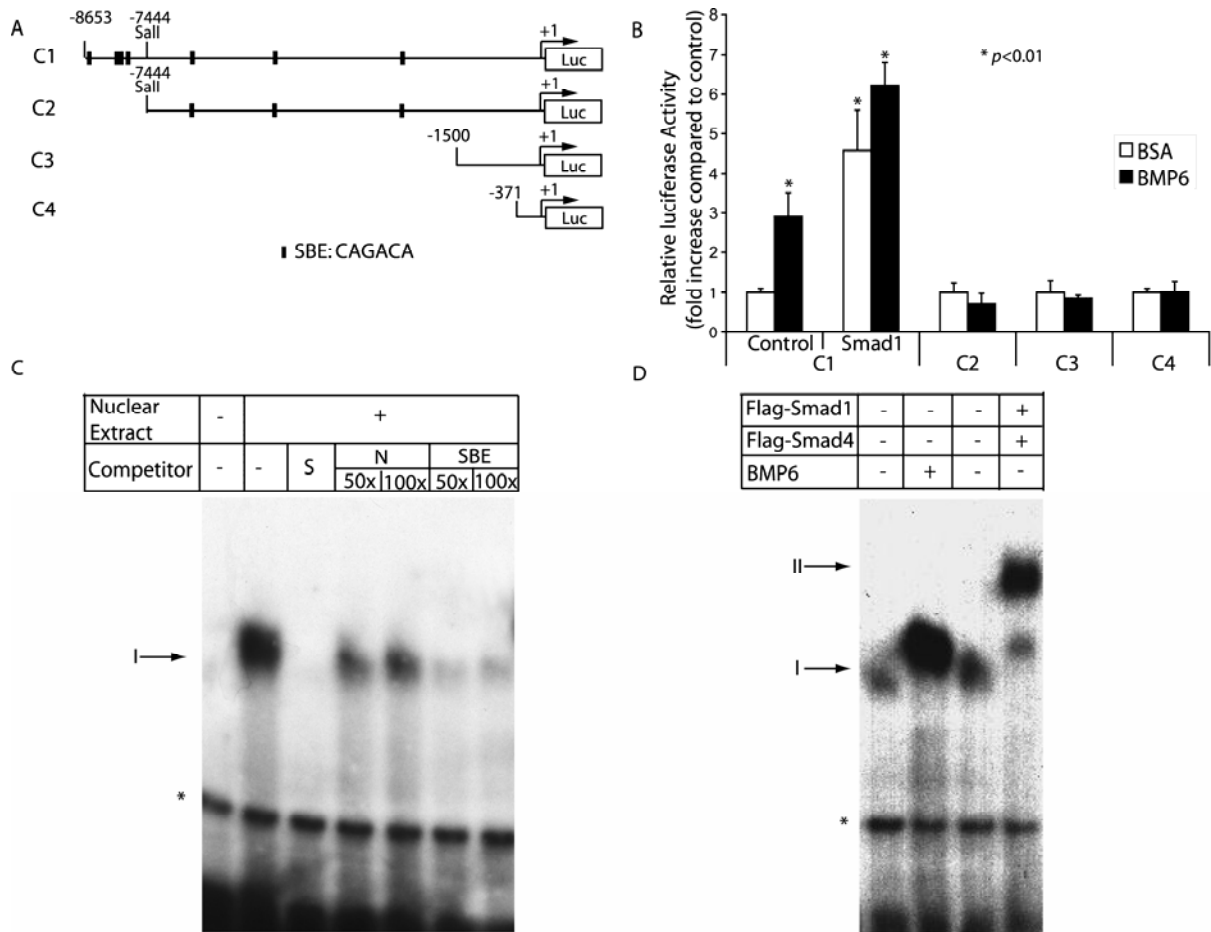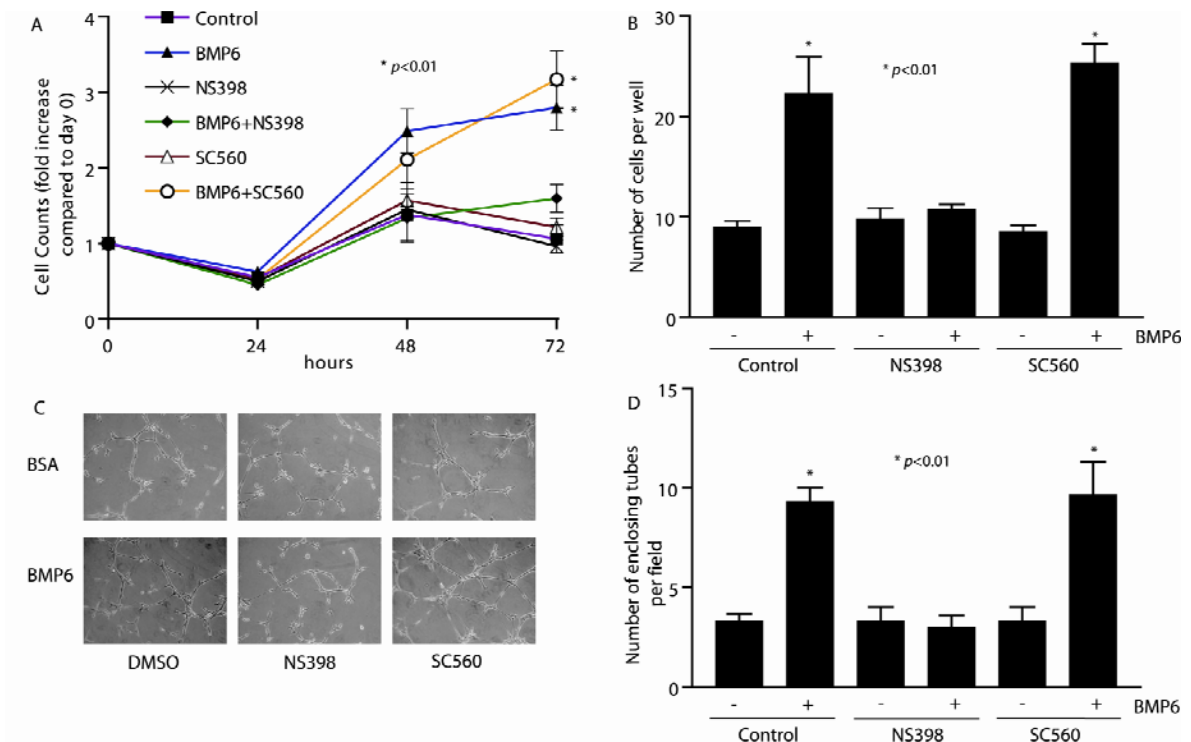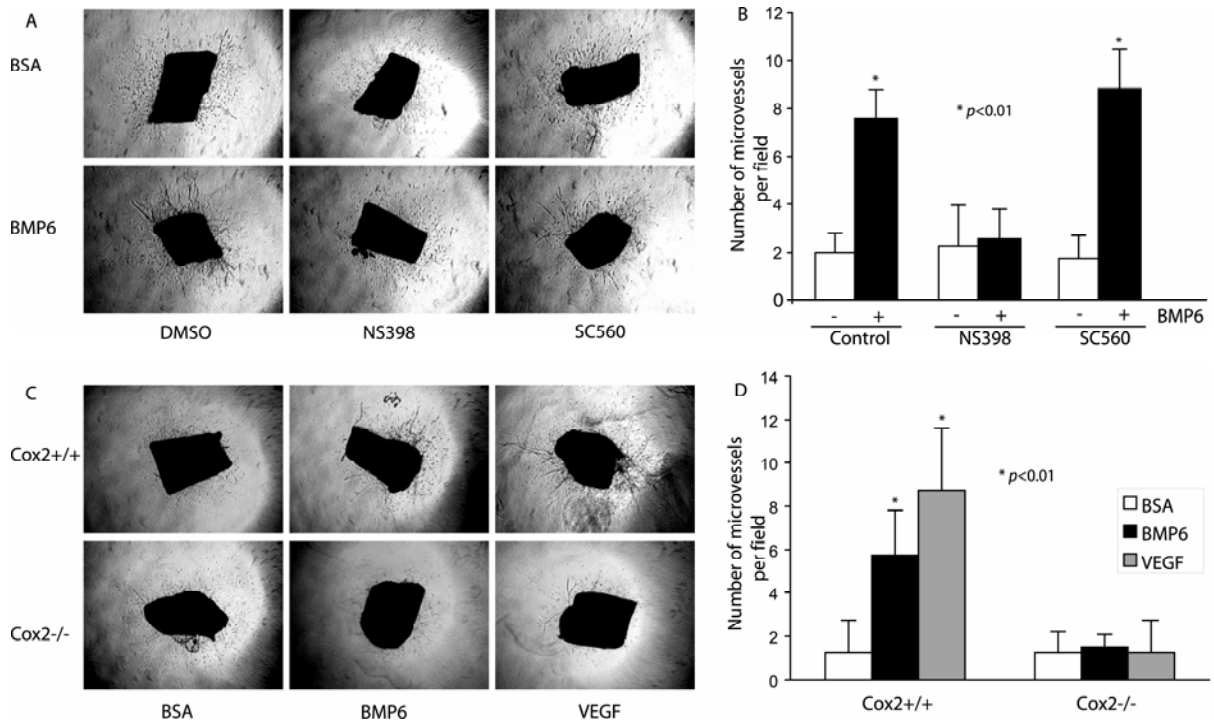
Functional Importance of Bmper in Multiple Organogenesis Determined by *in vivo* Deletion Studies

ABSTRACT

Targeted deletion of *Bmper* encoding an extracellular regulator of BMP signals results in perinatal lethality and skeletal deformation. Bmper transcripts, which are represented by knock-in GFP expression, were detected in lung mesenchyma and ventricular cardiomyocytes at perinatal stage. Loss of Bmper activity caused a delayed lung branching morphogenesis with condensed alveoli separated by thicken mesenchyme. *In vitro* cardiomyocyte assays revealed a pro-hypertrophy activity of BMP2. In addition, cardiomyocytes lacking endogenous *Bmper* were larger in size even in the absence of pharmacological induced hypertrophy. Real-time PCR showed upregulation of cardiac differentiation markers and Bmp signaling components in both BMP2 treated wild-type cells and *Bmper* mutants. This result suggests that Bmper serves as an anti-hypertrophy factor by attenuating BMP activity. The phenotypes associated with Bmper deficiency reveals Bmper as a potential therapeutic target in both physiologic and pathologic events in which BMP signaling is involved.

INTRODUTION

BMP-binding endothelial precursor-derived regulator (Bmper) was first found enriched in a fetal liver kinase 1(Flk1)-positive population of differentiating mouse ES[144]. *Bmper* encodes a protein that has 5 cysteine-rich (CR) von Willebrand C-like domains, similar to several BMP extracellular antagonists including Chordin. *BMPER* mRNA expression is highest in heart, lung and skin in adults. The expression pattern of *BMPER* in developing embryos is highly dynamic. At E10.5, *in situ* hybridization revealed Bmper expression in two important early angiogenesis regions, the yolk sac where BMP2, BMP4 and BMP6 activity has been found[184], and the aorto-gonadal-mesonephric (AGM) region, which contains EC cell precursors and where a high level of BMP4 is found[185]. At E14.5, *Bmper* expression is detected in cartilages of the developing skeleton including vertebral bodies, ribs, and in the lung mesenchyme[183,241].

Studies show evidence supporting both anti- or pro-BMP activity for Bmper. For example, ectopic expression of Bmper dorsalizes *Xenopus* embryos[144,186]. Bmper inhibits BMP-induced osteoblast and chondrocyte differentiation in vitro[187]. Bmper inhibits BMP4-dependent activity in both reporter assay and ES cell differentiation system[144]. Other studies are consistent with Bmper having a pro-BMP effect. Bmper activity is important for the formation of cross-veins in fly wing [188,189,190,191]. Bmper enhances phosphorylation of Smad1 stimulated by BMP4 in COS7 cells [192]. Injection of both BMPER and BMP4 RNA in animal caps synergistically induces the expression of the mesoderm marker, *Xbra* [186]. A hypothesis by Hammerschmidt's group suggests that Bmper activity is dependent on its proteolytic processing; uncleaved Bmper is anti-BMP whereas cleaved Bmper is pro-BMP because only uncleaved Bmper can bind to the extracellular matrix[193].

47

To clarify the exact function of Bmper in embryonic development and its role in BMP pathway, I performed *in vivo* targeted deletion of *Bmper*. The expression pattern of Bmper in lung and heart has been further characterized using a knock-in GFP encoding cassette under control of the Bmper promoter. *Bmper* null mice exhibit perinatal lethality and defects in development of the skeleton, lung, and heart. Targeted deletion of *Bmper* in lung resulted in defects in branching morphogenesis and increased mesenchymal tissues. Cardiomyocytes with Bmper deficiency undergo hypertrophy and display elevated BMP pathway activity. These data demonstrate the importance of Bmper in balancing BMP signaling and regulating organogenesis.

METARIALS AND METHODS

Reagents

Phospho-Smad1/5/8 antibody was purchased from Cell Signaling. Thyroid transcription factor 1 (TTF1) antibody was the product from GeneTex, Inc. Anti pro-surfactant C (pro-SPC) antibody and anti calcitonin gene-related peptide (CGRP) were kind gift from Dr. Jeffrey Whitsett. Anti-Clara Cell Secretory Protein (CCSP) and anti-SPB were from Upstate.

Target deletion of mouse *BMPER* gene

Mice with Bmper deficiency were generated with standard gene targeting methods[242]. The targeting construct was generated by using *pOSfrt* [243] as the backbone, which contains (*i*) a 4.4-kb PCR-generated fragment from genomic DNA that includes the *BMPER* promoter; (*ii*) a 700-bp cDNA encoding EGFP (CLONTECH); (*iii*) a 300-bp bovine growth hormone poly(A) addition region; and (*iv*) a 2.0-kb PCR-generated genomic fragment from second intron of the *BMPER* gene. Embryonic stem (ES) cells (129/ ola) were electroporated with the target construct. ES colonies, which were G418/ganciclovir-resistant, were identified by the PCR-based assay. Homologous recombination was confirmed by Southern analysis using both 5' and 3', diagnostic probes. The targeted ES cells were injected into C57BL/6 blastocysts[242]. Male chimeras were mated to wild-type C57BL/6 females to establish an isogenic line, and all experiments were conducted on the resulting hybrid background.

Genotyping of *BMPER* mutant mice

Genomic DNA of BMPER deficient mice were isolated and digested with *Hpa*I (5' probe) and *Nhe*I (3' probe) to identify wild-type [240] and targeted alleles. *BMPER* homologous mutants were generated by timed heterozygous matings. A PCR analysis has

been developed to genotype the embryos and pups. PCR samples were denatured in 95°C for

60 sec then subjected to 35 cycles of three step amplification, a 30-sec 94°C denaturation,

30-sec 68°C annealing and 45-sec 72°C extension step. A 608-bp product (primers berwtf

and bergtr) represents the WT allele and a 455-bp (primers berkof and bergtr) product

indicates the target allele. PCR primers: berwtf: 5'-

CTGCATCCACCCCTGTAAGTTTCTAG-3';

berkof: 5'-GTCCTCTGATGGTCAAAGTCCTG -3';

bergtr: 5'-CCAAGCCCAACGCTCCCTGCTGAAATCC-3'.

Southern blotting analysis

Southern blotting analysis was carried out as previously described (Matzuk et al.,

1992). Genomic DNA was digested with either *Hpa*I or *Nhe*I and electrophoresed in a 1%

agarose gel. Both 5' and 3' probe was labeled with [α-^{32}P] deoxycytidine triphosphate by

random oligopriming. Membranes containing DNA have hybridized with labeled probes in

65°C for one hour. The locations of radioactive probe hybridization on membrane were

detected by autoradiography.

Immunohistochemistry

Mouse tissues were fixed overnight in 4% paraformaldehyde/phosphate buffered

saline (PBS), dehydrated in a series concentration of ethanol, paraffin embedded and

sectioned at 5 μm. Immunohistochemistry was performed as described. Sections were first

deparaffinized by xylene and rehydrated in graded ethanol series.   Slides have been

incubated for 15 min with Antigen unmask reagent (Vector Laboratories, Burlingame, CA) in

coplin jar in steamer for antigen retrieval. Blocking was achieved with 2.5% horse serum for

10 min. Primary antibody incubations were performed for 30 min at room temperature (RT).

Biotinylated secondary antibodies (Vector Laboratories) were added to sections for 10 min, followed by signal detection using Vector NovaRED reagent (Vector Laboratories).

Embryonic Mouse Cardiomyocytes Isolation and hypertrophy study

Mouse Cardiomyocytes were prepared from hearts of E 18.5 embryos using a commercially available cardiomyocyte isolation kit (Worthington Biochemical) as previously described[244]. Hearts were minced and incubated with trypsin and collagenase in 37 ºC overnight. To reduce the total numbers of fibroblasts, cells were first preplated on untreated plastic flasks for 1 hour. Nonadherent portion of cells, which were enriched for cardiomyocytes, were cultured in minimum essential medium [245] containing Earle's salt with glutamine and 10% horse serum and 5% FBS. Cells were plated on laminin-coated tissue culture plates at a density of 1×10^5 cells/cm^2 and grown at 37°C in 5% CO_2. Cells were cultured for 48 hours before starting the experiments. After overnight serum starvation, cells were treated with control vehicle, BMP2 (100 ng/ml), and PE (100 μM) for 48 hrs. Cardiomyocytes were labeled with anti-β myosin heavy chain (βMHC) and florescent images were taken for measurement.

RNA isolation and real-time PCR

Total RNA was extracted from cells and tissues by using RNeasy Kits (Qiagen, Valencia, CA). The RNA isolation was performed according to the manufacturer's instructions. First-stand cDNA was synthesized using 500 ng of total RNA with 200 U of Superscript II RNase H-RT (Invitrogen) in a final volume of 20 μl. The resulting products were then treated with RNase A for 30 min at 37°C and purified thereafter with Qiaquick PCR purification kit (QIAGEN, Mississauga, Ontario). Realtime PCRs were carried out using 7500 Real-time PCR system (Applied Biosystems, Foster City, CA).

RESULTS

Deletion of *BMPER* by homologuous recombination.

Based on the expression and functional studies, we hypothesized that the regulatory role of Bmper on BMP signals could be very important in embryonic development, especially in the early steps in blood vessel formation. Since *Bmper* expression is first detected at E 7.0 (mid-gastrulation)[183], *Bmper* null embryos are expected to survive until at least that stage. For these reasons, a targeting deletion of *Bmper* in mice has been designed to characterize the exact role of Bmper *in vivo*. I made a targeting construct for generating *Bmper-/-* mice (Figure 3.1*A*). The targeting vector contains a green fluorescent protein (GFP) expression cassette and a neomycin resistance marker under the control of the MC1 promoter. Thymidine kinase (TK) encoded in the targeting vector is used for counterselection against nonhomologous integration. Mouse 129/Ola ES cells were transfected with the target vector in collaboration with the UNC Animal Models Core Facility. Homologous recombination of ES cells was first selected by growing cells in G418 and gancycolvir, followed by PCR screening and Southern blotting using 5' and 3' probes with HpaI and NheI as the diagnostic enzymes (Figure 3.1*B*). Targeted ES clones were microinjected into the blastocysts derived from C57Bl/6 embryos and implanted into pseudo-pregnant recipient females to create chimeras. Chimeras with targeted *BMPER* deletion and GFP knock-in were first mated with C57Bl/6 wild-type mice to generate heterozygous (HT, +/-) mice. Pups were genotyped with two pairs of primers, one for the WT allele and the other for the targeted allele. HT mice were mated to create *BMPER-/-* mice with a mixed C57Bl/6 and 129/Ola background. *BMPER-/-* mice were confirmed by PCR and southern blotting (Figure 3.1*C*).

The amount of *Bmper* transcript in hearts and lungs of control and mutant pups was determined by RT-PCR (Figure 3.1*D*).

Perinatal lethality and skeletal defects of *Bmper* deficient mice.

Bmper-/- mice died immediately after birth, while WT and HT littermates exhibited no lethality (Table 3.1). At E18.5, *BMPER-/-* embryos had a reasonable survival rate based on Mendelian ratios, even though they had smaller trunks and shorter tails than their WT and HT siblings (Figure 3.1*E*). No obvious gross defects were observed at E 13.5 except *Bmper-/-* embryos had a kink at the tip of their tails (data not shown).

Expression of *Bmper* in the lung and heart at perinatal stage.

Previous *in situ* and *nLacZ*-knocked-in data reveal the presence of Bmper in developing lung and heart during E10.5 to E14.5[183,241]. We observed the distribution of Bmper in these two organs at P0 by locating GFP expression (Figure 3.2). Bmper was expressed in lung mesenchymal cells among maturing alveoli. In heart, ventricular cardiomyocytes are the major cell type to express Bmper.

Lung morphogenesis defects in *Bmper* mutants.

Bmper-/- mice were previously shown to have defects in lung maturity[241]. Delayed lung branching morphogenesis was observed as early as E17.5 (Figure 3.3). At E18.5, *Bmper* deficient lungs displayed fewer terminal sacs especially in the peripheral region, which were separated by thicken interstitial mesenchyme. Compared with well developed lungs from WT siblings, *Bmper-/-* lungs had smaller terminal sacs due to the lack of alveolar expansion at P0 (Figure 3.3). There is an increased ratio of type II epithelial cells to total distal cells in E18.5 mutant lungs according to pro-SPC (type II epithelial cell marker) staining (Figure 3.4*A* and *B*). Neuroepithelial bodies formed by pulmonary neuroendocrine

cells (PNEC), which were marked by Calcitonin gene-related peptide (CGRP) were also not altered in *Bmper* null lungs (Figure 3.4*A*). At adulthood, HT lungs exhibited reduced surfactant production without noticeable decrease in type II cell numbers compared with WT ones, while Clara cells, which are CCSP positive, were not affected (Figure 3.4*C* and data not shown).

Hypertropy phenotype in *Bmper* deficient cardiomyocytes.

To investigate the importance of Bmp pathway in cardiomyocyte function, an *in vitro* hypertrophy assay were performed using E18.5 cardiomyocytes isolated from *Bmper+/+, +/- , and -/-* embryos. Each genotype of cells were treated with control vehicle, Bmp2 (100 ng/ml), and PE (100 μM). A total of 100 cells per condition were measured for surface size. As expected, PE induced about a 30% cell size increase in WT cells, while Bmp2 stimulated cells were almost 2 times larger than control cells (Figure 3.5*A* and *B*). *Bmper* deficient cells underwent hypertrophy without any treatment and were unresponsive to Bmp2 or PE induced hypertrophy (Figure 3.5*A* and *B*).

Upregulation of cardiac markers and BMP signaling molecules in *Bmper* null cardiomyocytes.

The mechanism of hypertrophy induced by BMP2 and *Bmper* deficiency was further characterized at the transcriptional level. Several cardiac markers and specific transcriptional factors including atrial natriuretic factor (ANF), αMHC, smooth muscle actin [246], Tbox5, and GATA4, were examined by real-time PCR. Both BMP2- and PE-induced WT cells had higher expression levels of these factors compared to cells under control condition (Figure 3.6*A*). *Bmper -/-* cells had elevated mRNA levels of cardiac specific markers despite treatments (Figure 3.6*A*). The expression of different components in the BMP pathway was

also assessed. BMP2 and PE positively regulated BMP signals by transcriptionally increase

of BMP ligands, receptors, and R-Smads, which also induce the upregulation of I-Smads,

Smurf1, and Noggin due to a negative feedback (Figure 3.6*B*, *C*, and data not shown). On

the other hand, *Bmper*-null cells showed an elevated activity of BMP pathways even under

basal conditions (Figure 3.6*B* and *C*). These results suggest that Bmper protects

cardiomyocytes from hypertrophy through modulation of BMP signals.

DISCUSSION

Our *in vivo* targeted deletion studies showed that Bmper is involved in multiple organogenetic processes and that its function is important for survival during the perinatal stage (Table 3.1). Since BMP pathways are well known as positive regulators for bone development, the skeleton malformation observed in our *Bmper* null embryos, similar to an independent knock-out study[241], are consistent with the pro-BMP activity of Bmper (Figure 3.1*D*).

The GFP staining pattern revealed the distribution of *Bmper* transcripts in the lung and heart at P0 (Figure 3.2*A* and *B*). *Bmper* expression was restricted to the lung mesenchyme from the onset of development (E10.5)[183,241] to P0 (Figure 3.2*A*). In the heart, Bmper was mainly expressed in ventricular cardiomyocytes and in the floor of left atrium (Figure 3.2*B* and data not shown). Double immunostaining with GFP and specific cell markers will be performed to further distinguish cell types expressing Bmper. Similar approaches will also be used on earlier stages of embryos and adult mice to demonstrate dynamic Bmper expression during development.

Bmper-/- lungs display an immature phenotype including delayed lung branching morphogenesis and smaller alveoli surrounded by abundant mesenchyme (Figure 3.3). Most lines of evidence (described in chapter I) suggest that BMP signals are involved in promoting the proliferation and survival of distal epithelial cells, rather than in regulating their differentiation[157,158]. Our data were consistent with these studies and showed an increased population of type II epithelial cells in E18.5 mutant lungs compared to WT ones (Figure 3.4*A* and *B*). Increased numbers of both epithelial and mesenchymal cells in *Bmper* deficient lungs support this model (Figure 3.7) that Bmper negatively regulates the proliferation and

survival of cells by antagonizing BMP4 activity. In this model, BMP4, which is secreted by distal epithelial, increases proliferation and reduces apoptosis. This activity is attenuated by Bmper released from surrounding mesenchyme. There is an overall pro-proliferation and anti-apoptosis effect on epithelium because of relatively high concentration of BMP4 and lower level of Bmper. In mesenchyme, an opposite effect is caused by the reverse concentration distribution of BMP4 and Bmper. More experiments will be performed to test this hypothesis. The difference in the apoptosis and proliferation between *Bmper* null lungs and controls will be analyzed by Tunel assay and the expression level of apoptotic related genes and cell proliferation factors will also be examined by real-time PCR and western blotting. This model will be further supported if the lung phenotype of *Bmper* null mice is relieved by crossing them with mice having conditional deletion of *Alk3* or *Bmp4* in lungs[159]. We have also observed a decreased surfactant synthesis in adult mutant lungs compared with WTs (Figure 3.4*C*). This suggests that Bmper may play an important role in maintaining the function of matured type II epithelial cells.

Our results indicate that both exogenous BMP2 treatment and endogenous Bmper reduction in cardiomyocytes stimulates hypertrophy (Figure 3.5*A* and *B*). Activation of the BMP pathway results in the upregulation of cardiac specific markers including ANF, SMA, and GATA4 (Figure 3.6*A*). *In vitro* studies show that Bmp2 can enhance myocardin transactivation activity to increase cardiac gene expression[247]. Myocardin serves as a cofactor for the serum response factor (SRF) pathway and overexpression of myocardin induced cardiomyocyte hypertrophy and upregulation of cardiac markers[248]. Further analysis of myocardin activity in BMP2 treated cardiomyocyte will be helpful to clarify the relationship between these two pro-hypertrophy signals.

We also observed that the reduction of Bmper in cardiomyocytes led to elevated levels of BMP signaling, which in turn induced hypertrophy even without the addition of BMP2 (Figure 3.5 and 3.6). This indicates that Bmper has anti-hypertrophy activity, which is dependent on its inhibition of BMP signals in cardiomyocyte. To test this hypothesis, we will repeat the *in vitro* hypertrophy study by utilizing recombinant Bmper protein and a BMP2 neutralizing antibody (R&D Systems). If Bmper acts as an antagonist of BMP signaling in cardiomyocytes, we should observe that the treatment of Bmper or the BMP2 blocking antibody will both inhibit BMP2 induced hypertrophy and rescue the mutant phenotype.

As previously described in the introduction, the BMP pathway is very important in early cardiac development especially in both cushion and valve formation. The *in vitro* study described here also shows that *Bmper* deficient cardiomyocytes display a hypertrophy phenotype. Several *in vivo* experiments will be performed to characterize the cardiac function in *Bmper+/-* mice compared with their WT littermates. First, echocardiography will measure the thickness of ventricular walls, the valvular regurgitation, and the cardiac output in both WT and mutant mice at basal condition. The hypertrophy phenotype can be induced using aortic banding, which is well established in our lab[249]. If mutant mice show more severe cardiac enlargement after the surgery, this will further support that Bmper protects heart from stress induced hypertrophy by antagonizing BMP activity.

Based on our observations of *Bmper* null mice phenotypes, the pro- or anti-BMP activity of Bmper are tissue specific. Earlier studies indicated that Bmper's effect on BMP signals relies on its proteolytic form and Bmper can also compete with Chordin for binding to BMP ligands[193]. Tissue specific expression pattern of BMP antagonists and/or the

58

unidentified proteinase, which cleaves Bmper, may be the reason for the complicated action of Bmper on BMP signaling. A microarry analysis on mouse embryonic fibroblasts (MEFs) isolated from control and *Bmper* mutant embryos were recently performed by Rusty Kelley in our lab. These data will be helpful in elucidating the exact regulatory role of Bmper on the BMP pathway.

FIGURE LEGENDS

FIG 3.1. The targeted deletion for the *Bmper* gene in ES cells and in mice. (A) Strategy for targeted deletion of *Bmper* gene. Homologous recombination between the targeting vector and the endogenous *Bmper* gene in the mouse ES cell results in the deletion of Exon 1 and 2 and the insertion of GFP expression cassette. (B) Southern blot analysis of DNA isolated from targeted ES clones, B6 and D10. WT, wild type. (C) Southern blot genotyping confirmed the targeted deletion of first two exons in *Bmper*. DNA was extracted from littermates of heterozygous matings at P0. (D) RT-PCR showed that *Bmper* mRNA levels were reduced or depleted in lungs and hearts from P0 mutants. GAPDH was used as endogenous control. (E) External morphology of *Bmper* nulls embryos at E18.5. From left to right, *Bmper+/+, +/-,* and, -/-.

FIG 3.2. Expression of *Bmper* in lungs and hearts observed with GFP staining at P0. (A) *Bmper* is expressed in lung mesenchymal cells. GFP staining was only observed in mutant tissues and WT lungs were used as a negative control. Positive staining is brown and count staining is blue. Arrows, GFP-positive cells. (B) *Bmper* expression is detected in ventricular cardiomyocytes in HT heart. Scale bars: 100 μm. Magnification, x 40 (insets in lower panel).

FIG 3.3. Lung morphogenesis defects in *Bmper* mutants during later embryonic and perinatal stages. HE staining of lungs from WT, HT, and KO lungs at E17.5, E18.5, and P0. *Bmper-/-* lungs showed delayed branching morphogenesis and inadequate expanded alveoli, which were separated by overgrowing interstitial mesechyme. Scale bars: 100 μm.

FIG 3.4. Increased type II epithelial cells in *Bmper* null lungs at perinatal stage and decreased surfactant synthesis in adult mutant lungs. (A) Pro-SPC and CGRP staining of control and mutant lungs at E18.5. The number of type II epithelial cells were increased in mutant lungs, while PNECs, CGRP positive cells were unaltered. Arrows, pro-SPC and CGRP positive cells. Scale bars: 50 μm. (B) Statistical analysis of type II cells ratio to total cells. Four random fields on slides were chosen for each genotype. *$p<0.01$; **$p<0.05$ determined by Student t-test. (C) Pro-SPC, SPB, CCSP staining of adult lungs. Reduced intensity of pro-SPC and SPB staining indicates decreased surfactant synthesis in HT lungs. Clara cells, which were labeled by CCSP, were not affected by *Bmper* deficiency. Arrows, pro-SPC, SPB, and CCSP positive cells. Scale bars: 100 μm. Magnification, x20; x40 (insets).

FIG 3.5. Cardiomyocyte hypertrophy induced by *Bmper* deficiency. (A) Immuno-florescent staining of cardiomyocytes with βMHC. Cardiomyocytes were isolated from E18.5 control and mutant embryos. Cells were serum starving overnight and treated with control, BMP2 (100 ng/ml), and PE (100 μM) for 48 hours. (B) Statistic analysis of 100 cell surface measurement for each genotype and treatment is shown. The *p*-value was determined by Student's t test. *$p<0.001$.

FIG 3.6. Elevated expression level of Cardiac markers and BMP pathway components in *Bmper* null cardiomyocytes. Real-time PCR analysis of BMP ligands (A), receptors and

R-smads (B), and I-smads and Noggin (C) in WT and KO cardiomyocytes. RNA were isolated from cardiomyocyted treated with control vehicle, BMP2 (100 ng/ml) and PE (100 μM) for 48 hours. The *p*-value was calculated by Student's t test. *p<0.001, **p<0.05.

FIG 3.7. Schematic model of BMP signaling and Bmper activity in distal embryonic lung. Epithelium releases BMP4 to promote the proliferation and reduce apoptosis, while mesenchyme secretes Bmper to inhibit BMP signals, which in turn causes decreased proliferation and enhanced apoptosis. Alk3 is expressed by both epithelial cells and mesenchymal ones and mediates BMP downstream effect in both tissues. Activation of BMP signaling is dependent on the different concentration ratio of BMP4 and Bmper locally.

Table 3.1 Breeding Database of *Bmper* Mutant MIce.

Status of animals on day 1	No. of animals of genotype:		
	-/-	+/-	+/+
Live	0	56	27
Dead	14	2	4
Expected	31	62	31

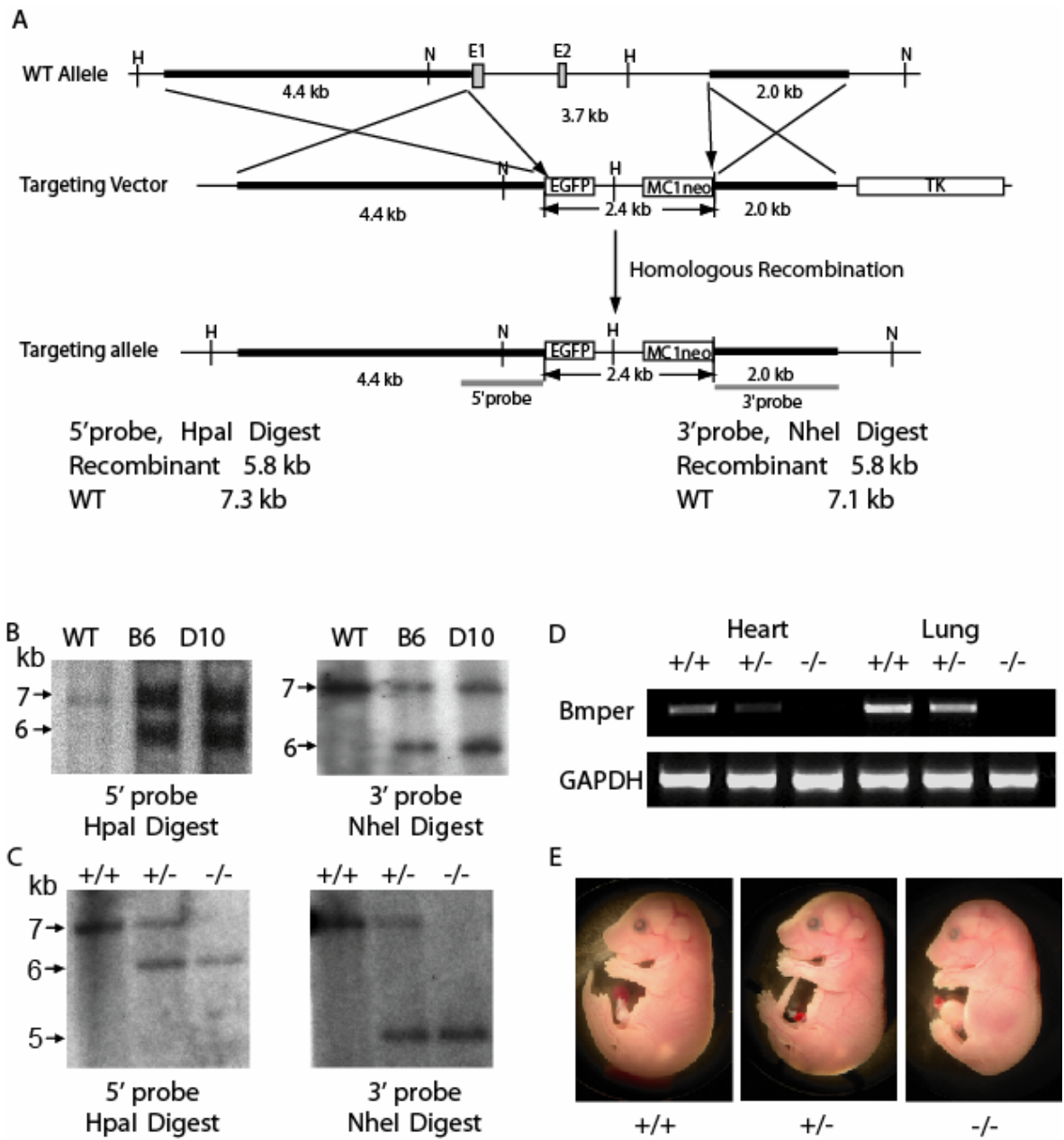**FIG 3.1. The targeted deletion for the *Bmper* gene in ES cells and in mice.**
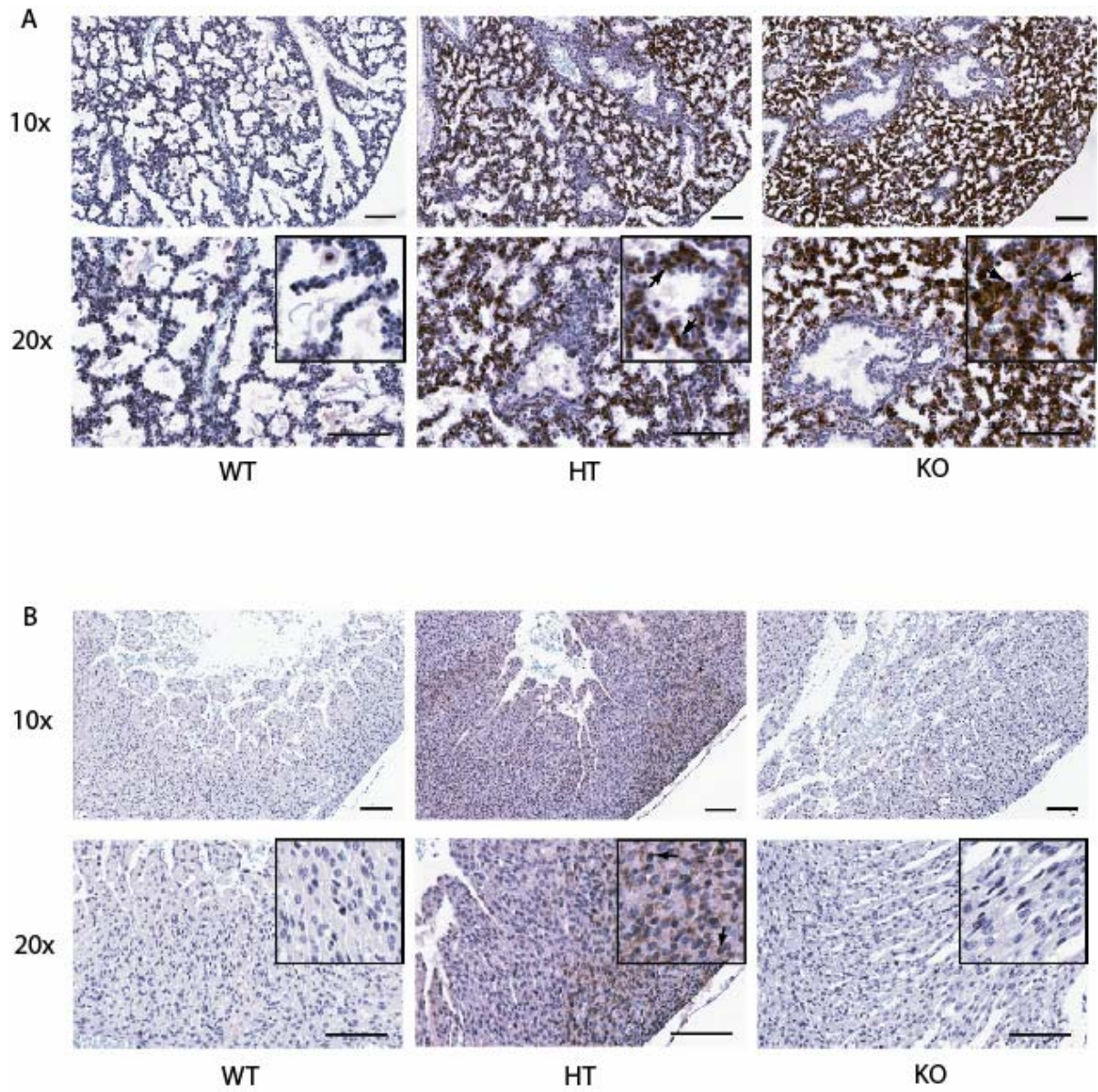
FIG 3.2. Expression of *Bmper* in lungs and hearts observed with GFP staining at P0.
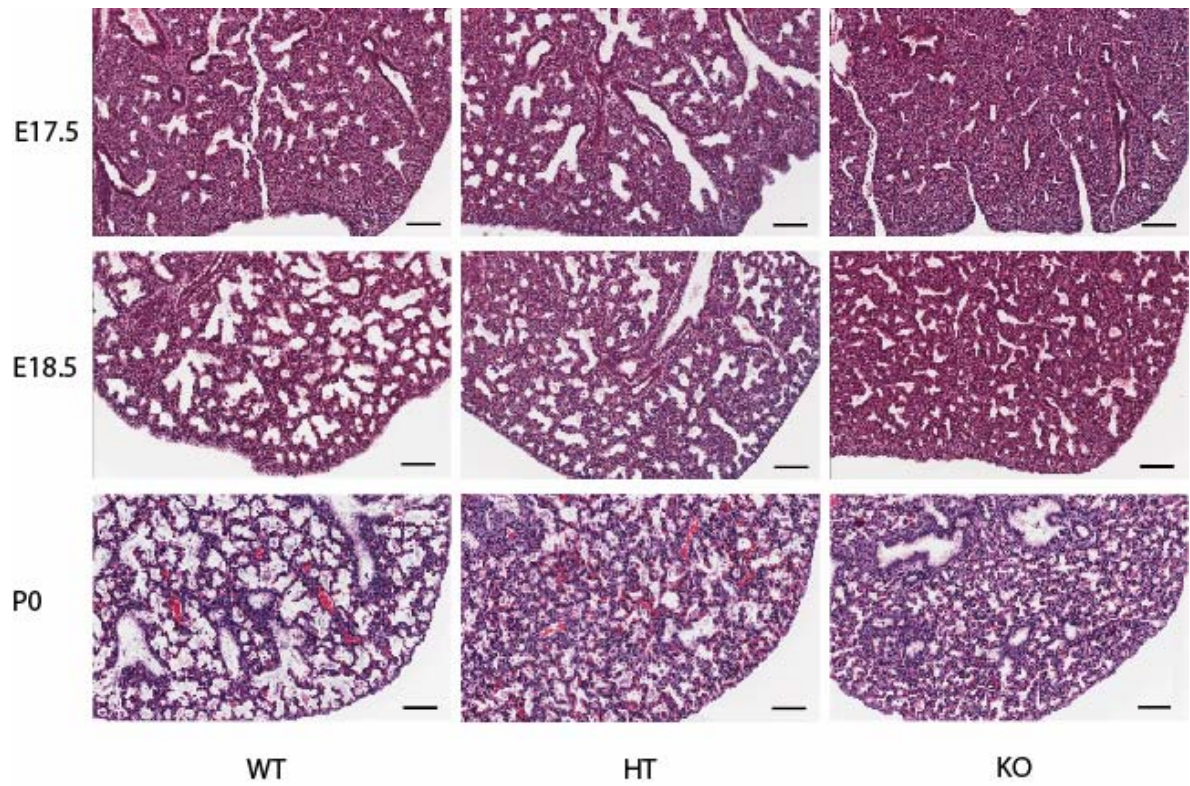
FIG 3.3. Lung morphogenesis defects in *Bmper* mutants during later embryonic and perinatal stages.
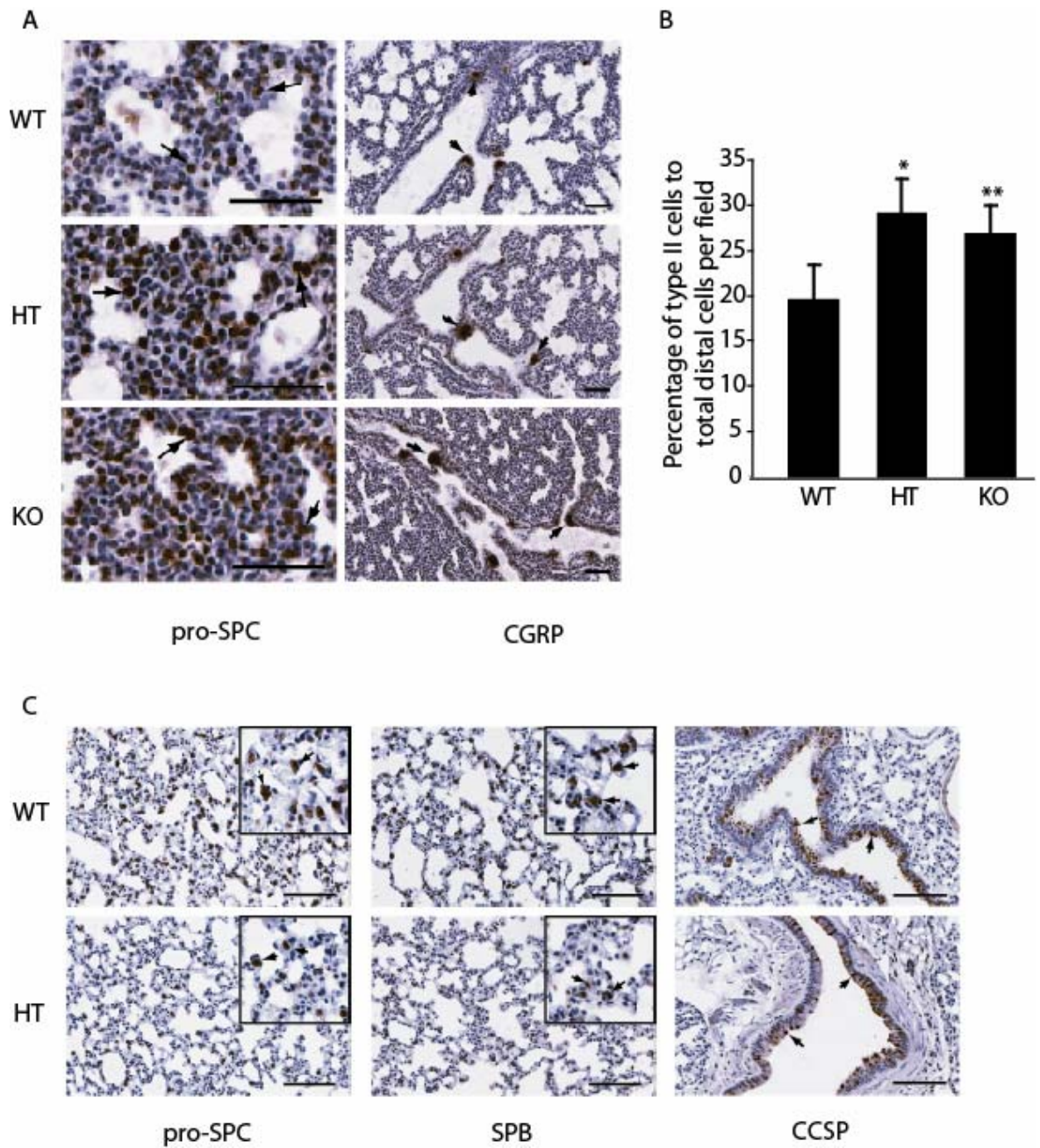
FIG 3.4. **Increased type II epithelial cells in *Bmper* null lungs at perinatal stage and decreased surfactant synthesis in adult mutant lungs.**

FIG 3.5. **Cardiomyocyte hypertrophy induced by *Bmper* deficiency.**

FIG 3.6. Elevated expression level of Cardiac markers and BMP pathway components in *Bmper* null cardiomyocytes.

68

FIG 3.7. Schematic model of BMP signaling and Bmper activity in distal embryonic lung.

CHAPTER IV

CONCLUSION AND FUTURE PLANS

We investigated the role of the BMP signaling during development. Our *in vitro* studies identified an important BMP downstream target, Cox2, which mediates BMP6-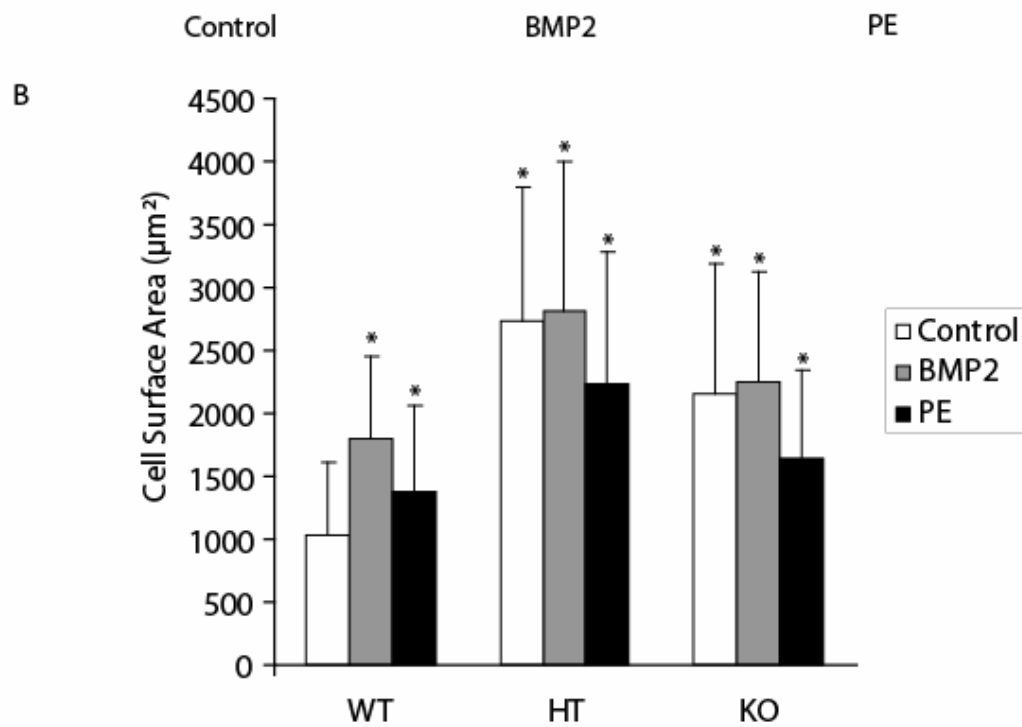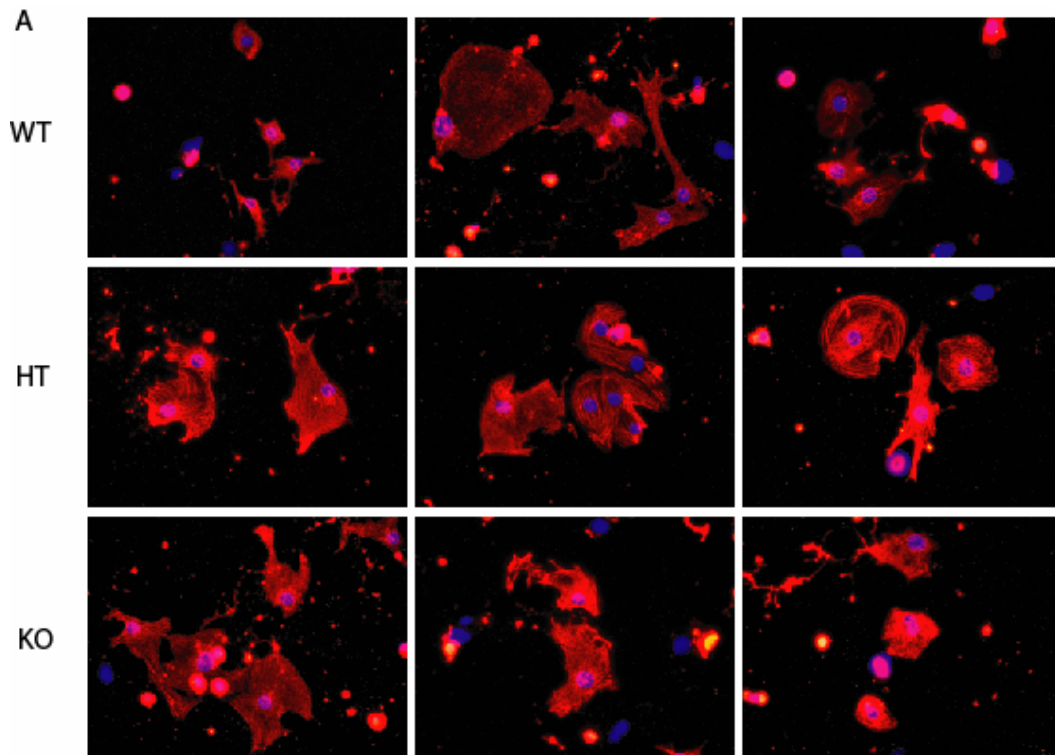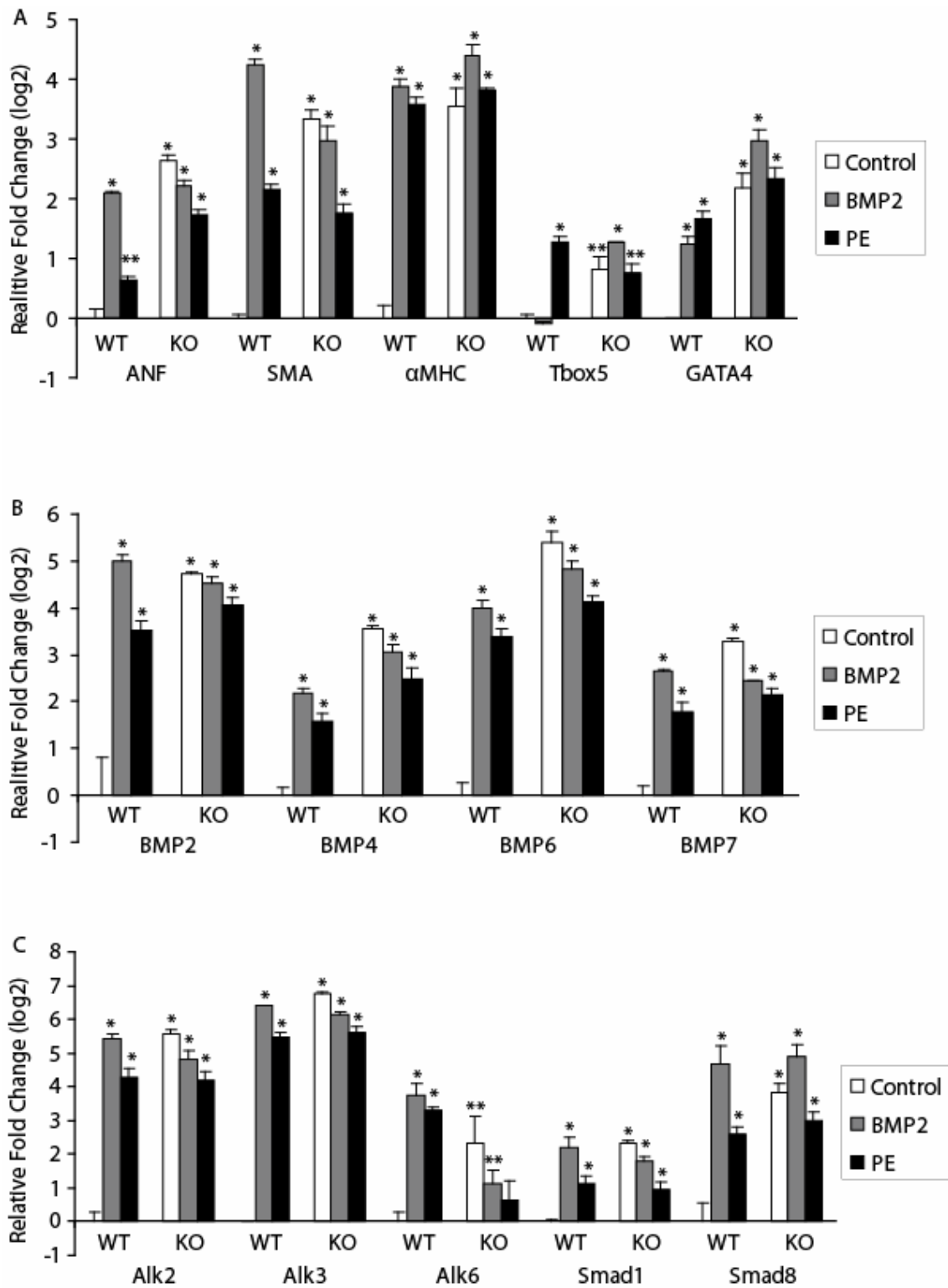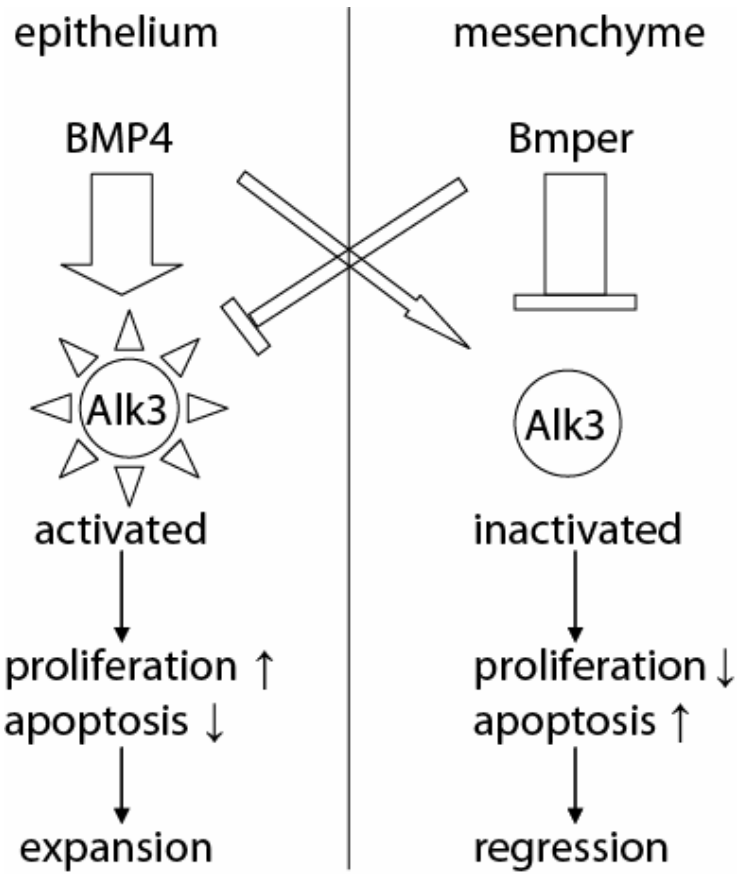induced EC activation in angiogenesis. *In vivo* deletion of a BMP extracellular regulator, Bmper, highlights the importance of BMP signaling in several organogenetic processes, including the development of the skeleton, lung, and heart.

Transcriptional activation of Cox2 promoter by BMP6 and other signals

Our reporter assays identified a SBE site in the Cox2 promoter region (Figure 2.5). The Cox2 promoter contains multiple transcriptional factor binding sites, including a cAMP-responsive element (CRE), nuclear factor interleukin-6 (NF-IL6) and nuclear factor κB (NFκB) elements[250-252]. The CRE binding site is important in response to the stimulation of *src* and *ras* in epithelial cells[253,254]. NFκB and NF-IL6 elements are crucial sites for transcriptionally regulation of *Cox2* by lipopolysaccharide and endotoxin in macrophage-like cells[255-257]. These promoter elements show redundancy in endotoxin response macrophage lineage[258]. In addition, BMP2 activates Cox2 transcription via a cbfa1 binding site on the Cox2 promoter in osteoblasts [218]. The Wnt pathway also transcriptionally upregulates Cox2 through a Tcf-4-binding element[217]. To find out whether other existing elements participate in BMP6-induced Cox2 upregulation, we propose to perform reporter assays using luciferase constructs with different combinations of mutant binding sites. If mutation of a certain

binding site(s) affects the BMP6-induced luciferase activity, we can identify which element(s) may be important for the upregulation of Cox2 by BMP6. Results from this assay can also be helpful for characterizing the crosstalk among BMP signaling and other growth factors such as VEGF and Wnt, which use Cox2 as a common downstream mediator.

Cox2-dependent PG synthesis in BMP6-mediated angiogenesis

Our *in vitro* data indicate that Cox2, instead of Cox1, mediates downstream effects in BMP6-induced angiogenesis. This finding is consistent with previous studies showing functional difference between these two enzymes, in spite of a 61% amino acid sequence homology[211,230,259]. Two mechanisms contribute to their different roles in physiological and pathological events. First, the Cox1 promoter lacks a TATA or CAAT box while the Cox2 promoter contains multiple transcriptional regulatory elements [259,260]. These features allow Cox1 to be a constitutive expressed enzyme whereas Cox2 expression is inducible, upon stimulation of multiple cytokines and growth factors. Second, the two isoforms of Cox exhibit different preferential functional coupling with prostaglandin synthases[261]. In the case of PGE_2 synthesis, Cox1 preferentially couples with cytosolic prostaglandin E synthase (cPGES), which is constitutively expressed to maintain PGE_2 production required for cellular homeostasis [262]. Cox2 selectively cooperates with an inducible microsomal prostaglandin E synthase-1 (mPGES-1) to increase PGE_2 production under the induction of cytokines and growth factors [263]. The upregulation of both Cox2 and mPGES-1 by IL-1β suggests that the coregulation of these two enzymes may be important for the increased production of PGE_2 by IL-1β stimulation [264,265]. To find out whether mPGES-1 is also upregulated by BMP6, the expression of mPGES-1 in BMP6-induced ECs can be examined by RT-PCR, Western

blotting. Once we confirm that the upregulation of mPGES-1 is at transcriptional level, the promoter region of *mPges-1* will be further examined by reporter assays.

BMP-induced Cox2 activity in cardiovascular diseases and tumorigenesis

The nonspecific non-steroidal anti-inflammatory drugs (NSAIDs) have been widely used in treating various inflammatory related diseases. One of the most common side effects is gastrointestinal (GI) syndrome, which is caused by the disruption GI integrity maintained by Cox1 [266]. Cox2 selective inhibitors have been used to reduce GI adverse events, but these drugs have increased the risk of cardiovascular disease compared with nonspecific inhibitors [267,268]. This may be related to differences in expression and product synthesis of the two Cox isoforms in vasculature. Cox1 is the predominant form in platelets and mediates the synthesis of TXA_2, which is a vasoconstrictor and positive regulator for platelet aggregation, whereas Cox2 is involved in producing PGI_2, which is a vasodilator and inhibitor of platelet aggregation [269,270]. Unlike the nonspecific inhibitors, which block production of both PGI_2 and TXA_2, Cox2 inhibitors selectively reduce production of PGI_2 by ECs without suppression of Cox1-derived TXA_2 [271]. The unbalance in biosynthesis between PGI_2 and TXA_2 results in drug-induced thrombosis, which is related to an increased incidence of cardiovascular diseases [272]. Our data demonstrates that BMP6 transcriptionally upregulates Cox2 in ECs (Figure 2.3 and 2.5) and also increases the biosynthesis of PGI_2 and PGE_2 derived from Cox2 (Figure 2.4). These findings suggest that BMPs can be used to reduce the risk of cardiovascular incidence related to Cox2 selective inhibitors. Additional transcriptional studies need to be conducted in other non-EC cell lines to test whether BMP6-induced Cox2 upregulation is restricted to ECs or is pleiotropic.

The pro-angiogenetic activity of Cox2 has been implicated as a promoting factor in carcinogenesis and the overexpression of Cox2 has been observed in breast [273] and colorectal cancer [274-276]. Inhibition of Cox2 activity by either genetic deletion or pharmacological inhibition reduces tumor growth, supporting the idea that Cox2 acts as a positive regulator in tumor development [277,278]. At the same time, the BMP signal pathway has also been linked to tumorigenesis. Mutations of *Smad4* and *Alk3* are found in familial juvenile polyposis [279]. *Alk3* is also mutated in the germ line of some families carrying an inherited type of breast cancer, called Cowden syndrome [280]. Both pro- and anti-tumor effects of BMP signaling have been reported. For example, overexpression of BMP6 and BMP7 was detected in metastatic prostate cancer cells [281-283]. Conversely, BMP7 is downregulated in nephroblastoma [284]. BMP4 and BMP6 transgenic mice show high resistance to 12-O-tetradecanoyl-phorbol-13-acetate-induced tumorigenesis compared to controls [285,286]. The pro-tumorigenesis aspect of BMP signaling in certain tumors may involve increased angiogenesis by upregulation of Cox2, demonstrated in our *in vitro* studies. A similar relationship has also been observed between VEGF and Cox2 in breast cancer, where they act synergistically to promote tumor angiogenesis [273]. Our studies suggest that the development of a more effective combination therapy, which targets both Cox2 and BMP signaling, may be an effective treatment in cancers showing elevated levels of these two pathways.

Tissue specific opposing activities of Bmper

Data from *Bmper* null studies reveal tissue specific pro- and anti-BMP activity of Bmper. Two models can be used to elucidate these opposing activities of Bmper (Figure 4.1). Firstly, similar to chordin, Bmper is proteolytically cleaved into N- and C-terminal

fragments, which form a heterodimer via disulfide bonds [144,193]. Both uncleaved and cleaved Bmper can strongly bind to BMPs, but only the uncleaved form is capable of binding to heparin in extracellular matrix [193]. The association of uncleaved Bmper with the extracellular matrix sequesters BMPs from their cell surface receptors and inhibits BMP signaling. The proteolytic cleavage releases Bmper from binding with the extracellular matrix and converts Bmper from an anti-BMP factor to a pro-BMP regulator. Both *in vitro* and *in vivo* studies can be performed to test this model. MECs can be treated with the control vehicle, BMP6 alone, BMP6 with the conditional media containing full-length Bmper with mutant cleavage site, or BMP6 with the conditional media containing cleaved Bmper fragments. The activity of BMP signaling can be determined by quantifying phospho-Smad1/5/8 and BMP downstream targets, including Id1 and Cox2 by real-time PCR and Western blotting. If only the full-length Bmper proteins but not the cleaved fragments are able to inhibit the BMP activity and block BMP-induced upregulation of Id1 and Cox2, this will suggest that proteolytic cleavage is the main force to switch Bmper from an anti-BMP factor to a pro-BMP regulator. To determine the role of Bmper on BMP signaling in specific tissues, the expression levels of BMP downstream targets and the amount of phospho-Smad1/5/8 in different tissues from *Bmper* knockout mice and WT ones will first be analyzed. For example, if Bmper is a negative regulator for BMP signaling in a certain tissue, then the *Bmper* deficient tissue should have elevated BMP signaling activity compared with WT. We next can determine the amount of full-length Bmper cleaved in that tissue by Western blotting. Our hypothesis will be supported if the predominant form of Bmper is full-length in the tissue that Bmper has an anti-BMP role, while cleaved fragments will be the majority in the tissue where Bmper is pro-BMP signaling.

The second model involves clathrin-coated pits (CCPs)-mediated endocytosis. Studies showed that BMP receptors (both type I and type II receptors) undergo constitutive endocytosis via CCPs [287]. Data from our lab (Rusty Kelley, unpublished data) suggests that the presence of Bmper can facilitate the endocytosis of BMP ligands in a cell-type specific manner. This receptor-dependent endocytosis is not required for phosphorylation of R-Smads, but is essential for transmitting R-Smads into the nucleus where they can regulate the transcriptional activity of downstream targets [287]. At the same time, internalized receptors either recycle to the plasma membrane, resulting in continual activation, or transport to lysosomes for degradation, and therefore attenuating BMP signaling [288]. According to our *in vitro* results (Rusty Kelley, unpublished data), Bmper promotes the degradation of internalized BMPs and partially inhibits Smad-dependent downstream signaling through endocytosis. Thus, Bmper exhibits an anti-BMP activity through CCRs-dependent endocytosis, which is cell-type specific and could also be tissue specific.
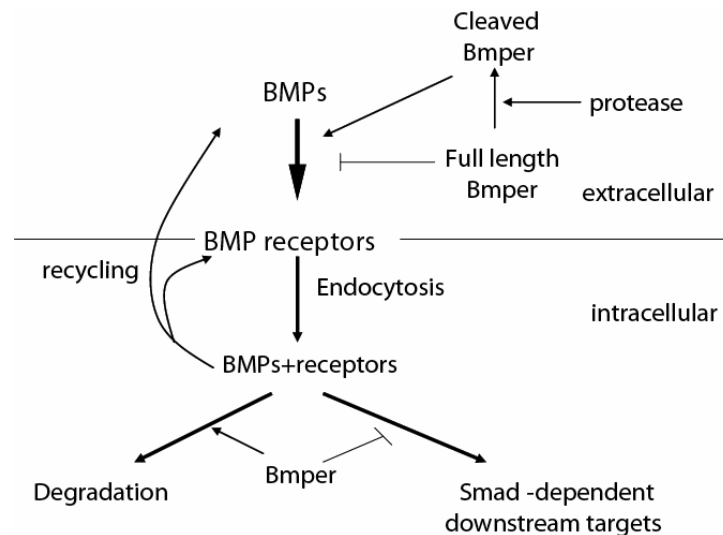

FIG. 4.1. Opposing effects of Bmper on BMP pathway dependent either on its cleavage forms or CCPs-mediated endocytosis.

Besides these two putative models, Bmper may exhibit its regulatory role in other ways. 1) BMP antagonist-dependent model. Bmper can modulate BMP signals by its interaction with other BMP antagonists such as Chordin, Noggin, or Gremlin. Competitive binding assays *in vitro* reveal that Bmper and Chordin compete for the binding to BMP2 [193]. This competitive binding between Bmper and Chordin provides the possibility that Bmper may act as a pro-BMP factor by blocking the interaction of Chordin with BMPs. More *in vitro* competitive binding experiments need to be done to test if Bmper can similarly compete with other BMP antagonists for their binding to BMPs. 2) BMP receptor complex model. As described in the introduction, the two forms of the BMP receptor complexs, PFC and BISC, determine the activation of either Smad-dependent or independent pathways [143]. Since the binding of Bmper to BMPs does not interfere with their interaction with the transmembrane receptors [193], this association may affect the preference in binding to the two different receptor complexes, favoring one pathway over the other. To test this hypothesis, we can examine the phospho-Smads and the MAPK activity after BMP4 treatment with or without co-treatment of Bmper *in vitro*. The phospho-Smads and the MAPK activity in different tissues of WT and *Bmper* null mice will also be analyzed to determine the role of Bmper in the regulation of Smad-dependent and Smad-independent signaling.

The role of Bmper in lung and heart development

The role of Bmper in lung and heart formation has been analyzed using the *Bmper* knockout mice. We have observed the overgrowth of both epithelial and mesenchymal cells in the distal region of *Bmper* null lung. We hypothesize that Bmper released from mesenchymal tissues negatively regulates the proliferation and survival of cells by antagonizing the activity of BMP4 secreted by the epithelium. To test this hypothesis, the

difference in the apoptosis and proliferation between *Bmper* null lungs and controls will be analyzed by Tunel assay. The expression level of apoptotic related genes and cell proliferation factors will also be examined by real-time PCR and Western blotting. The anti-BMP activity of Bmper will be further supported if the lung phenotype of *Bmper* null mice is relieved by crossing them with mice having conditional deletion of *Alk3* or *Bmp4* in lungs[159].

Our *in vitro* study shows that BMP2 can induce hypertrophy in WT cardiomyocytes, where as *Bmper* knockout cardiomyocytes display a hypertrophy phenotype without any treatment and have an elevated level of BMP signaling. This indicated that Bmper serves as an anti-hypertrophy factor by attenuating BMP activity. To test this hypothesis, we will repeat the *in vitro* hypertrophy study by utilizing the recombinant Bmper protein and a BMP2 specific neutralizing antibody (R&D Systems). If Bmper acts as an antagonist of BMP signaling in cardiomyocytes, we should observe that the addition of Bmper or the BMP2 blocking antibody will both inhibit BMP2 induced hypertrophy and rescue the knockout phenotype.

BMP signaling is involved in early cardiac development especially in both cushion and valve formation (described in the introduction). Bmper plays an important role in heart formation through its interaction with the BMP pathway. Several *in vivo* experiments will be performed to characterize the cardiac function in *Bmper+/-* mice compared with their WT littermates. First, echocardiography will measure the thickness of ventricular walls, the valvular regurgitation, and the cardiac output in both WT and mutant mice at basal condition. The hypertrophy phenotype can be induced *in vivo* by aortic banding, which is well established in our lab [249]. If *Bmper+/-* mice develop more severe ventricular enlargement

and heart failure after the surgery, this will further support that Bmper protects the heart from

hypertrophy by antagonizing BMP activity.

Retinal angiogenesis in *Bmper deficient mice*

To further characterize the role of Bmper and BMP signals in angiogenesis, we

propose to adapt an *in vivo* retinal angiogenesis model to our *Bmper* heterozygous mice. We

have detected the enrichment of *Bmper* expression in retina (Figure 4.2*A*), which strongly

suggests the involvement of Bmper in retinal development. Normal retinal vessels start to

form from the central optic disc to peripheral areas during P0 to about P11. In the following

two weeks, vascular plexuses are established by sprouting and remodeling[289,290]. To

determine if the reduced Bmper amount leads to abnormal vascular formation, the retinal

vasculature of WT and *Bmper+/-* mice at early postnatal (P6) and adult stage will be

examined by whole-mount isolectin staining (normal P14 retina staining shown in Figure

4.2*B*). Disruption of retinal vasculature either postnatally or during the adult period in

Bmper deficient mice will demonstrate that Bmper participates in retinal angiogenesis

through modulating BMP signals.

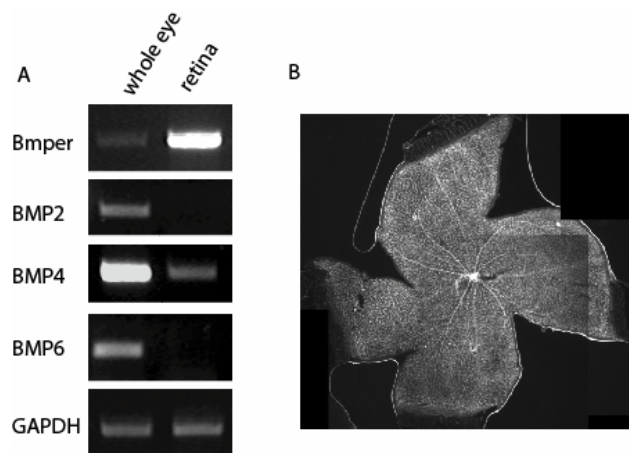
FIG 4.2. Expression of Bmper and BMPs in retina and whole-mount retinopathy. (A)
RT-PCR analysis of Bmper and BMP ligands in whole eye and retina from WT adult mice.
(B) Whole-mount isolectin staining of P14 WT retina.

In addition to studying the influence of Bmper in normal retinal vascular development, its effect on hypoxia-driven neovascularization will also be investigated by oxygen induced retinopathy (OIR) [291-294]. In this experiment, *Bmper+/-* pups and their WT littermates will be exposed to 75% oxygen from P7 to P12. The high concentrations of oxygen will cause the regression of the capillary network in the center of the retina in WT mice. Pups will be returned to normoxia at P12. The now poor vasculature results in hypoxia, which will induce the release of pro-angiogenetic factors, including VEGF and PDGF. These signals promote the pathologic vessel growth at the interface between retina and vitreous until P22. Vascular formation at different stages (P14, P17, and P20) will be documented by whole-mount isolectin stain. Expression levels of genes related to angiogenesis and the BMP pathway will also be determined by real-time PCR. These data will provide direct evidence to identify the role of Bmper in angiogenesis.

In conclusion, we have identified Cox2 as one of the essential downstream targets in BMP-induced angiogenesis by *in vitro* reporter assays and EC functional assays. Cox2 may also serve as an important mediator in connecting the BMP pathway with other pro-angiogenetic growth factor signals such as VEGF. Similar approaches can be applied to characterize potential downstream targets in BMP-mediated vascular remodeling events. Second, we examined the role of a BMP extracellular regulator, Bmper, in heart and lung formation during early development using an *in vivo* targeted deletion study. *Bmper* deficiency caused not only abnormalities in lung morphogenesis with the overgrowth of distal lung epithelium and mesenchyme, but also hypertrophy in cultured cardiomyocytes. An elevated BMP signaling activity was observed in *Bmper* null cardiomyocytes by real-time PCR, strongly suggesting an anti-BMP effect of Bmper in cardiomyocytes. Further

characterization of *Bmper* deficient mice will reveal more helpful information in elucidating

the tissue specific opposing activities of Bmper on the BMP pathway. As Cox2 mediates

BMP downstream effects and Bmper serves as a regulator for proper BMP activity, they both

can serve as therapeutic targets in heart disease and in tumorigenesis resulting from abnormal

BMP activities.

REFERENCES

1.   Risau W, Sariola H, Zerwes HG, et al. Vasculogenesis and angiogenesis in embryonic-stem-cell-derived embryoid bodies. Development. 1988;102:471-478.

2.   Wilting J, Christ B. Embryonic angiogenesis: a review. Naturwissenschaften. 1996;83:153-164.

3.   Risau W, Flamme I. Vasculogenesis. Annu Rev Cell Dev Biol. 1995;11:73-91.

4.   Hanahan D. Signaling vascular morphogenesis and maintenance. Science. 1997;277:48-50.

5.   Ferrara N, Alitalo K. Clinical applications of angiogenic growth factors and their inhibitors. Nat Med. 1999;5:1359-1364.

6.   Folkman J. Angiogenesis in cancer, vascular, rheumatoid and other disease. Nat Med. 1995;1:27-31.

7.   Taipale J, Makinen T, Arighi E, Kukk E, Karkkainen M, Alitalo K. Vascular endothelial growth factor receptor-3. Curr Top Microbiol Immunol. 1999;237:85-96.

8.   Ten Have-Opbroek AA. Lung development in the mouse embryo. Exp Lung Res. 1991;17:111-130.

9.   Warburton D, Schwarz M, Tefft D, Flores-Delgado G, Anderson KD, Cardoso WV. The molecular basis of lung morphogenesis. Mech Dev. 2000;92:55-81.

10.   Scheuermann DW. Comparative histology of pulmonary neuroendocrine cell system in mammalian lungs. Microsc Res Tech. 1997;37:31-42.

11.   Beier HM, Kirchner C, Mootz U. Uteroglobin-like antigen in the pulmonary epithelium and secretion of the lung. Cell Tissue Res. 1978;190:15-25.

12.   Burri PH. Fetal and postnatal development of the lung. Annu Rev Physiol. 1984;46:617-628.

13.   Williams MC, Mason RJ. Development of the type II cell in the fetal rat lung. Am Rev Respir Dis. 1977;115:37-47.

14. Sekine K, Ohuchi H, Fujiwara M, et al. Fgf10 is essential for limb and lung formation. Nat Genet. 1999;21:138-141.

15. De Moerlooze L, Spencer-Dene B, Revest J, Hajihosseini M, Rosewell I, Dickson C. An important role for the IIIb isoform of fibroblast growth factor receptor 2 (FGFR2) in mesenchymal-epithelial signalling during mouse organogenesis. Development. 2000;127:483-492.

16. Crisera CA, Connelly PR, Marmureanu AR, et al. Esophageal atresia with tracheoesophageal fistula: suggested mechanism in faulty organogenesis. J Pediatr Surg. 1999;34:204-208.

17. Crisera CA, Connelly PR, Marmureanu AR, et al. TTF-1 and HNF-3beta in the developing tracheoesophageal fistula: further evidence for the respiratory origin of the distal esophagus'. J Pediatr Surg. 1999;34:1322-1326.

18. Crisera CA, Maldonado TS, Longaker MT, Gittes GK. Defective fibroblast growth factor signaling allows for nonbranching growth of the respiratory-derived fistula tract in esophageal atresia with tracheoesophageal fistula. J Pediatr Surg. 2000;35:1421-1425.

19. Ioannides AS, Henderson DJ, Spitz L, Copp AJ. Role of Sonic hedgehog in the development of the trachea and oesophagus. J Pediatr Surg. 2003;38:29-36; discussion 29-36.

20. Litingtung Y, Lei L, Westphal H, Chiang C. Sonic hedgehog is essential to foregut development. Nat Genet. 1998;20:58-61.

21. Miller LA, Wert SE, Clark JC, Xu Y, Perl AK, Whitsett JA. Role of Sonic hedgehog in patterning of tracheal-bronchial cartilage and the peripheral lung. Dev Dyn. 2004;231:57-71.

22. Pepicelli CV, Lewis PM, McMahon AP. Sonic hedgehog regulates branching morphogenesis in the mammalian lung. Curr Biol. 1998;8:1083-1086.

23. Hoffman JI, Kaplan S. The incidence of congenital heart disease. J Am Coll Cardiol. 2002;39:1890-1900.

24. Sissman NJ. Developmental landmarks in cardiac morphogenesis: comparative chronology. Am J Cardiol. 1970;25:141-148.

25. Schultheiss TM, Xydas S, Lassar AB. Induction of avian cardiac myogenesis by anterior endoderm. Development. 1995;121:4203-4214.

26. Waldo KL, Kumiski DH, Wallis KT, et al. Conotruncal myocardium arises from a secondary heart field. Development. 2001;128:3179-3188.

27. Kelly RG, Brown NA, Buckingham ME. The arterial pole of the mouse heart forms from Fgf10-expressing cells in pharyngeal mesoderm. Dev Cell. 2001;1:435-440.

28. Camenisch TD, Molin DG, Person A, et al. Temporal and distinct TGFbeta ligand requirements during mouse and avian endocardial cushion morphogenesis. Dev Biol. 2002;248:170-181.

29. Person AD, Klewer SE, Runyan RB. Cell biology of cardiac cushion development. Int Rev Cytol. 2005;243:287-335.

30. Armstrong EJ, Bischoff J. Heart valve development: endothelial cell signaling and differentiation. Circ Res. 2004;95:459-470.

31. Schroeder JA, Jackson LF, Lee DC, Camenisch TD. Form and function of developing heart valves: coordination by extracellular matrix and growth factor signaling. J Mol Med. 2003;81:392-403.

32. Marguerie A, Bajolle F, Zaffran S, et al. Congenital heart defects in Fgfr2-IIIb and Fgf10 mutant mice. Cardiovasc Res. 2006;71:50-60.

33. Ilagan R, Abu-Issa R, Brown D, et al. Fgf8 is required for anterior heart field development. Development. 2006;133:2435-2445.

34. Vincentz JW, McWhirter JR, Murre C, Baldini A, Furuta Y. Fgf15 is required for proper morphogenesis of the mouse cardiac outflow tract. Genesis. 2005;41:192-201.

35. Nanba D, Kinugasa Y, Morimoto C, et al. Loss of HB-EGF in smooth muscle or endothelial cell lineages causes heart malformation. Biochem Biophys Res Commun. 2006;350:315-321.

36. Leveen P, Pekny M, Gebre-Medhin S, Swolin B, Larsson E, Betsholtz C. Mice deficient for PDGF B show renal, cardiovascular, and hematological abnormalities. Genes Dev. 1994;8:1875-1887.

37. Hellstrom M, Kalen M, Lindahl P, Abramsson A, Betsholtz C. Role of PDGF-B and PDGFR-beta in recruitment of vascular smooth muscle cells and pericytes during embryonic blood vessel formation in the mouse. Development. 1999;126:3047-3055.

38. Soriano P. Abnormal kidney development and hematological disorders in PDGF beta-receptor mutant mice. Genes Dev. 1994;8:1888-1896.

39.   Bjarnegard M, Enge M, Norlin J, et al. Endothelium-specific ablation of PDGFB leads to pericyte loss and glomerular, cardiac and placental abnormalities. Development. 2004;131:1847-1857.

40.   Bartram U, Speer CP. The role of transforming growth factor beta in lung development and disease. Chest. 2004;125:754-765.

41.   de Caestecker M. The transforming growth factor-beta superfamily of receptors. Cytokine Growth Factor Rev. 2004;15:1-11.

42.   Saharinen J, Hyytiainen M, Taipale J, Keski-Oja J. Latent transforming growth factor-beta binding proteins (LTBPs)--structural extracellular matrix proteins for targeting TGF-beta action. Cytokine Growth Factor Rev. 1999;10:99-117.

43.   Annes JP, Munger JS, Rifkin DB. Making sense of latent TGFbeta activation. J Cell Sci. 2003;116:217-224.

44.   Wozney JM. The bone morphogenetic protein family and osteogenesis. Mol Reprod Dev. 1992;32:160-167.

45.   Daopin S, Piez KA, Ogawa Y, Davies DR. Crystal structure of transforming growth factor-beta 2: an unusual fold for the superfamily. Science. 1992;257:369-373.

46.   Mittl PR, Priestle JP, Cox DA, McMaster G, Cerletti N, Grutter MG. The crystal structure of TGF-beta 3 and comparison to TGF-beta 2: implications for receptor binding. Protein Sci. 1996;5:1261-1271.

47.   Hinck AP, Archer SJ, Qian SW, et al. Transforming growth factor beta 1: three-dimensional structure in solution and comparison with the X-ray structure of transforming growth factor beta 2. Biochemistry. 1996;35:8517-8534.

48.   Griffith DL, Keck PC, Sampath TK, Rueger DC, Carlson WD. Three-dimensional structure of recombinant human osteogenic protein 1: structural paradigm for the transforming growth factor beta superfamily. Proc Natl Acad Sci U S A. 1996;93:878-883.

49.   Scheufler C, Sebald W, Hulsmeyer M. Crystal structure of human bone morphogenetic protein-2 at 2.7 A resolution. J Mol Biol. 1999;287:103-115.

50.   Thompson TB, Woodruff TK, Jardetzky TS. Structures of an ActRIIB:activin A complex reveal a novel binding mode for TGF-beta ligand:receptor interactions. Embo J. 2003;22:1555-1566.

51. McPherron AC, Lee SJ. GDF-3 and GDF-9: two new members of the transforming growth factor-beta superfamily containing a novel pattern of cysteines. J Biol Chem. 1993;268:3444-3449.

52. Kirsch T, Sebald W, Dreyer MK. Crystal structure of the BMP-2-BRIA ectodomain complex. Nat Struct Biol. 2000;7:492-496.

53. Hart PJ, Deep S, Taylor AB, Shu Z, Hinck CS, Hinck AP. Crystal structure of the human TbetaR2 ectodomain--TGF-beta3 complex. Nat Struct Biol. 2002;9:203-208.

54. Attisano L, Carcamo J, Ventura F, Weis FM, Massague J, Wrana JL. Identification of human activin and TGF beta type I receptors that form heteromeric kinase complexes with type II receptors. Cell. 1993;75:671-680.

55. Nishitoh H, Ichijo H, Kimura M, et al. Identification of type I and type II serine/threonine kinase receptors for growth/differentiation factor-5. J Biol Chem. 1996;271:21345-21352.

56. Yamashita H, ten Dijke P, Huylebroeck D, et al. Osteogenic protein-1 binds to activin type II receptors and induces certain activin-like effects. J Cell Biol. 1995;130:217-226.

57. Gouedard L, Chen YG, Thevenet L, et al. Engagement of bone morphogenetic protein type IB receptor and Smad1 signaling by anti-Mullerian hormone and its type II receptor. J Biol Chem. 2000;275:27973-27978.

58. Wrana JL, Attisano L, Wieser R, Ventura F, Massague J. Mechanism of activation of the TGF-beta receptor. Nature. 1994;370:341-347.

59. ten Dijke P, Yamashita H, Ichijo H, et al. Characterization of type I receptors for transforming growth factor-beta and activin. Science. 1994;264:101-104.

60. ten Dijke P, Yamashita H, Sampath TK, et al. Identification of type I receptors for osteogenic protein-1 and bone morphogenetic protein-4. J Biol Chem. 1994;269:16985-16988.

61. Wrana JL, Attisano L, Carcamo J, et al. TGF beta signals through a heteromeric protein kinase receptor complex. Cell. 1992;71:1003-1014.

62. Ebisawa T, Tada K, Kitajima I, et al. Characterization of bone morphogenetic protein-6 signaling pathways in osteoblast differentiation. J Cell Sci. 1999;112 (Pt 20):3519-3527.

63.   Onichtchouk D, Chen YG, Dosch R, et al. Silencing of TGF-beta signalling by the pseudoreceptor BAMBI. Nature. 1999;401:480-485.

64.   Grotewold L, Plum M, Dildrop R, Peters T, Ruther U. Bambi is coexpressed with Bmp-4 during mouse embryogenesis. Mech Dev. 2001;100:327-330.

65.   Tsang M, Kim R, de Caestecker MP, Kudoh T, Roberts AB, Dawid IB. Zebrafish nma is involved in TGFbeta family signaling. Genesis. 2000;28:47-57.

66.   Karaulanov E, Knochel W, Niehrs C. Transcriptional regulation of BMP4 synexpression in transgenic Xenopus. Embo J. 2004;23:844-856.

67.   Sekiya T, Oda T, Matsuura K, Akiyama T. Transcriptional regulation of the TGF-beta pseudoreceptor BAMBI by TGF-beta signaling. Biochem Biophys Res Commun. 2004;320:680-684.

68.   Heldin CH, Miyazono K, ten Dijke P. TGF-beta signalling from cell membrane to nucleus through SMAD proteins. Nature. 1997;390:465-471.

69.   Kretzschmar M, Liu F, Hata A, Doody J, Massague J. The TGF-beta family mediator Smad1 is phosphorylated directly and activated functionally by the BMP receptor kinase. Genes Dev. 1997;11:984-995.

70.   Derynck R, Gelbart WM, Harland RM, et al. Nomenclature: vertebrate mediators of TGFbeta family signals. Cell. 1996;87:173.

71.   Derynck R, Zhang Y, Feng XH. Smads: transcriptional activators of TGF-beta responses. Cell. 1998;95:737-740.

72.   Massague J. TGF-beta signal transduction. Annu Rev Biochem. 1998;67:753-791.

73.   Cheng J, Grande JP. Transforming growth factor-beta signal transduction and progressive renal disease. Exp Biol Med (Maywood). 2002;227:943-956.

74.   Massague J, Seoane J, Wotton D. Smad transcription factors. Genes Dev. 2005;19:2783-2810.

75.   Shi Y, Massague J. Mechanisms of TGF-beta signaling from cell membrane to the nucleus. Cell. 2003;113:685-700.

76.   Chai J, Wu JW, Yan N, Massague J, Pavletich NP, Shi Y. Features of a Smad3 MH1-DNA complex. Roles of water and zinc in DNA binding. J Biol Chem. 2003;278:20327-20331.

77. Kretzschmar M, Doody J, Timokhina I, Massague J. A mechanism of repression of TGFbeta/ Smad signaling by oncogenic Ras. Genes Dev. 1999;13:804-816.

78. Wicks SJ, Lui S, Abdel-Wahab N, Mason RM, Chantry A. Inactivation of smad-transforming growth factor beta signaling by Ca(2+)-calmodulin-dependent protein kinase II. Mol Cell Biol. 2000;20:8103-8111.

79. Matsuura I, Denissova NG, Wang G, He D, Long J, Liu F. Cyclin-dependent kinases regulate the antiproliferative function of Smads. Nature. 2004;430:226-231.

80. Ho J, Cocolakis E, Dumas VM, Posner BI, Laporte SA, Lebrun JJ. The G protein-coupled receptor kinase-2 is a TGFbeta-inducible antagonist of TGFbeta signal transduction. Embo J. 2005;24:3247-3258.

81. Pera EM, Ikeda A, Eivers E, De Robertis EM. Integration of IGF, FGF, and anti-BMP signals via Smad1 phosphorylation in neural induction. Genes Dev. 2003;17:3023-3028.

82. Grimm OH, Gurdon JB. Nuclear exclusion of Smad2 is a mechanism leading to loss of competence. Nat Cell Biol. 2002;4:519-522.

83. Zhu H, Kavsak P, Abdollah S, Wrana JL, Thomsen GH. A SMAD ubiquitin ligase targets the BMP pathway and affects embryonic pattern formation. Nature. 1999;400:687-693.

84. Feng XH, Filvaroff EH, Derynck R. Transforming growth factor-beta (TGF-beta)-induced down-regulation of cyclin A expression requires a functional TGF-beta receptor complex. Characterization of chimeric and truncated type I and type II receptors. J Biol Chem. 1995;270:24237-24245.

85. Zhang Y, Chang C, Gehling DJ, Hemmati-Brivanlou A, Derynck R. Regulation of Smad degradation and activity by Smurf2, an E3 ubiquitin ligase. Proc Natl Acad Sci U S A. 2001;98:974-979.

86. Ebisawa T, Fukuchi M, Murakami G, et al. Smurf1 interacts with transforming growth factor-beta type I receptor through Smad7 and induces receptor degradation. J Biol Chem. 2001;276:12477-12480.

87. Kavsak P, Rasmussen RK, Causing CG, et al. Smad7 binds to Smurf2 to form an E3 ubiquitin ligase that targets the TGF beta receptor for degradation. Mol Cell. 2000;6:1365-1375.

88.   Watanabe M, Masuyama N, Fukuda M, Nishida E. Regulation of intracellular dynamics of Smad4 by its leucine-rich nuclear export signal. EMBO Rep. 2000;1:176-182.

89.   Wu RY, Zhang Y, Feng XH, Derynck R. Heteromeric and homomeric interactions correlate with signaling activity and functional cooperativity of Smad3 and Smad4/DPC4. Mol Cell Biol. 1997;17:2521-2528.

90.   Lo RS, Chen YG, Shi Y, Pavletich NP, Massague J. The L3 loop: a structural motif determining specific interactions between SMAD proteins and TGF-beta receptors. Embo J. 1998;17:996-1005.

91.   Hayashi H, Abdollah S, Qiu Y, et al. The MAD-related protein Smad7 associates with the TGFbeta receptor and functions as an antagonist of TGFbeta signaling. Cell. 1997;89:1165-1173.

92.   Souchelnytskyi S, Nakayama T, Nakao A, et al. Physical and functional interaction of murine and Xenopus Smad7 with bone morphogenetic protein receptors and transforming growth factor-beta receptors. J Biol Chem. 1998;273:25364-25370.

93.   Feng XH, Zhang Y, Wu RY, Derynck R. The tumor suppressor Smad4/DPC4 and transcriptional adaptor CBP/p300 are coactivators for smad3 in TGF-beta-induced transcriptional activation. Genes Dev. 1998;12:2153-2163.

94.   Pouponnot C, Jayaraman L, Massague J. Physical and functional interaction of SMADs and p300/CBP. J Biol Chem. 1998;273:22865-22868.

95.   Shen X, Hu PP, Liberati NT, Datto MB, Frederick JP, Wang XF. TGF-beta-induced phosphorylation of Smad3 regulates its interaction with coactivator p300/CREB-binding protein. Mol Biol Cell. 1998;9:3309-3319.

96.   Topper JN, DiChiara MR, Brown JD, et al. CREB binding protein is a required coactivator for Smad-dependent, transforming growth factor beta transcriptional responses in endothelial cells. Proc Natl Acad Sci U S A. 1998;95:9506-9511.

97.   Macias-Silva M, Abdollah S, Hoodless PA, Pirone R, Attisano L, Wrana JL. MADR2 is a substrate of the TGFbeta receptor and its phosphorylation is required for nuclear accumulation and signaling. Cell. 1996;87:1215-1224.

98.   Abdollah S, Macias-Silva M, Tsukazaki T, Hayashi H, Attisano L, Wrana JL. TbetaRI phosphorylation of Smad2 on Ser465 and Ser467 is required for Smad2-Smad4 complex formation and signaling. J Biol Chem. 1997;272:27678-27685.

99.   Souchelnytskyi S, Tamaki K, Engstrom U, Wernstedt C, ten Dijke P, Heldin CH. Phosphorylation of Ser465 and Ser467 in the C terminus of Smad2 mediates interaction with Smad4 and is required for transforming growth factor-beta signaling. J Biol Chem. 1997;272:28107-28115.

100.   ten Dijke P, Miyazono K, Heldin CH. Signaling inputs converge on nuclear effectors in TGF-beta signaling. Trends Biochem Sci. 2000;25:64-70.

101.   Dennler S, Itoh S, Vivien D, ten Dijke P, Huet S, Gauthier JM. Direct binding of Smad3 and Smad4 to critical TGF beta-inducible elements in the promoter of human plasminogen activator inhibitor-type 1 gene. Embo J. 1998;17:3091-3100.

102.   Massague J, Chen YG. Controlling TGF-beta signaling. Genes Dev. 2000;14:627-644.

103.   Shi Y, Wang YF, Jayaraman L, Yang H, Massague J, Pavletich NP. Crystal structure of a Smad MH1 domain bound to DNA: insights on DNA binding in TGF-beta signaling. Cell. 1998;94:585-594.

104.   Zawel L, Dai JL, Buckhaults P, et al. Human Smad3 and Smad4 are sequence-specific transcription activators. Mol Cell. 1998;1:611-617.

105.   Kusanagi K, Inoue H, Ishidou Y, Mishima HK, Kawabata M, Miyazono K. Characterization of a bone morphogenetic protein-responsive Smad-binding element. Mol Biol Cell. 2000;11:555-565.

106.   Korchynskyi O, ten Dijke P. Identification and functional characterization of distinct critically important bone morphogenetic protein-specific response elements in the Id1 promoter. J Biol Chem. 2002;277:4883-4891.

107.   Seoane J, Le HV, Shen L, Anderson SA, Massague J. Integration of Smad and forkhead pathways in the control of neuroepithelial and glioblastoma cell proliferation. Cell. 2004;117:211-223.

108.   Chen X, Rubock MJ, Whitman M. A transcriptional partner for MAD proteins in TGF-beta signalling. Nature. 1996;383:691-696.

109.   Chen X, Weisberg E, Fridmacher V, Watanabe M, Naco G, Whitman M. Smad4 and FAST-1 in the assembly of activin-responsive factor. Nature. 1997;389:85-89.

110.   Shibuya H, Yamaguchi K, Shirakabe K, et al. TAB1: an activator of the TAK1 MAPKKK in TGF-beta signal transduction. Science. 1996;272:1179-1182.

111.   Yamaguchi K, Nagai S, Ninomiya-Tsuji J, et al. XIAP, a cellular member of the inhibitor of apoptosis protein family, links the receptors to TAB1-TAK1 in the BMP signaling pathway. Embo J. 1999;18:179-187.

112.   Shim JH, Xiao C, Paschal AE, et al. TAK1, but not TAB1 or TAB2, plays an essential role in multiple signaling pathways in vivo. Genes Dev. 2005;19:2668-2681.

113.   Edlund S, Bu S, Schuster N, et al. Transforming growth factor-beta1 (TGF-beta)-induced apoptosis of prostate cancer cells involves Smad7-dependent activation of p38 by TGF-beta-activated kinase 1 and mitogen-activated protein kinase kinase 3. Mol Biol Cell. 2003;14:529-544.

114.   Yu L, Hebert MC, Zhang YE. TGF-beta receptor-activated p38 MAP kinase mediates Smad-independent TGF-beta responses. Embo J. 2002;21:3749-3759.

115.   Arsura M, Panta GR, Bilyeu JD, et al. Transient activation of NF-kappaB through a TAK1/IKK kinase pathway by TGF-beta1 inhibits AP-1/SMAD signaling and apoptosis: implications in liver tumor formation. Oncogene. 2003;22:412-425.

116.   Yue J, Mulder KM. Activation of the mitogen-activated protein kinase pathway by transforming growth factor-beta. Methods Mol Biol. 2000;142:125-131.

117.   Moustakas A, Heldin CH. Non-Smad TGF-beta signals. J Cell Sci. 2005;118:3573-3584.

118.   Cate RL, Mattaliano RJ, Hession C, et al. Isolation of the bovine and human genes for Mullerian inhibiting substance and expression of the human gene in animal cells. Cell. 1986;45:685-698.

119.   De Jong FH. Inhibin. Physiol Rev. 1988;68:555-607.

120.   Ling N, Ying SY, Ueno N, et al. Pituitary FSH is released by a heterodimer of the beta-subunits from the two forms of inhibin. Nature. 1986;321:779-782.

121.   Vale W, Rivier J, Vaughan J, et al. Purification and characterization of an FSH releasing protein from porcine ovarian follicular fluid. Nature. 1986;321:776-779.

122.   Dickson MC, Martin JS, Cousins FM, Kulkarni AB, Karlsson S, Akhurst RJ. Defective haematopoiesis and vasculogenesis in transforming growth factor-beta 1 knock out mice. Development. 1995;121:1845-1854.

123. Sanford LP, Ormsby I, Gittenberger-de Groot AC, et al. TGFbeta2 knockout mice have multiple developmental defects that are non-overlapping with other TGFbeta knockout phenotypes. Development. 1997;124:2659-2670.

124. Proetzel G, Pawlowski SA, Wiles MV, et al. Transforming growth factor-beta 3 is required for secondary palate fusion. Nat Genet. 1995;11:409-414.

125. Urist MR. Bone: formation by autoinduction. Science. 1965;150:893-899.

126. Hogan BL. Bone morphogenetic proteins: multifunctional regulators of vertebrate development. Genes Dev. 1996;10:1580-1594.

127. Balemans W, Van Hul W. Extracellular regulation of BMP signaling in vertebrates: a cocktail of modulators. Dev Biol. 2002;250:231-250.

128. Shimasaki S, Moore RK, Otsuka F, Erickson GF. The bone morphogenetic protein system in mammalian reproduction. Endocr Rev. 2004;25:72-101.

129. Zhao GQ, Garbers DL. Male germ cell specification and differentiation. Dev Cell. 2002;2:537-547.

130. Tobin JF, Celeste AJ. Bone morphogenetic proteins and growth differentiation factors as drug targets in cardiovascular and metabolic disease. Drug Discov Today. 2006;11:405-411.

131. Kawabata M, Imamura T, Miyazono K. Signal transduction by bone morphogenetic proteins. Cytokine Growth Factor Rev. 1998;9:49-61.

132. Macias-Silva M, Hoodless PA, Tang SJ, Buchwald M, Wrana JL. Specific activation of Smad1 signaling pathways by the BMP7 type I receptor, ALK2. J Biol Chem. 1998;273:25628-25636.

133. David L, Mallet C, Mazerbourg S, Feige JJ, Bailly S. Identification of BMP9 and BMP10 as functional activators of the orphan activin receptor-like kinase 1 (ALK1) in endothelial cells. Blood. 2007;109:1953-1961.

134. Kawabata M, Inoue H, Hanyu A, Imamura T, Miyazono K. Smad proteins exist as monomers in vivo and undergo homo- and hetero-oligomerization upon activation by serine/threonine kinase receptors. Embo J. 1998;17:4056-4065.

135. Friedle H, Knochel W. Cooperative interaction of Xvent-2 and GATA-2 in the activation of the ventral homeobox gene Xvent-1B. J Biol Chem. 2002;277:23872-23881.

136. Hollnagel A, Oehlmann V, Heymer J, Ruther U, Nordheim A. Id genes are direct targets of bone morphogenetic protein induction in embryonic stem cells. J Biol Chem. 1999;274:19838-19845.

137. Hussein SM, Duff EK, Sirard C. Smad4 and beta-catenin co-activators functionally interact with lymphoid-enhancing factor to regulate graded expression of Msx2. J Biol Chem. 2003;278:48805-48814.

138. Ladher R, Mohun TJ, Smith JC, Snape AM. Xom: a Xenopus homeobox gene that mediates the early effects of BMP-4. Development. 1996;122:2385-2394.

139. Miyama K, Yamada G, Yamamoto TS, et al. A BMP-inducible gene, dlx5, regulates osteoblast differentiation and mesoderm induction. Dev Biol. 1999;208:123-133.

140. Peiffer DA, Von Bubnoff A, Shin Y, et al. A Xenopus DNA microarray approach to identify novel direct BMP target genes involved in early embryonic development. Dev Dyn. 2005;232:445-456.

141. Rastegar S, Friedle H, Frommer G, Knochel W. Transcriptional regulation of Xvent homeobox genes. Mech Dev. 1999;81:139-149.

142. Yoshida Y, Tanaka S, Umemori H, et al. Negative regulation of BMP/Smad signaling by Tob in osteoblasts. Cell. 2000;103:1085-1097.

143. Nohe A, Hassel S, Ehrlich M, et al. The mode of bone morphogenetic protein (BMP) receptor oligomerization determines different BMP-2 signaling pathways. J Biol Chem. 2002;277:5330-5338.

144. Moser M, Binder O, Wu Y, et al. BMPER, a novel endothelial cell precursor-derived protein, antagonizes bone morphogenetic protein signaling and endothelial cell differentiation. Mol Cell Biol. 2003;23:5664-5679.

145. Adelman CA, Chattopadhyay S, Bieker JJ. The BMP/BMPR/Smad pathway directs expression of the erythroid-specific EKLF and GATA1 transcription factors during embryoid body differentiation in serum-free media. Development. 2002;129:539-549.

146. Walmsley M, Ciau-Uitz A, Patient R. Adult and embryonic blood and endothelium derive from distinct precursor populations which are differentially programmed by BMP in Xenopus. Development. 2002;129:5683-5695.

147. Langenfeld EM, Langenfeld J. Bone morphogenetic protein-2 stimulates angiogenesis in developing tumors. Mol Cancer Res. 2004;2:141-149.

148.	Rothhammer T, Bataille F, Spruss T, Eissner G, Bosserhoff AK. Functional implication of BMP4 expression on angiogenesis in malignant melanoma. Oncogene. 2006.

149.	Valdimarsdottir G, Goumans MJ, Rosendahl A, et al. Stimulation of Id1 expression by bone morphogenetic protein is sufficient and necessary for bone morphogenetic protein-induced activation of endothelial cells. Circulation. 2002;106:2263-2270.

150.	Kiyono M, Shibuya M. Bone morphogenetic protein 4 mediates apoptosis of capillary endothelial cells during rat pupillary membrane regression. Mol Cell Biol. 2003;23:4627-4636.

151.	Weaver M, Batts L, Hogan BL. Tissue interactions pattern the mesenchyme of the embryonic mouse lung. Dev Biol. 2003;258:169-184.

152.	King JA, Marker PC, Seung KJ, Kingsley DM. BMP5 and the molecular, skeletal, and soft-tissue alterations in short ear mice. Dev Biol. 1994;166:112-122.

153.	Bellusci S, Henderson R, Winnier G, Oikawa T, Hogan BL. Evidence from normal expression and targeted misexpression that bone morphogenetic protein (Bmp-4) plays a role in mouse embryonic lung morphogenesis. Development. 1996;122:1693-1702.

154.	Verschueren K, Dewulf N, Goumans MJ, et al. Expression of type I and type IB receptors for activin in midgestation mouse embryos suggests distinct functions in organogenesis. Mech Dev. 1995;52:109-123.

155.	Dewulf N, Verschueren K, Lonnoy O, et al. Distinct spatial and temporal expression patterns of two type I receptors for bone morphogenetic proteins during mouse embryogenesis. Endocrinology. 1995;136:2652-2663.

156.	Bragg AD, Moses HL, Serra R. Signaling to the epithelium is not sufficient to mediate all of the effects of transforming growth factor beta and bone morphogenetic protein 4 on murine embryonic lung development. Mech Dev. 2001;109:13-26.

157.	Weaver M, Yingling JM, Dunn NR, Bellusci S, Hogan BL. Bmp signaling regulates proximal-distal differentiation of endoderm in mouse lung development. Development. 1999;126:4005-4015.

158.	Lu MM, Yang H, Zhang L, Shu W, Blair DG, Morrisey EE. The bone morphogenic protein antagonist gremlin regulates proximal-distal patterning of the lung. Dev Dyn. 2001;222:667-680.

159. Eblaghie MC, Reedy M, Oliver T, Mishina Y, Hogan BL. Evidence that autocrine signaling through Bmpr1a regulates the proliferation, survival and morphogenetic behavior of distal lung epithelial cells. Dev Biol. 2006;291:67-82.

160. Nakajima Y, Yamagishi T, Hokari S, Nakamura H. Mechanisms involved in valvuloseptal endocardial cushion formation in early cardiogenesis: roles of transforming growth factor (TGF)-beta and bone morphogenetic protein (BMP). Anat Rec. 2000;258:119-127.

161. Keyes WM, Logan C, Parker E, Sanders EJ. Expression and function of bone morphogenetic proteins in the development of the embryonic endocardial cushions. Anat Embryol (Berl). 2003;207:135-147.

162. Delot EC, Bahamonde ME, Zhao M, Lyons KM. BMP signaling is required for septation of the outflow tract of the mammalian heart. Development. 2003;130:209-220.

163. Kim RY, Robertson EJ, Solloway MJ. Bmp6 and Bmp7 are required for cushion formation and septation in the developing mouse heart. Dev Biol. 2001;235:449-466.

164. Abdelwahid E, Rice D, Pelliniemi LJ, Jokinen E. Overlapping and differential localization of Bmp-2, Bmp-4, Msx-2 and apoptosis in the endocardial cushion and adjacent tissues of the developing mouse heart. Cell Tissue Res. 2001;305:67-78.

165. Jones CM, Lyons KM, Hogan BL. Involvement of Bone Morphogenetic Protein-4 (BMP-4) and Vgr-1 in morphogenesis and neurogenesis in the mouse. Development. 1991;111:531-542.

166. Lyons KM, Hogan BL, Robertson EJ. Colocalization of BMP 7 and BMP 2 RNAs suggests that these factors cooperatively mediate tissue interactions during murine development. Mech Dev. 1995;50:71-83.

167. Solloway MJ, Robertson EJ. Early embryonic lethality in Bmp5;Bmp7 double mutant mice suggests functional redundancy within the 60A subgroup. Development. 1999;126:1753-1768.

168. Mishina Y, Suzuki A, Ueno N, Behringer RR. Bmpr encodes a type I bone morphogenetic protein receptor that is essential for gastrulation during mouse embryogenesis. Genes Dev. 1995;9:3027-3037.

169. Roelen BA, Goumans MJ, van Rooijen MA, Mummery CL. Differential expression of BMP receptors in early mouse development. Int J Dev Biol. 1997;41:541-549.

170. Yuasa S, Itabashi Y, Koshimizu U, et al. Transient inhibition of BMP signaling by Noggin induces cardiomyocyte differentiation of mouse embryonic stem cells. Nat Biotechnol. 2005;23:607-611.

171. Choi M, Stottmann RW, Yang YP, Meyers EN, Klingensmith J. The bone morphogenetic protein antagonist noggin regulates mammalian cardiac morphogenesis. Circ Res. 2007;100:220-228.

172. Ma L, Lu MF, Schwartz RJ, Martin JF. Bmp2 is essential for cardiac cushion epithelial-mesenchymal transition and myocardial patterning. Development. 2005;132:5601-5611.

173. Rivera-Feliciano J, Tabin CJ. Bmp2 instructs cardiac progenitors to form the heart-valve-inducing field. Dev Biol. 2006;295:580-588.

174. Liu W, Selever J, Wang D, et al. Bmp4 signaling is required for outflow-tract septation and branchial-arch artery remodeling. Proc Natl Acad Sci U S A. 2004;101:4489-4494.

175. Kingsley DM, Bland AE, Grubber JM, et al. The mouse short ear skeletal morphogenesis locus is associated with defects in a bone morphogenetic member of the TGF beta superfamily. Cell. 1992;71:399-410.

176. Solloway MJ, Dudley AT, Bikoff EK, Lyons KM, Hogan BL, Robertson EJ. Mice lacking Bmp6 function. Dev Genet. 1998;22:321-339.

177. Dudley AT, Robertson EJ. Overlapping expression domains of bone morphogenetic protein family members potentially account for limited tissue defects in BMP7 deficient embryos. Dev Dyn. 1997;208:349-362.

178. Gaussin V, Van de Putte T, Mishina Y, et al. Endocardial cushion and myocardial defects after cardiac myocyte-specific conditional deletion of the bone morphogenetic protein receptor ALK3. Proc Natl Acad Sci U S A. 2002;99:2878-2883.

179. Song L, Fassler R, Mishina Y, Jiao K, Baldwin HS. Essential functions of Alk3 during AV cushion morphogenesis in mouse embryonic hearts. Dev Biol. 2007;301:276-286.

180. Zimmerman LB, De Jesus-Escobar JM, Harland RM. The Spemann organizer signal noggin binds and inactivates bone morphogenetic protein 4. Cell. 1996;86:599-606.

181. Bachiller D, Klingensmith J, Kemp C, et al. The organizer factors Chordin and Noggin are required for mouse forebrain development. Nature. 2000;403:658-661.

182. Stottmann RW, Anderson RM, Klingensmith J. The BMP antagonists Chordin and Noggin have essential but redundant roles in mouse mandibular outgrowth. Dev Biol. 2001;240:457-473.

183. Coffinier C, Ketpura N, Tran U, Geissert D, De Robertis EM. Mouse Crossveinless-2 is the vertebrate homolog of a Drosophila extracellular regulator of BMP signaling. Mech Dev. 2002;119 Suppl 1:S179-184.

184. Farrington SM, Belaoussoff M, Baron MH. Winged-helix, Hedgehog and Bmp genes are differentially expressed in distinct cell layers of the murine yolk sac. Mech Dev. 1997;62:197-211.

185. Marshall CJ, Kinnon C, Thrasher AJ. Polarized expression of bone morphogenetic protein-4 in the human aorta-gonad-mesonephros region. Blood. 2000;96:1591-1593.

186. Coles E, Christiansen J, Economou A, Bronner-Fraser M, Wilkinson DG. A vertebrate crossveinless 2 homologue modulates BMP activity and neural crest cell migration. Development. 2004;131:5309-5317.

187. Binnerts ME, Wen X, Cante-Barrett K, et al. Human Crossveinless-2 is a novel inhibitor of bone morphogenetic proteins. Biochem Biophys Res Commun. 2004;315:272-280.

188. Garcia-Bellido A, de Celis JF. Developmental genetics of the venation pattern of Drosophila. Annu Rev Genet. 1992;26:277-304.

189. Conley CA, Silburn R, Singer MA, et al. Crossveinless 2 contains cysteine-rich domains and is required for high levels of BMP-like activity during the formation of the cross veins in Drosophila. Development. 2000;127:3947-3959.

190. Ralston A, Blair SS. Long-range Dpp signaling is regulated to restrict BMP signaling to a crossvein competent zone. Dev Biol. 2005;280:187-200.

191. O'Connor MB, Umulis D, Othmer HG, Blair SS. Shaping BMP morphogen gradients in the Drosophila embryo and pupal wing. Development. 2006;133:183-193.

192. Kamimura M, Matsumoto K, Koshiba-Takeuchi K, Ogura T. Vertebrate crossveinless 2 is secreted and acts as an extracellular modulator of the BMP signaling cascade. Dev Dyn. 2004;230:434-445.

193. Rentzsch F, Zhang J, Kramer C, Sebald W, Hammerschmidt M. Crossveinless 2 is an essential positive feedback regulator of Bmp signaling during zebrafish gastrulation. Development. 2006;133:801-811.

194. Larrain J, Bachiller D, Lu B, Agius E, Piccolo S, De Robertis EM. BMP-binding modules in chordin: a model for signalling regulation in the extracellular space. Development. 2000;127:821-830.

195. Oelgeschlager M, Larrain J, Geissert D, De Robertis EM. The evolutionarily conserved BMP-binding protein Twisted gastrulation promotes BMP signalling. Nature. 2000;405:757-763.

196. Chang C, Holtzman DA, Chau S, et al. Twisted gastrulation can function as a BMP antagonist. Nature. 2001;410:483-487.

197. Ross JJ, Shimmi O, Vilmos P, et al. Twisted gastrulation is a conserved extracellular BMP antagonist. Nature. 2001;410:479-483.

198. Scott IC, Blitz IL, Pappano WN, Maas SA, Cho KW, Greenspan DS. Homologues of Twisted gastrulation are extracellular cofactors in antagonism of BMP signalling. Nature. 2001;410:475-478.

199. Larrain J, Oelgeschlager M, Ketpura NI, Reversade B, Zakin L, De Robertis EM. Proteolytic cleavage of Chordin as a switch for the dual activities of Twisted gastrulation in BMP signaling. Development. 2001;128:4439-4447.

200. Graf D, Timmons PM, Hitchins M, et al. Evolutionary conservation, developmental expression, and genomic mapping of mammalian Twisted gastrulation. Mamm Genome. 2001;12:554-560.

201. Piccolo S, Agius E, Lu B, Goodman S, Dale L, De Robertis EM. Cleavage of Chordin by Xolloid metalloprotease suggests a role for proteolytic processing in the regulation of Spemann organizer activity. Cell. 1997;91:407-416.

202. Marques G, Musacchio M, Shimell MJ, Wunnenberg-Stapleton K, Cho KW, O'Connor MB. Production of a DPP activity gradient in the early Drosophila embryo through the opposing actions of the SOG and TLD proteins. Cell. 1997;91:417-426.

203. Scott IC, Blitz IL, Pappano WN, et al. Mammalian BMP-1/Tolloid-related metalloproteinases, including novel family member mammalian Tolloid-like 2, have differential enzymatic activities and distributions of expression relevant to patterning and skeletogenesis. Dev Biol. 1999;213:283-300.

204. Shimmi O, O'Connor MB. Physical properties of Tld, Sog, Tsg and Dpp protein interactions are predicted to help create a sharp boundary in Bmp signals during dorsoventral patterning of the Drosophila embryo. Development. 2003;130:4673-4682.

205. Oelgeschlager M, Reversade B, Larrain J, Little S, Mullins MC, De Robertis EM. The pro-BMP activity of Twisted gastrulation is independent of BMP binding. Development. 2003;130:4047-4056.

206. Schulte-Merker S, Lee KJ, McMahon AP, Hammerschmidt M. The zebrafish organizer requires chordino. Nature. 1997;387:862-863.

207. Ducy P, Karsenty G. The family of bone morphogenetic proteins. Kidney Int. 2000;57:2207-2214.

208. Miyazono K, ten Dijke P, Heldin CH. TGF-beta signaling by Smad proteins. Adv Immunol. 2000;75:115-157.

209. Hata A, Seoane J, Lagna G, Montalvo E, Hemmati-Brivanlou A, Massague J. OAZ uses distinct DNA- and protein-binding zinc fingers in separate BMP-Smad and Olf signaling pathways. Cell. Vol. 100; 2000:229-240.

210. Henningfeld KA, Friedle H, Rastegar S, Knochel W. Autoregulation of Xvent-2B; direct interaction and functional cooperation of Xvent-2 and Smad1. J Biol Chem. 2002;277:2097-2103.

211. Koki AT, Masferrer JL. Celecoxib: a specific COX-2 inhibitor with anticancer properties. Cancer Control. 2002;9:28-35.

212. Bolli R, Shinmura K, Tang XL, et al. Discovery of a new function of cyclooxygenase (COX)-2: COX-2 is a cardioprotective protein that alleviates ischemia/reperfusion injury and mediates the late phase of preconditioning. Cardiovasc Res. 2002;55:506-519.

213. Garcia Rodriguez LA. The effect of NSAIDs on the risk of coronary heart disease: fusion of clinical pharmacology and pharmacoepidemiologic data. Clin Exp Rheumatol. 2001;19:S41-44.

214. Gottlieb S. COX 2 inhibitors may increase risk of heart attack. Bmj. 2001;323:471.

215. Wang Y, Kodani E, Wang J, et al. Cardioprotection during the final stage of the late phase of ischemic preconditioning is mediated by neuronal NO synthase in concert with cyclooxygenase-2. Circ Res. 2004;95:84-91.

216. Shinmura K, Tang XL, Wang Y, et al. Cyclooxygenase-2 mediates the cardioprotective effects of the late phase of ischemic preconditioning in conscious rabbits. Proc Natl Acad Sci U S A. 2000;97:10197-10202.

217. Araki Y, Okamura S, Hussain SP, et al. Regulation of cyclooxygenase-2 expression by the Wnt and ras pathways. Cancer Res. 2003;63:728-734.

218. Chikazu D, Li X, Kawaguchi H, et al. Bone morphogenetic protein 2 induces cyclo-oxygenase 2 in osteoblasts via a Cbfal binding site: role in effects of bone morphogenetic protein 2 in vitro and in vivo. J Bone Miner Res. 2002;17:1430-1440.

219. He XR, Zhang C, Patterson C. Universal mouse reference RNA derived from neonatal mice. Biotechniques. 2004;37:464-468.

220. Eisen MB, Spellman PT, Brown PO, Botstein D. Cluster analysis and display of genome-wide expression patterns. Proc Natl Acad Sci U S A. 1998;95:14863-14868.

221. Ruef J, Meshel AS, Hu Z, et al. Flavopiridol inhibits smooth muscle cell proliferation in vitro and neointimal formation In vivo after carotid injury in the rat. Circulation. 1999;100:659-665.

222. Masson VV, Devy L, Grignet-Debrus C, et al. Mouse Aortic Ring Assay: A New Approach of the Molecular Genetics of Angiogenesis. Biol Proced Online. 2002;4:24-31.

223. Luque A, Carpizo DR, Iruela-Arispe ML. ADAMTS1/METH1 inhibits endothelial cell proliferation by direct binding and sequestration of VEGF165. J Biol Chem. 2003;278:23656-23665.

224. Thiemermann C. Biosynthesis and interaction of endothelium-derived vasoactive mediators. Eicosanoids. 1991;4:187-202.

225. Kirtikara K, Raghow R, Laulederkind SJ, Goorha S, Kanekura T, Ballou LR. Transcriptional regulation of cyclooxygenase-2 in the human microvascular endothelial cell line, HMEC-1: control by the combinatorial actions of AP2, NF-IL-6 and CRE elements. Mol Cell Biochem. 2000;203:41-51.

226. Jobin C, Morteau O, Han DS, Balfour Sartor R. Specific NF-kappaB blockade selectively inhibits tumour necrosis factor-alpha-induced COX-2 but not constitutive COX-1 gene expression in HT-29 cells. Immunology. 1998;95:537-543.

227. Zhang Y, Feng X, We R, Derynck R. Receptor-associated Mad homologues synergize as effectors of the TGF-beta response. Nature. 1996;383:168-172.

228. Nakao A, Imamura T, Souchelnytskyi S, et al. TGF-beta receptor-mediated signalling through Smad2, Smad3 and Smad4. Embo J. 1997;16:5353-5362.

229. Maliekal TT, Anto RJ, Karunagaran D. Differential activation of Smads in HeLa and SiHa cells that differ in their response to transforming growth factor-beta. J Biol Chem. 2004;279:36287-36292.

230. Kuwano T, Nakao S, Yamamoto H, et al. Cyclooxygenase 2 is a key enzyme for inflammatory cytokine-induced angiogenesis. Faseb J. 2004;18:300-310.

231. Akarasereenont PC, Techatraisak K, Thaworn A, Chotewuttakorn S. The expression of COX-2 in VEGF-treated endothelial cells is mediated through protein tyrosine kinase. Mediators Inflamm. 2002;11:17-22.

232. Wu G, Luo J, Rana JS, Laham R, Sellke FW, Li J. Involvement of COX-2 in VEGF-induced angiogenesis via P38 and JNK pathways in vascular endothelial cells. Cardiovasc Res. 2006;69:512-519.

233. Wang H, Charles PC, Wu Y, et al. Gene Expression Profile Signatures Indicate a Role for Wnt Signaling in Endothelial Commitment From Embryonic Stem Cells. Circ Res. 2006.

234. Goppelt-Struebe M. Regulation of prostaglandin endoperoxide synthase (cyclooxygenase) isozyme expression. Prostaglandins Leukot Essent Fatty Acids. 1995;52:213-222.

235. Sheng H, Shao J, Washington MK, DuBois RN. Prostaglandin E2 increases growth and motility of colorectal carcinoma cells. J Biol Chem. 2001;276:18075-18081.

236. Sheng H, Shao J, Morrow JD, Beauchamp RD, DuBois RN. Modulation of apoptosis and Bcl-2 expression by prostaglandin E2 in human colon cancer cells. Cancer Res. 1998;58:362-366.

237. Ben-Av P, Crofford LJ, Wilder RL, Hla T. Induction of vascular endothelial growth factor expression in synovial fibroblasts by prostaglandin E and interleukin-1: a potential mechanism for inflammatory angiogenesis. FEBS Lett. 1995;372:83-87.

238. Tsuji S, Kawano S, Tsujii M, et al. [Mucosal microcirculation and angiogenesis in gastrointestinal tract]. Nippon Rinsho. 1998;56:2247-2252.

239. Damrongsri D, Geva S, Salvi GE, Williams RC, Limwongse V, Offenbacher S. Cyclooxygenase-2 inhibition selectively attenuates bone morphogenetic protein-6 synthesis and bone formation during guided tissue regeneration in a rat model. Clin Oral Implants Res. 2006;17:38-47.

240.	Evans SM, Tai LJ, Tan VP, Newton CB, Chien KR. Heterokaryons of cardiac myocytes and fibroblasts reveal the lack of dominance of the cardiac muscle phenotype. Mol Cell Biol. 1994;14:4269-4279.

241.	Ikeya M, Kawada M, Kiyonari H, et al. Essential pro-Bmp roles of crossveinless 2 in mouse organogenesis. Development. 2006;133:4463-4473.

242.	Dai Q, Zhang C, Wu Y, et al. CHIP activates HSF1 and confers protection against apoptosis and cellular stress. Embo J. 2003;22:5446-5458.

243.	Caron KM, Smithies O. Extreme hydrops fetalis and cardiovascular abnormalities in mice lacking a functional Adrenomedullin gene. Proc Natl Acad Sci U S A. 2001;98:615-619.

244.	Kedar V, McDonough H, Arya R, Li HH, Rockman HA, Patterson C. Muscle-specific RING finger 1 is a bona fide ubiquitin ligase that degrades cardiac troponin I. Proc Natl Acad Sci U S A. 2004;101:18135-18140.

245.	Li Q, Estepa G, Memet S, Israel A, Verma IM. Complete lack of NF-kappaB activity in IKK1 and IKK2 double-deficient mice: additional defect in neurulation. Genes Dev. 2000;14:1729-1733.

246.	Uren A, Reichsman F, Anest V, et al. Secreted frizzled-related protein-1 binds directly to Wingless and is a biphasic modulator of Wnt signaling. J Biol Chem. 2000;275:4374-4382.

247.	Izumi M, Fujio Y, Kunisada K, et al. Bone morphogenetic protein-2 inhibits serum deprivation-induced apoptosis of neonatal cardiac myocytes through activation of the Smad1 pathway. J Biol Chem. 2001;276:31133-31141.

248.	Xing W, Zhang TC, Cao D, et al. Myocardin induces cardiomyocyte hypertrophy. Circ Res. 2006;98:1089-1097.

249.	Willis MS, Ike C, Li L, Wang DZ, Glass DJ, Patterson C. Muscle ring finger 1, but not muscle ring finger 2, regulates cardiac hypertrophy in vivo. Circ Res. 2007;100:456-459.

250.	Inoue H, Nanayama T, Hara S, Yokoyama C, Tanabe T. The cyclic AMP response element plays an essential role in the expression of the human prostaglandin-endoperoxide synthase 2 gene in differentiated U937 monocytic cells. FEBS Lett. 1994;350:51-54.

251. Inoue H, Yokoyama C, Hara S, Tone Y, Tanabe T. Transcriptional regulation of human prostaglandin-endoperoxide synthase-2 gene by lipopolysaccharide and phorbol ester in vascular endothelial cells. Involvement of both nuclear factor for interleukin-6 expression site and cAMP response element. J Biol Chem. 1995;270:24965-24971.

252. Kosaka T, Miyata A, Ihara H, et al. Characterization of the human gene (PTGS2) encoding prostaglandin-endoperoxide synthase 2. Eur J Biochem. 1994;221:889-897.

253. Subbaramaiah K, Telang N, Ramonetti JT, et al. Transcription of cyclooxygenase-2 is enhanced in transformed mammary epithelial cells. Cancer Res. 1996;56:4424-4429.

254. Xie W, Herschman HR. v-src induces prostaglandin synthase 2 gene expression by activation of the c-Jun N-terminal kinase and the c-Jun transcription factor. J Biol Chem. 1995;270:27622-27628.

255. Hwang D, Jang BC, Yu G, Boudreau M. Expression of mitogen-inducible cyclooxygenase induced by lipopolysaccharide: mediation through both mitogen-activated protein kinase and NF-kappaB signaling pathways in macrophages. Biochem Pharmacol. 1997;54:87-96.

256. Inoue H, Tanabe T. Transcriptional role of the nuclear factor kappa B site in the induction by lipopolysaccharide and suppression by dexamethasone of cyclooxygenase-2 in U937 cells. Biochem Biophys Res Commun. 1998;244:143-148.

257. Wadleigh DJ, Reddy ST, Kopp E, Ghosh S, Herschman HR. Transcriptional activation of the cyclooxygenase-2 gene in endotoxin-treated RAW 264.7 macrophages. J Biol Chem. 2000;275:6259-6266.

258. Mestre JR, Mackrell PJ, Rivadeneira DE, Stapleton PP, Tanabe T, Daly JM. Redundancy in the signaling pathways and promoter elements regulating cyclooxygenase-2 gene expression in endotoxin-treated macrophage/monocytic cells. J Biol Chem. 2001;276:3977-3982.

259. Morita I. Distinct functions of COX-1 and COX-2. Prostaglandins Other Lipid Mediat. 2002;68-69:165-175.

260. Tanabe T, Tohnai N. Cyclooxygenase isozymes and their gene structures and expression. Prostaglandins Other Lipid Mediat. 2002;68-69:95-114.

261. Park JY, Pillinger MH, Abramson SB. Prostaglandin E2 synthesis and secretion: the role of PGE2 synthases. Clin Immunol. 2006;119:229-240.

262. Tanioka T, Nakatani Y, Semmyo N, Murakami M, Kudo I. Molecular identification of cytosolic prostaglandin E2 synthase that is functionally coupled with cyclooxygenase-1 in immediate prostaglandin E2 biosynthesis. J Biol Chem. 2000;275:32775-32782.

263. Murakami M, Naraba H, Tanioka T, et al. Regulation of prostaglandin E2 biosynthesis by inducible membrane-associated prostaglandin E2 synthase that acts in concert with cyclooxygenase-2. J Biol Chem. 2000;275:32783-32792.

264. Jakobsson PJ, Thoren S, Morgenstern R, Samuelsson B. Identification of human prostaglandin E synthase: a microsomal, glutathione-dependent, inducible enzyme, constituting a potential novel drug target. Proc Natl Acad Sci U S A. 1999;96:7220-7225.

265. Thoren S, Jakobsson PJ. Coordinate up- and down-regulation of glutathione-dependent prostaglandin E synthase and cyclooxygenase-2 in A549 cells. Inhibition by NS-398 and leukotriene C4. Eur J Biochem. 2000;267:6428-6434.

266. Silverstein FE, Faich G, Goldstein JL, et al. Gastrointestinal toxicity with celecoxib vs nonsteroidal anti-inflammatory drugs for osteoarthritis and rheumatoid arthritis: the CLASS study: A randomized controlled trial. Celecoxib Long-term Arthritis Safety Study. Jama. 2000;284:1247-1255.

267. Bresalier RS, Sandler RS, Quan H, et al. Cardiovascular events associated with rofecoxib in a colorectal adenoma chemoprevention trial. N Engl J Med. 2005;352:1092-1102.

268. Solomon SD, McMurray JJ, Pfeffer MA, et al. Cardiovascular risk associated with celecoxib in a clinical trial for colorectal adenoma prevention. N Engl J Med. 2005;352:1071-1080.

269. Cullen L, Kelly L, Connor SO, Fitzgerald DJ. Selective cyclooxygenase-2 inhibition by nimesulide in man. J Pharmacol Exp Ther. 1998;287:578-582.

270. McAdam BF, Catella-Lawson F, Mardini IA, Kapoor S, Lawson JA, FitzGerald GA. Systemic biosynthesis of prostacyclin by cyclooxygenase (COX)-2: the human pharmacology of a selective inhibitor of COX-2. Proc Natl Acad Sci U S A. 1999;96:272-277.

271. FitzGerald GA. Mechanisms of platelet activation: thromboxane A2 as an amplifying signal for other agonists. Am J Cardiol. 1991;68:11B-15B.

272.   FitzGerald GA. COX-2 and beyond: Approaches to prostaglandin inhibition in human disease. Nat Rev Drug Discov. 2003;2:879-890.

273.   Kirkpatrick K, Ogunkolade W, Elkak A, et al. The mRNA expression of cyclo-oxygenase-2 (COX-2) and vascular endothelial growth factor (VEGF) in human breast cancer. Curr Med Res Opin. 2002;18:237-241.

274.   Eberhart CE, Coffey RJ, Radhika A, Giardiello FM, Ferrenbach S, DuBois RN. Up-regulation of cyclooxygenase 2 gene expression in human colorectal adenomas and adenocarcinomas. Gastroenterology. 1994;107:1183-1188.

275.   Elder DJ, Baker JA, Banu NA, Moorghen M, Paraskeva C. Human colorectal adenomas demonstrate a size-dependent increase in epithelial cyclooxygenase-2 expression. J Pathol. 2002;198:428-434.

276.   Hao X, Bishop AE, Wallace M, et al. Early expression of cyclo-oxygenase-2 during sporadic colorectal carcinogenesis. J Pathol. 1999;187:295-301.

277.   Oshima M, Dinchuk JE, Kargman SL, et al. Suppression of intestinal polyposis in Apc delta716 knockout mice by inhibition of cyclooxygenase 2 (COX-2). Cell. 1996;87:803-809.

278.   Steinbach G, Lynch PM, Phillips RK, et al. The effect of celecoxib, a cyclooxygenase-2 inhibitor, in familial adenomatous polyposis. N Engl J Med. 2000;342:1946-1952.

279.   De Bosscher K, Hill CS, Nicolas FJ. Molecular and functional consequences of Smad4 C-terminal missense mutations in colorectal tumour cells. Biochem J. 2004;379:209-216.

280.   Zhou XP, Woodford-Richens K, Lehtonen R, et al. Germline mutations in BMPR1A/ALK3 cause a subset of cases of juvenile polyposis syndrome and of Cowden and Bannayan-Riley-Ruvalcaba syndromes. Am J Hum Genet. 2001;69:704-711.

281.   Thomas BG, Hamdy FC. Bone morphogenetic protein-6: potential mediator of osteoblastic metastases in prostate cancer. Prostate Cancer Prostatic Dis. 2000;3:283-285.

282.   De Pinieux G, Flam T, Zerbib M, et al. Bone sialoprotein, bone morphogenetic protein 6 and thymidine phosphorylase expression in localized human prostatic adenocarcinoma as predictors of clinical outcome: a clinicopathological and immunohistochemical study of 43 cases. J Urol. 2001;166:1924-1930.

283. Masuda H, Fukabori Y, Nakano K, Takezawa Y, T CS, Yamanaka H. Increased expression of bone morphogenetic protein-7 in bone metastatic prostate cancer. Prostate. 2003;54:268-274.

284. Higinbotham KG, Karavanova ID, Diwan BA, Perantoni AO. Deficient expression of mRNA for the putative inductive factor bone morphogenetic protein-7 in chemically initiated rat nephroblastomas. Mol Carcinog. 1998;23:53-61.

285. Blessing M, Nanney LB, King LE, Hogan BL. Chemical skin carcinogenesis is prevented in mice by the induced expression of a TGF-beta related transgene. Teratog Carcinog Mutagen. 1995;15:11-21.

286. Wach S, Schirmacher P, Protschka M, Blessing M. Overexpression of bone morphogenetic protein-6 (BMP-6) in murine epidermis suppresses skin tumor formation by induction of apoptosis and downregulation of fos/jun family members. Oncogene. 2001;20:7761-7769.

287. Hartung A, Bitton-Worms K, Rechtman MM, et al. Different routes of bone morphogenic protein (BMP) receptor endocytosis influence BMP signaling. Mol Cell Biol. 2006;26:7791-7805.

288. Katzmann DJ, Babst M, Emr SD. Ubiquitin-dependent sorting into the multivesicular body pathway requires the function of a conserved endosomal protein sorting complex, ESCRT-I. Cell. 2001;106:145-155.

289. Dorrell MI, Aguilar E, Friedlander M. Retinal vascular development is mediated by endothelial filopodia, a preexisting astrocytic template and specific R-cadherin adhesion. Invest Ophthalmol Vis Sci. 2002;43:3500-3510.

290. Fruttiger M. Development of the mouse retinal vasculature: angiogenesis versus vasculogenesis. Invest Ophthalmol Vis Sci. 2002;43:522-527.

291. Smith LE, Wesolowski E, McLellan A, et al. Oxygen-induced retinopathy in the mouse. Invest Ophthalmol Vis Sci. 1994;35:101-111.

292. Alon T, Hemo I, Itin A, Pe'er J, Stone J, Keshet E. Vascular endothelial growth factor acts as a survival factor for newly formed retinal vessels and has implications for retinopathy of prematurity. Nat Med. 1995;1:1024-1028.

293. Stone J, Itin A, Alon T, et al. Development of retinal vasculature is mediated by hypoxia-induced vascular endothelial growth factor (VEGF) expression by neuroglia. J Neurosci. 1995;15:4738-4747.

294.   Brooks SE, Gu X, Samuel S, et al. Reduced severity of oxygen-induced retinopathy in eNOS-deficient mice. Invest Ophthalmol Vis Sci. 2001;42:222-228.